Inkjet printed organic electronic devices for biomedical diagnosis

Eloïse Bihar

▶ To cite this version:

HAL Id: tel-01668466
https://theses.hal.science/tel-01668466

Submitted on 20 Dec 2017

N°d'ordre NNT : 2016LYSEM036

THESE de DOCTORAT DE L'UNIVERSITE DE LYON
opérée au sein de
l'Ecole des Mines de Saint-Etienne

Ecole Doctorale N° 488
Sciences, Ingénierie, Santé

Spécialité de doctorat : Microélectronique
Discipline : Bioélectronique

Soutenue publiquement le 19/12/2016, par :
Eloïse Bihar

Réalisation de dispositifs biomédicaux par impression jet d'encre

Devant le jury composé de :

Daniel, Susan	Professeure associée	Cornell University	Présidente
De Mello John	Professeur	Imperial College London	Rapporteur
Kaltenbrunner, Martin	Professeur associé	Johannes Kepler University	Rapporteur
Rivnay, Jonathan	Maitre de conférence	Northwestern university	Examinateur
Reverdy Bruas, Nadège	Maitre de conférence	Grenoble INP Pagora	Examinatrice
Malliaras, George	Professeur	Ecole des Mines de Saint-Etienne	Directeur de thèse
Saadaoui, Mohamed	Chargé de recherche	Ecole des Mines de Saint-Etienne	Co-directeur de thèse
Hervé, Thierry	CEO	Microvitae technologies	Invité

Spécialités doctorales	Responsables :	Spécialités doctorales	Responsables
SCIENCES ET GENIE DES MATERIAUX	K. Wolski Directeur de recherche	MATHEMATIQUES APPLIQUEES	O. Roustant, Maître-assistant
MECANIQUE ET INGENIERIE	S. Drapier, professeur	INFORMATIQUE	O. Boissier, Professeur
GENIE DES PROCEDES	F. Gruy, Maître de recherche	IMAGE, VISION, SIGNAL	JC. Pinoli, Professeur
SCIENCES DE LA TERRE	B. Guy, Directeur de recherche	GENIE INDUSTRIEL	A. Dolgui, Professeur
SCIENCES ET GENIE DE L'ENVIRONNEMENT	D. Graillot, Directeur de recherche	MICROELECTRONIQUE	S. Dauzere Peres, Professeur

EMSE : Enseignants-chercheurs et chercheurs autorisés à diriger des thèses de doctorat (titulaires d'un doctorat d'État ou d'une HDR)

ABSI	Nabil	CR	Génie industriel	CMP
AVRIL	Stéphane	PR2	Mécanique et ingénierie	CIS
BALBO	Flavien	PR2	Informatique	FAYOL
BASSEREAU	Jean-François	PR	Sciences et génie des matériaux	SMS
BATTAIA-GUSCHINSKAYA	Olga	CR	Génie industriel	FAYOL
BATTON-HUBERT	Mireille	PR2	Sciences et génie de l'environnement	FAYOL
BERGER DOUCE	Sandrine	PR2	Sciences de gestion	FAYOL
BIGOT	Jean Pierre	MR(DR2)	Génie des Procédés	SPIN
BILAL	Essaid	DR	Sciences de la Terre	SPIN
BLAYAC	Sylvain	MA(MDC)	Microélectronique	CMP
BOISSIER	Olivier	PR1	Informatique	FAYOL
BONNEFOY	Olivier	MA(MDC)	Génie des Procédés	SPIN
BORBELY	Andras	MR(DR2)	Sciences et génie des matériaux	SMS
BOUCHER	Xavier	PR2	Génie Industriel	FAYOL
BRODHAG	Christian	DR	Sciences et génie de l'environnement	FAYOL
BRUCHON	Julien	MA(MDC)	Mécanique et ingénierie	SMS
BURLAT	Patrick	PR1	Génie Industriel	FAYOL
COURNIL	Michel	PR0	Génie des Procédés	DIR
DAUZERE-PERES	Stéphane	PR1	Génie Industriel	CMP
DEBAYLE	Johan	CR	Image Vision Signal	CIS
DELAFOSSE	David	PR0	Sciences et génie des matériaux	SMS
DELORME	Xavier	MA(MDC)	Génie industriel	FAYOL
DESRAYAUD	Christophe	PR1	Mécanique et ingénierie	SMS
DOLGUI	Alexandre	PR0	Génie Industriel	FAYOL
DRAPIER	Sylvain	PR1	Mécanique et ingénierie	SMS
FAVERGEON	Loïc	CR	Génie des Procédés	SPIN
FEILLET	Dominique	PR1	Génie Industriel	CMP
FRACZKIEWICZ	Anna	DR	Sciences et génie des matériaux	SMS
GARCIA	Daniel	MR(DR2)	Génie des Procédés	SPIN
GAVET	Yann	MA(MDC)	Image Vision Signal	CIS
GERINGER	Jean	MA(MDC)	Sciences et génie des matériaux	CIS
GOEURIOT	Dominique	DR	Sciences et génie des matériaux	SMS
GONDRAN	Natacha	MA(MDC)	Sciences et génie de l'environnement	FAYOL
GRAILLOT	Didier	DR	Sciences et génie de l'environnement	SPIN
GROSSEAU	Philippe	DR	Génie des Procédés	SPIN
GRUY	Frédéric	PR1	Génie des Procédés	SPIN
GUY	Bernard	DR	Sciences de la Terre	SPIN
HAN	Woo-Suck	MR	Mécanique et ingénierie	SMS
HERRI	Jean Michel	PR1	Génie des Procédés	SPIN
KERMOUCHE	Guillaume	PR2	Mécanique et Ingénierie	SMS
KLOCKER	Helmut	DR	Sciences et génie des matériaux	SMS
LAFOREST	Valérie	MR(DR2)	Sciences et génie de l'environnement	FAYOL
LERICHE	Rodolphe	CR	Mécanique et ingénierie	FAYOL
LI	Jean-Michel		Microélectronique	CMP
MALLIARAS	Georges	PR1	Microélectronique	CMP
MAURINE	Philippe	Ingénieur de recherche	Microélectronique	CMP
MOLIMARD	Jérôme	PR2	Mécanique et ingénierie	CIS
MONTHEILLET	Frank	DR	Sciences et génie des matériaux	SMS
MOUTTE	Jacques	CR	Génie des Procédés	SPIN
NEUBERT	Gilles	PR	Génie industriel	FAYOL
NIKOLOVSKI	Jean-Pierre	Ingénieur de recherche		CMP
NORTIER	Patrice	PR1		SPIN
OWENS	Rosin	MA(MDC)	Microélectronique	CMP
PICARD	Gauthier	MA(MDC)	Informatique	FAYOL
PIJOLAT	Christophe	PR0	Génie des Procédés	SPIN
PIJOLAT	Michèle	PR1	Génie des Procédés	SPIN
PINOLI	Jean Charles	PR0	Image Vision Signal	CIS
POURCHEZ	Jérémy	MR	Génie des Procédés	CIS
ROBISSON	Bruno	Ingénieur de recherche	Microélectronique	CMP
ROUSSY	Agnès	MA(MDC)	Génie industriel	CMP
ROUSTANT	Olivier	MA(MDC)	Mathématiques appliquées	FAYOL
ROUX	Christian	PR	Image Vision Signal	CIS
STOLARZ	Jacques	CR	Sciences et génie des matériaux	SMS
TRIA	Assia	Ingénieur de recherche	Microélectronique	CMP
VALDIVIESO	François	PR2	Sciences et génie des matériaux	SMS
VIRICELLE	Jean Paul	DR	Génie des Procédés	SPIN
WOLSKI	Krzystof	DR	Sciences et génie des matériaux	SMS
XIE	Xiaolan	PR1	Génie industriel	CIS
YUGMA	Gallian	CR	Génie industriel	CMP

ENISE : Enseignants-chercheurs et chercheurs autorisés à diriger des thèses de doctorat (titulaires d'un doctorat d'État ou d'une HDR)

BERGHEAU	Jean-Michel	PU	Mécanique et Ingénierie	ENISE
BERTRAND	Philippe	MCF	Génie des procédés	ENISE
DUBUJET	Philippe	PU	Mécanique et Ingénierie	ENISE
FEULVARCH	Eric	MCF	Mécanique et Ingénierie	ENISE
FORTUNIER	Roland	PR	Sciences et Génie des matériaux	ENISE
GUSSAROV	Andrey	Enseignant contractuel	Génie des procédés	ENISE
HAMDI	Hédi	MCF	Mécanique et Ingénierie	ENISE
LYONNET	Patrick	PU	Mécanique et Ingénierie	ENISE
RECH	Joël	PU	Mécanique et Ingénierie	ENISE
SMUROV	Igor	PU	Mécanique et Ingénierie	ENISE
TOSCANO	Rosario	PU	Mécanique et Ingénierie	ENISE
ZAHOUANI	Hassan	PU	Mécanique et Ingénierie	ENISE

Table of contents

Résumé

De nos jours, le domaine biomédical est en pleine croissance avec le développement de nouveaux dispositifs thérapeutiques, pour le diagnostic, le traitement ou la prévention de maladies chroniques ou cardiovasculaires telles que diabète, ou infarctus. Ces dernières années ont connu l'émergence des polymères semi-conducteurs.   Ceux-ci présentent à la fois des propriétés ioniques et électroniques utiles pour les applications éléctrophysiologiques et semblent être une alternative intéressante aux matériaux inorganiques utilisés dans le secteur du biomédical. Poursuivant l'objectif de créer des dispositifs imprimés, j'ai démarré mes travaux de thèse en sélectionnant le PEDOT:PSS composé de deux polymère : le poly*(3,4-éthylènedioxythiophène)* (PEDOT) et le poly*(styrène sulfonate)* de sodium (PSS). ce polymère étant un parfait candidat comme matériau pour la transduction des signaux biologiques en signaux électriques pour les applications biomédicales visées.

Tout d'abord, j'ai axé mes travaux de recherche sur le développement et l'optimisation d'une encre conductrice à base de PEDOT:PSS, parfait candidat comme matériau, pour la transduction des signaux biologiques en signaux électriques, compatible avec le process jet d'encre, pour la réalisation de dispositifs imprimés.

Puis mes travaux se sont orientés vers la conception et l'étude d'électrodes imprimées sur supports papiers, tatous et textiles permettant des enregistrements long termes d'électrocardiogrammes (ECG) ou électromyogrammes (EMG), présentant des performances similaires aux électrodes commerciales, utilisant un système d'acquisition spécifique pour la mesure d'activités électriques de tissus musculaires. Des mesures d'impédance ont été effectuées afin de les caractériser les électrodes. Un gel ionique biocompatible a été imprimée afin de diminuer l'impédance des électrodes PEDOT :PSS sur textile ce qui a permis d'atteindre des performances électriques similaires aux électrodes commerciales.

Puis dans un second temps, je me suis penchée sur l'impression et la caractérisation sur support papier de transistor organique électrochimique (OECT). Les premiers résultats ont permis d'envisager la fonctionnalisation des transistors afin de permettre la détection d'éléments biologiques ou chimiques comme le glucose et l'alcool. Des tests ont été réalisés en laboratoire et ont permis d'établir la sensibilité et le seuil de détection des dispositifs sur

support papier. Egalement des encres avec différentes fonctionnalités ont été formulées afin de fonctionnaliser les transistors et effectuer les mesures de détection biologique.

Ces travaux proposent une nouvelle voie pour la conception de dispositifs innovants biomédicaux à bas couts, imprimés, permettant la personnalisation des produits pouvant être intégrés dans des dispositifs biomédicaux portables ou dans des vêtements « intelligents ».

Abstract

Currently, there is a tremendous effort on the development of biomedical devices in healthcare industry for the early diagnosis, prevention or treatment of chronic disease such as diabetes or cardiovascular disease. For example, the study of electrical activity of the biological tissues or cells also known as electrophysiology, can provide useful information regarding the medical status of a patient such as malfunctions in the neural or cardiovascular system. With the evolution of microelectronics industry and their direct implementation in the biomedical arena, innovative tools and technologies have come to the fore enabling more reliable and cost-effective treatment. During the last decade, conducting polymers have attracted special attention due to their unique set of features such as combined ionic and electronic conduction, soft nature and ease in processability rendering them an ideal alternative to the inorganic materials used for electrophysiological applications. Driven by the technological demands for low-cost and large area electronics, in this thesis I focus on the integration of the especially promising conducting polymer namely Poly*(3,4-ethylenedioxythiophene)* polystyrene sulfonate (PEDOT:PSS) with additive printing technologies toward the realization of high performances biomedical devices.

In the first part, I focus on the printing techniques and their recent applications in electronics with a loop on the inkjet technique and the functionalized inks for the fabrication of the biomedical devices tested during this thesis.

Following, I emphasize on the fabrication of inkjet-printed PEDOT:PSS based biopotential electrodes on a wide variety of substrates (i.e., paper, textiles, tattoo paper) for use in electrophysiological applications such as electrocardiography (ECG) and electromyography (EMG) on human volunteers. In an initial approach, electrodes on paper were investigated for long-term ECG recordings obtained by simply placing two fingers on the electrodes which

exhibited good signal quality over a period of 3 months. This convenient-to-use and inexpensive platform enables future integration of devices with portable devices (i.e., smart phones). In a second approach, printed wearable electrodes were fabricated, on top of commercially available stretchable textile. In an attempt to improve the electrode-skin interface, a new cholinium lactate-based ionic liquid gel was as well inkjet-printed directly on the textile. The resulting electrodes yielded recordings of comparable quality to Ag/AgCl electrodes highlighting their potential as customizable health monitoring devices for cutaneous applications. Last but not least, conformable printed tattoo electrodes were realized toward the ultimate goal of fully integrated e-skin platform. In order to enable a reliable connection of the tattoo with the electronic acquisition system, the conventional wiring was replaced by a simple contact between the tattoo and a similarly ink-jet printed textile electrode. The proposed tattoo-textile electrode system was able to detect the biceps activity during muscle contraction for a period of seven hours.

In the last part, I present the potentiality of inkjet printing method for the realization of more complex circuits such as the organic electrochemical transistor (OECTs) as high performing biomedical devices. OECTs, owing to their inherent signal amplification properties can be ideal transducers for biosensing applications. As proof of concept, a paper disposable breathalyzer comprised of a printed OECT and modified with alcohol dehydrogenase was used for the direct alcohol detection in breath, enabling future integration with wearable devices for real-time health monitoring.

Overall, conducting polymers such as PEDOT:PSS hold great promise to interface electronics with biology. Their compatibility with inkjet-printing technologies allows the realization of low-cost and large area electronic devices, toward next-generation of fully integrated smart biomedical devices.

Acknowledgements

List of figures

Abbreviations list

ADH	Alcohol dehydrogenase
APTS	(3-Aminopropyl)triethoxysilane
BrAC	Breath alcohol concentration
BAC	Blood alcohol concentration
CIJ	Continuous InkJet
CP	Conducting polymer
CVDs	Cardiovascular diseases
DMF	DimethylFormamide
DMSO	DimethylSulfoxide
DOD	Drop on Demand
ECG	Electrocardiography
EEG	Electroencephalography
EIS	Electrochemical Impedance
EMG	Electromyography
EOG	Electrooculography
FETs	Field Effect transistors
GOPs	Glycidoxypropyltrimethoxysilane
GOx	Glucose oxidase
IL	Ionic liquid
NADH	Nicotinamide adenine dinucleotide
NADP	Nicotinamide adenine dinucleotide phosphate
ITO	Indium Tin Oxide
OECT	Organic ElectroChemical Transistor
OLED	Organic light Emitting Diode
PBS	Phosphate buffer solution

PEDOT:PSS	Poly (3,4-ethylenedioxythiophene) Poly(styrene sulfonate)
RFID	Radio Frequency IDentification
SNR	Signal to noise ratio
UV	Ultraviolet

Chapter 1

Introduction

This chapter is based on the following publication:

"Fabrication approaches for conducting polymer devices"

D. Koutsouras, **E. Bihar*,** J. Fairfield, M. Saadaoui, G. G. Malliaras, Green Materials for Electronics, in press.*

In a context of improving the medical devices and equipments to enable a better access for healthcare, new technologies emerged as promising alternatives to conventional fabrication approaches to develop state of the art medical care with reduced manufacturing costs. To assess this challenge, printing technologies could fit requirements for an easy transfer of lab prototypes to industry at large scale production.

During my PhD, I tried to demonstrate the potential of inkjet printing technique to fabricate new devices for biomedical applications such as electrophysiology or biosensing by the use of conducting polymers which offer a unique set of features to replace inorganic materials. In this context, I presented in the first chapter, the printing technologies with a special focus on a digital-writing approach, inkjet process. Then, I will present some developments on functional inks for electronic applications, especially PEDOT:PSS inks which I used for the fabrication of the devices presented in this thesis.

1.1 Introduction to printing technologies: a case study on conducting polymer

The term "printed electronics" comes from bridging the fields of both printing and electronics; this union of two fields allow for simpler methodology to fabricate inexpensive electronic components. The market for printed electronics has been estimated around 57 billion USD in 2019 by IDTechEx [1], and there are significant opportunities for companies to enter this market. Advantages for printing techniques include direct ink transfer to substrates and a reduction in the number of manufacturing steps. Furthermore, motivations for the continued use of printing arise from its flexibility, high processing speeds, ease of customization, reduction in manufacturing costs, the possibility of printing on inexpensive flexible plastic or paper substrates, and the ability to print with different types of materials.

Recently, there has been a growing interest to adapt classical printing techniques to be able to print new functional materials, especially with electronic inks for device fabrication. This idea has the potential to open up new markets and opportunities for both industry and academia. By exchanging traditional graphic inks for electrically functional inks, one can directly print or fabricate interconnections, antennas, sensors etc. By using printing techniques, one can avoid the large number of processing steps (lithography, etching, etc.) used in conventional electronic fabrication techniques.

Technologies such as screen printing or inkjet are promising technologies, and have been extensively studied over the last few decades. They are envisaged to replace traditional manufacturing technologies, such as lithography, to fabricate new electronic components. In this part, we will describe the different printing techniques with an emphasis on conducting materials. We will separate the topic into two categories: contact and non-contact printing.

1.1.1 Contact printing technologies

1.1.1.1. Gravure

Gravure printing is a process coming from intaglio developed in the 19th century. It uses a rotary printing press and operates at high speed processing (up to 100 m/min). It is adapted for large volume runs such as books or magazines. Gravure is based on the direct transfer of the

ink to the substrate from an engraved cylinder to the substrate (Figure 1.1). This cylinder is electroplated, for instance with copper, and engraved electromechanically or by laser to create microcells. A chromium zinc layer is generally added to protect the cylinder. The volume of the ink that is deposited is determined by the geometry of the microcells. Then, the ink is transferred by capillary force from the microcells to the substrate when a pressure is applied between the gravure cylinder and the substrate. Moreover, a doctor blade station is used in order to remove any excess ink and to ensure good film uniformity. Gravure allows designs with high resolution up to 20 µm and presents a good printing quality and process reproducibility. It is compatible with a wide range of solvents or water based inks. The required viscosity of the inks is comprised between 10 mPa.s and 500 mPa.s. Nevertheless this process exhibits some limitations in terms of maintenance and cost of manufacturing mainly due to the price and the weight of cylinders.
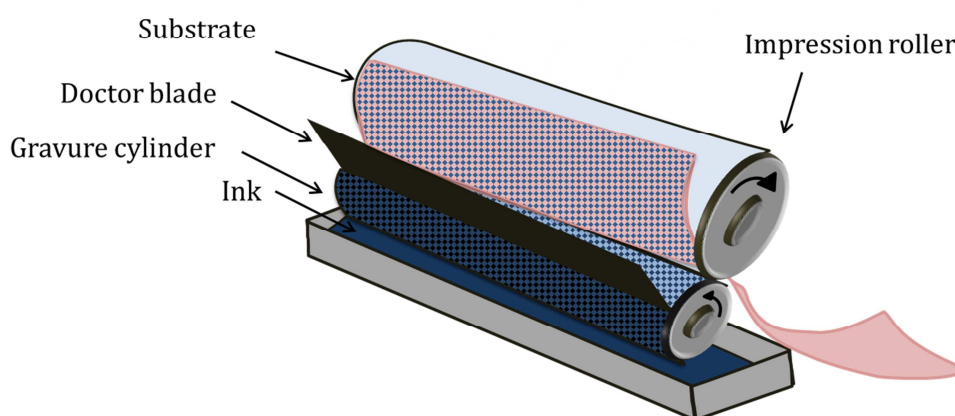
Figure 1.1 **Gravure process.**

This technique has been studied for electronic applications such as for the realization of Field Effect Transistors (FETs) or photovoltaic cells[2]. A few groups tested the printability of conducting polymers to print functional multilayers to fabricate FETs [3] or to realize solar cells with laboratory gravure modules [4-6] . Gravure-printed PEDOT:PSS electrodes demonstrated high mechanical flexibility and stretchability in comparison with conventional Indium Tin Oxide (ITO) on flexible substrates. For instance, Hübler et al. fabricated photovoltaic cells by printing PEDOT:PSS as the anode and P3HT: PCBM as the photoactive and hole transport layers on paper [4]. Yang et al. used an industrial gravure printing proofer to process photovoltaic module, where they print conducting polymers on flexible substrates already

coated with ITO [7]. Recently, gravure has been investigated to realize impedance-based electrochemical biosensors [8] which paves the way to fabricate new generation of flexible devices for biological applications.

1.1.1.2. Flexography

Conventionally Flexography is used for printing food packages and magazines. Flexography is compatible with flexible substrates such as plastics or cardboards. It is a process combining a system of cylinders and a flexible relief plate (Figure 1.2). An engraved anilox roll is used to transfer the ink from the pan. The amount of the ink is fixed by the volume of the microcells' cylinder. A doctor blade ensures that the thickness of the ink is uniform. Then, the printing of the ink is assured by the contact between the substrate and the plate cylinder. These plates are usually made from rubber or photopolymer materials and produced by photolithography.

This technology is compatible with a wide variety of inks: UV cured inks, solvent or water based inks with a viscosity ranging from 10 to 100 cP. Resolution up to 50 µm can be reached. The use of the plates lowers the cost of fabrication and allows the printing of large volume runs with high processing speed (up to 180 m/min). The costs are reduced in comparison with gravure but plates can be degraded with the use of solvents. One of the major undesirable effects of this process is the "halo" which appears on the edge of the printed pattern. The default comes from the deformation of the plate when the pressure is applied between the plate and the substrate squeezing the ink.
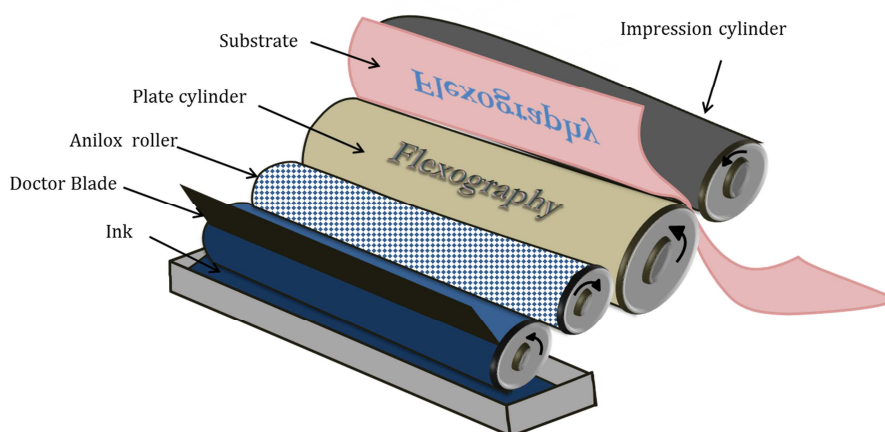
Figure 1.2 **Flexography process.**

Only few studies chose this approach for printed electronic applications [9,10]. Hübler et al [11] use a laboratory flexographic test printing device to print the gate and contact electrodes using conducting polymers to fabricate transistors. Krebs et al [12] reported using this process to improve the wettability of surface to slot die conducting polymer while Yu et al [13] printed the silver layer to realize grids to replace ITO in polymer cells.

1.1.1.3. Screen printing

Screen printing is a simple and versatile technique used in many applications such as textiles or advertisements. It has been originally invented in China, and imported into Europe in the 18th century and developed in the second half of the 20th century. The first patent was published in 1907 by Samuel Simon, and the technique became more popular in the sixties with artists such as Andy Warhol [14].

Screen printing is a stencil method that uses a mesh stretched over a frame to transfer the ink to the substrate. The ink is pushed into the opening of the mesh through a squeegee (Figure 1.3). The mesh is usually made from nylon, polyester or a stainless steel. Two different categories of screen printing have been developed and can be integrated for roll to roll manufacturing: the flatbed screen or the rotary screen. The flatbed screen (Figure 1.3.A) is used in laboratories or in production and the rotary is adapted for large scale process with a production speed up to 100 m/min. In this case, the squeegee and the ink are placed in the rotary screen (Figure 1.3.B) making the maintenance procedure difficult. The printing resolution can be up to 100µm and depends on parameters such as the surface energy of the substrate, the ink viscosity, the mesh size and counts.
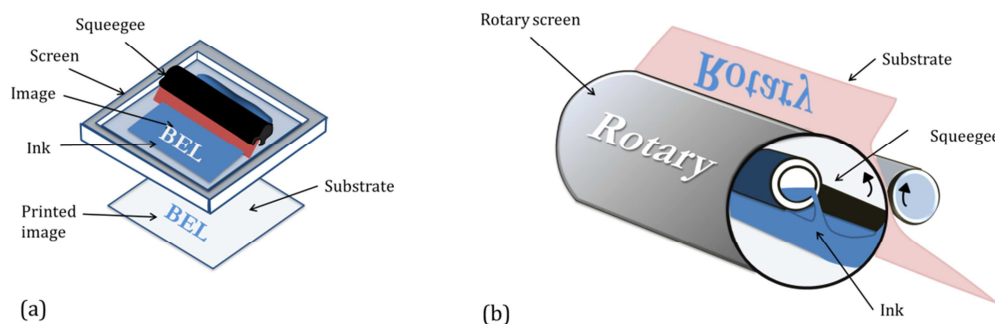
Figure 1.3 **Screen printing.** (a) Flatbed screen printing. (b) Rotary screen printing

Screen printing is one of the most robust technologies that have been developed those last few years as it is compatible with a wide range of substrates such as textiles, clothes, papers, glass etc. This process requires high viscosity inks (up to 10 000 cP) and the deposited thickness can go up to few hundreds of microns. Screen printing is already used to print interconnections for printed circuits boards and antennas for RFIDs (Radio Frequency IDentification), active layers [15] and electrodes [16,17] for solar cells or organic thin film transistors [18], and emitting layers in OLEDS [19-21] (Figure 1.4). Many studies [22-24] and patents [25-27] have reported the use of screen printing for biosensing applications. They demonstrated the feasibility of such devices to detect bio elements or to fabricate amperometric biosensors.

(A)   (B)
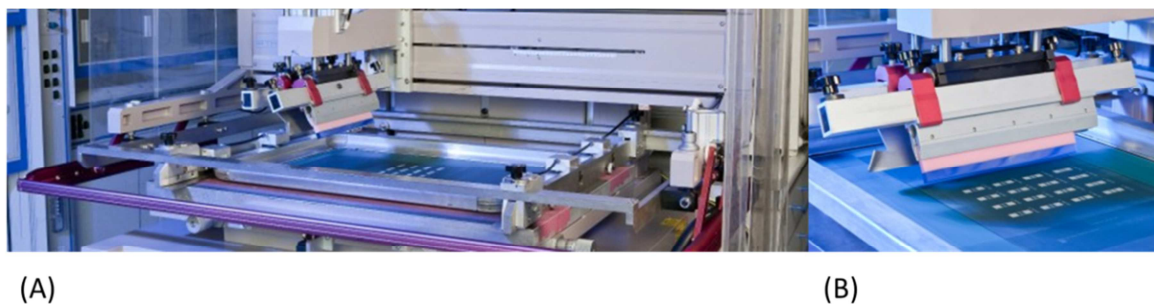
Figure 1.4 **(a). (b). Screen printer using Clevios™ ink** [Reproduced with permission from Heraeus]

1.2.1   Non-contact printing technologies

Non-contact printing technologies are digital-writing approaches and present many advantages because they do not require masks and the geometry can be customized and changed on demand. Also, the ink is digitally delivered to the substrate thus limiting the waste of materials and allowing to process designs at low cost.

1.2.1.1   Aerosol jet

Aerosol jet printing of ink has been developed since the 2000s and shows a promising future for industrial applications. This technology allows printing a large range of ink viscosities (from 1 cP to 2500 cP). The principle is based on the ejection of fluids even with

nanoparticles from a chamber to the substrate (Figure 1.5), a new technology which uses the atomization of suspension by an ultrasonic or a pneumatic system. The formed droplets are guided by a jet stream up to the printing nozzles. The aerosol printing can produce conformal coating and resolution down to 10µm with processing speed up to 1.2 m/min.
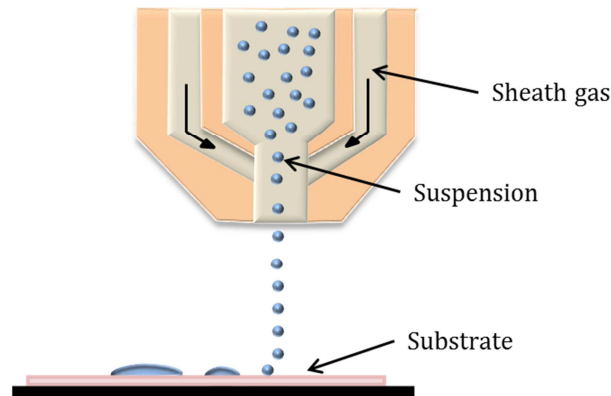
Figure 1.5 **Aerosol process**

Few studies mention aerosol printing in literature[28,29]. Recently, it has been evaluated for diverse applications such as solar cells and thin film transistors. For instance, aerosol jet has been used to print the conducting polymer as an active layer in solar cells [30] and to fabricate electrodes for Thin Film Transistors (TFTs) [31]. Aerosol has been also studied for the deposition of DNA or enzymatic layers and for the functionalization of electrodes in biological sensors [32].

1.2.1.2 Inkjet

Inkjet is a non-contact technology commonly used for daily use printing applications (home or office). This process can be integrated in industry in roll to roll processes in the production line. Advances in these technologies have been seen recently, for instance, the standardization and commercialization of 3D printing and the creation of new functional inks for electronics.

A. History

The physics behind Inkjet has been first described in 1878 by Lord Rayleigh [33], the pioneer in studying the mechanism of the liquid jets' instability. The first patent was deposited by Elmqvist [34] in 1951 at Siemens-Elema Company.

In the early 1960s, Sweet developed a model [35] in Stanford University, in which he assumes that the trajectory of ejected droplets can be controlled electrostatically through an externally applied electric field. This process has been called Continuous Inkjet (CIJ) and it is still used for some applications. Later, a drop on demand (DOD) technology was proposed in 1972 by Zoltan [36], Kyser and Sears [37] as an alternative to CIJ. A single droplet is formed and detached by each of the nozzles.

In the late 1970s, John Vaught [38] from Hewlett Packard and Ichiro Endo [39] from Canon developed a DOD system based on the formation and the ejection of ink using a heating element known as thermal inkjet. In the 1990s, with the standardization of personal computers, Inkjet became a daily used technology with the commercialization of inexpensive printers.

B. Basic principles

The Inkjet mechanism is based on the ejection of fluid droplets, released from a chamber under the variation of internal pressure in the printhead cavity and through nozzles. This fluid ejection depends on rheological parameters such as the ink's properties (surface tension, viscosity, density) and the chamber's pressure. The resolution can reach 20 µm depending on the nozzle diameter, drop volume, and drop to drop spacing. Originally, two technologies have been developed for Inkjet: Continuous Inkjet (CIJ) and Drop on Demand technology (DOD) (Figure 1.6.)
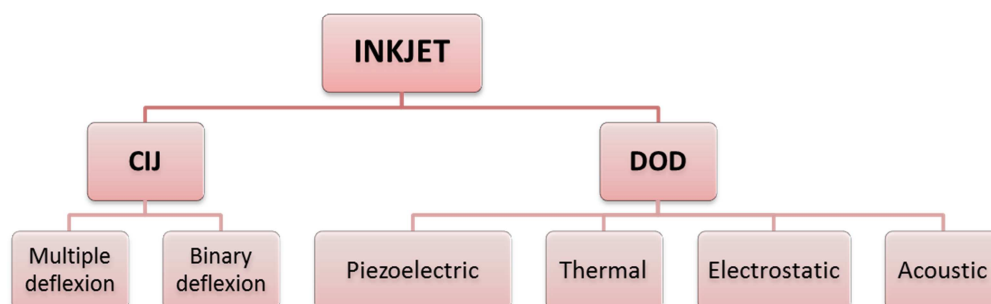
Figure 1. 6 **Inkjet technology**

- **CIJ (Continuous Inkjet) printing**

The Continuous Inkjet technology consists of the generation and the ejection of continuous drops. Those droplets pass through an electrostatic charging electrode and then a high-voltage deflector plate leads trajectory deviation towards a recycling recipient. Two different categories of CIJ have been developed: the binary and the multiple deflections. In a binary deflection system, (Figure 1.7) there are two states regulated by the electrostatic deflector. The drops charged during the printing step are going directly to the substrate and the non-charged ones are deviated and collected in a gutter and then recycled. In a multiple deflection system, the non-charged drops are going to the gutter to be reprocessed while the charged drops are deviated to be deposited onto the substrate.

Drop generator

Charge electrode

High voltage deflector Plate

Gutter

Printed pattern

Substrate
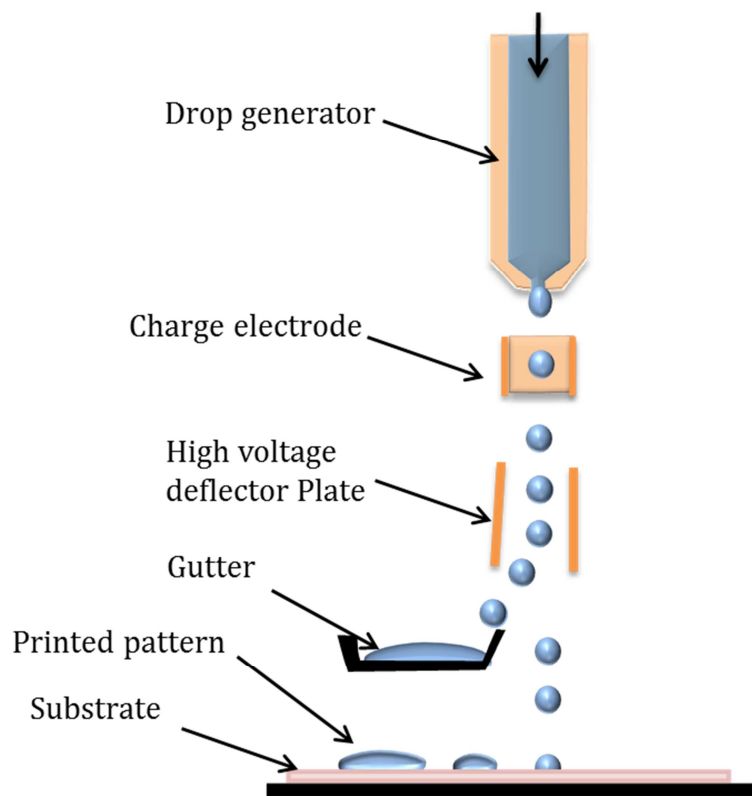
Figure 1.7 **Binary Continuous Inkjet system**

CIJ technology is used in industry for marking and encoding the products before commercialization. It presents advantages such as good printing resolution down to 50 µm, high ejection frequencies of droplets up to 60 kHz at high printing speed, and good process

stability without the nozzles clogging. However, this technique shows limitations regarding the type of inks which have to match the requirements of the system especially for the electrostatic charging step. Printing of complex designs and customization is not easy because of the continuous ejection of the drops. This is why this technology has never been adopted for printed electronics because of issues due to the possible ink contamination during the recycling of the ink.

- **(DOD) Drop-On-Demand inkjet printing : piezoelectric or Thermal**

The drop-on-demand technique can be divided into 4 categories: piezoelectric, thermal, electrostatic and acoustic inkjet. Thermal and piezoelectric inkjets are the technologies mainly adopted in industry and laboratories.

In the thermal inkjet, a local increase in the temperature of the ink generally up to 300°C and using a heating element creates an air bubble within the ink. This change in local pressure provokes the formation and the ejection of individual droplets (Figure 1.8. A). Today, thermal inkjet is widely used for graphic printing and especially for home printers. However, requirements for heating before ejection make this process very limited in term of inks. A few studies mentioned the possibility to use this technology to fabricate biosensors [40,41]. For instance, Setti et al [42] reported fabricating an amperometric sensor for the detection of glucose.

The piezoelectric inkjet technology is based on the use of piezo membrane. This membrane is mechanically deformed when an external voltage is applied, causing a change in the pressure in the chamber. This causes the formation of the drop in the aperture in the printhead, and the expulsion of the ink relieves the pressure in the printhead as shown in Figure 1.8. B. This mechanism is compatible with different printable materials. In this process, the nozzle generates few-picoliter droplets, the best resolution is around 20 µm, and the viscosity range of inkjet is from to 5-20 cP.
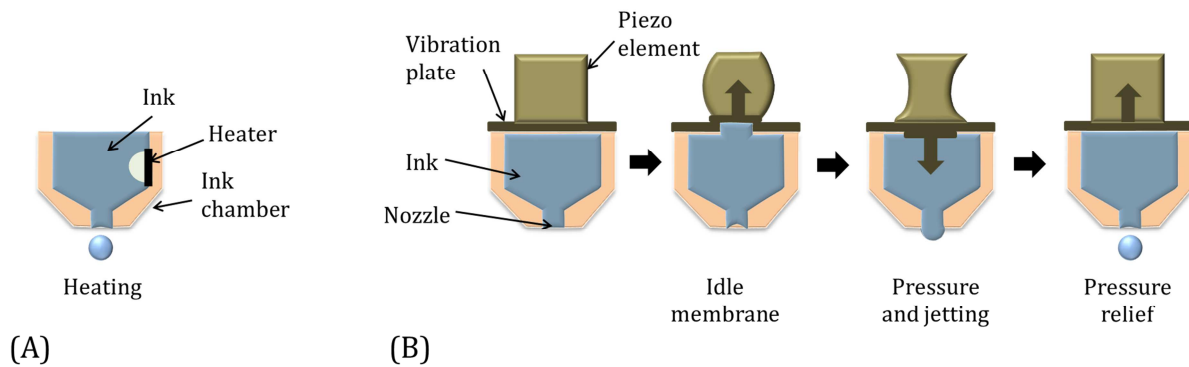
Figure 1.8 **(a). Thermal inkjet. (b) Drop-on-demand inkjet process**

With the rise in printed electronics, several companies like FujiFilm, Ceradrop, and Meyer Burger developed new inkjet machines that can print different functional materials using piezo-DOD technology (Figure 1.9). The printing parameters can be tuned such as the voltage applied to the piezo element, the drop spacing, the waveform, and the temperature of the ink. Some printers offer the possibility to realize the alignment to print complete devices with several layers and different inks. The machines show flexibility and are easy to use, making the process adaptable to different materials.

Figure 1.9 **Inkjet printer using Clevios™ ink** [Reproduced with permission from Heraeus]

Inkjet offers many possibilities for new developments. In the literature, this technology is widely studied for diverse electronic applications such as Organic Thin Film Transistors [43,44], polymer light emitting diodes [45,46], and recently polymer solar cells [47-49] and sensing

applications [50]. Studies demonstrated the feasibility to manufacture micrometer [51,52] or submicrometer [53] dimensions OTFTs controlling the hydrophobicity of the substrate and printing the drain, source and gate of the transistor with a commercial PEDOT:PSS ink. Barathan et al [54] combined inkjet with spincoating to pattern electroluminescent devices. Inkjet has also been studied to print the active layer of solar cells ([55,56]) with a device efficiency above 3%. Printed conducting polymers have also been studied for chemical sensing such as ammonia detection [57,58].

C. Printability requirements

In the DOD technology, the formation and ejection of the droplet depend on different rheological parameters of the ink such as viscosity, density, and surface tension (Figure 1.10).

(A)   (B)
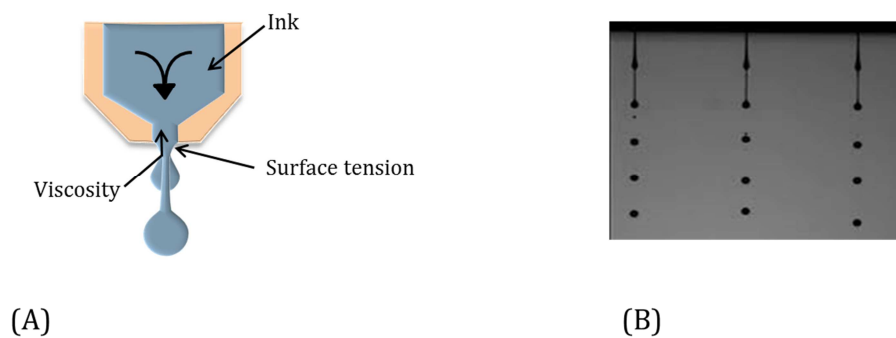
Figure 1.10 **Drop formation in the nozzle** (a). Schematic of the drop formation (b). Photograph of the ejection of the drop

Printability of the ink depends on these rheological parameters combined with the characteristics of the printhead: nozzle diameter, frequency of the drops ejection, applied voltage, channel, and pressure in the chamber. Rheological behavior of the ink can be described with dimensionless parameters called the Reynolds number and Weber number or Ohnesorge number respectively defined as below

$$Re = \frac{v\,\rho R}{\mu}\,;\, We = \frac{v^2\,\rho R}{\sigma};\, Oh = \frac{\sqrt{We}}{Re} = \frac{\mu}{\sqrt{\rho R \sigma}} \qquad (1)$$

Where μ is the viscosity of the ink (Pa.s), ρ the density (kg/m^3), σ the surface tension (mN/m) and R the radius of the nozzle (m), and v is the velocity (m/s).

These numbers are directly dependent on the fluid's rheological properties and predict the ejection of the ink from the nozzle. In the 1980s, Fromm defined criteria for ink printability such as $Z = \frac{1}{Oh} > 2$ [59]. Later, Reis and Derby [60,61] discussed Fromm's assumption and propose their own rheological requirements for ink jetting. Using a numerical simulation of drop formation, Reis suggested that the condition $1 < Z < 10$ is more adapted in order to match the ink with the printing requirements. They propose a chart [61] where one can define which area is the most adequate combing the above-mentioned dimensionless number with DOD printing. The lower limit corresponds to a high viscosity that prevents the jetting and the upper limits to the formation of unwanted satellite drops. This theory is often used in the literature [62-64] for the formulation in new functional inks dedicated to inkjet printing technology.

1.2   Inks

Graphic inks are widely present on the market and used in daily life. Over the last few years, with the concern of environmental issues and to reduce the fabrication costs of electronic components, a new trend has emerged in formulating new conducting inks which exhibit different electrical properties. Manufacturers are developing novel inks with specific functions which can fit specific requirements for diverse applications such as photovoltaics or TFTs. In this section we describe the main categories of inks used in electronic applications.

1.2.1 Metallic inks

The inks are usually composed of metallic nanoparticles, for instance gold, silver, or copper in suspension. Surfactants can be added to the formulation for the tuning of the surface tension to fit the requirements of printing process. Many manufacturers offer a large choice of metallic inks for printing processes and the market is in expansion. A plethora of different methods exist to produce nanoparticles, such as chemical reactions or mechanical attrition. The first method is based on the use of precursors [65] where an organic complex containing metal salt is dissolved in a solvent. For the mechanical attrition, a ball milling [66] is used to nanosize the metal powder. Sizes of nanoparticles can vary from few to hundreds of

nanometers and they can be in different shapes like nanoplates or nanospheres depending on the preparation conditions. Those nanoparticles are usually embedded in organic shell polymers of few nanometers for protection against oxidation and for better dispersion in organic solvents or even water, to fabricate the ink. One of the most common polymers for embedding nanoparticles is the poly(vinyl pyrrolidone) (PVP).

Thermal curing is a key step in the fabrication of metal structures. After printing, the annealing step allows the evaporation of organic compounds and the coalescence of nanoparticles. New types of curing named selective such as microwave curing [67], laser sintering [68], or photonic sintering [69] permit the coalescence of nanoparticles without thermomechanical degradation or damage to plastic substrates. The metal film obtained from printing nanoparticles ink usually exhibits an electrical conductivity of about 10 to 30% of that of the bulk metal, depending on the thermal cycle, the substrate thermal properties and the size and the shape of the nanoparticles [70].

1.2.2 Dielectric inks

Dielectric inks are usually used in printed electronics to fabricate the resistive or the isolating layer in the circuits or as separation layer. They can be UV based inks also composed of nanoparticles (TiO_2, $BaTiO_3$)[71]. UV curable inks comprise monomers, oligomers, photoinitiators and additives. Photoinitiators absorb energy from UV leading to the polymerization of the monomers, for instance acrylic monomers after exposure to UV light (Fig. 1.11).
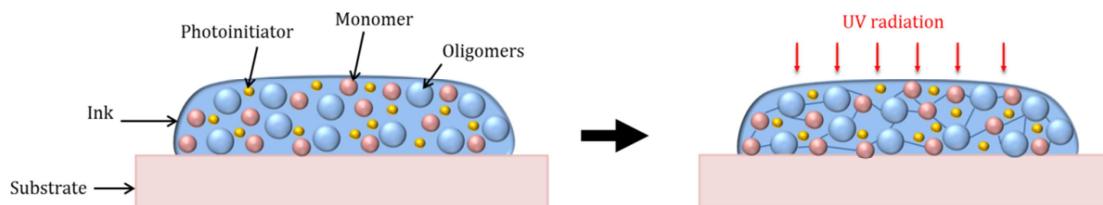
Figure 1.11 **UV polymerization.**

Such UV inks offer advantages such as facile processing without clogging the nozzle. They avoid the evaporation of volatile organic compounds from the ink since polymerization occurs without the need of a drying step. The polymerization step takes few seconds

depending on the power source of the UV and can be easily integrated into a roll-to-roll process.

1.2.3 *Conducting polymer inks*

Over the last few years, many studies have been conducted to develop as well as to better understand physics of organic semiconductors. A growing interest has thus risen in finding new conducting polymers (CP).

Since their discovery in the 1970s by Alan Heeger, Alan MacDiarmid, and Hideki Shirakawa, CPs have been broadly studied due to their electrical conductivity, high mechanical flexibility, and long term stability[72]. In the 70's Polyacetylene was found to be oxidized with chlorine bromine or iodine vapor and reached an electrical conductivity up to 10^5 S/m. This discovery led researchers to the Nobel Prize in Chemistry in 2000. Since that discovery, Polyacetylene has been ruled out because of its instability in air and insolubility in solvents making this highly CP difficult to process in industrial environment . With the emergence of printed electronics, CPs are formulated in new innovative inks. Polyaniline, polypyrroles, polythiophenes and poly(3,4-ethylenedioxythiophene) polystyrene sulfonate (PEDOT:PSS) are especially considered for diverse electronic applications.

CP offer advantages such as low cost, and ease of processing for many applications like the transistors, the organic light emitting diodes and photovoltaics (OLED and OPV) and appear to be good candidates to replace inorganic semiconductors. CP present a distinctive chemical structure, comprised of conjugated double bonds along the backbone that allows the transfer of electrons[73]. They are dispersed in organic solvents, and secondary dopant solvents such as Ethylene Glycol or DMSO can be added to the formulation to boost the electrical conductivity and to fix the viscosity while surfactants such as Triton X-100 can tune the surface tension to match to the substrate surface energy .

Polypyrrole is a dielectric polymer that can be doped by oxidation process to reach a conductivity of 100 S/cm [74]. The chemical structure of this polymer is showed figure 1.12. This polymer is usually electrochemically deposited [75] and has been used for applications

such as capacitors [76] or chemical sensors [77]. Only few studies mention Polypyrrole as an ink for printed electronics applications[78,79].

Polypyrrole

Figure 1.12 **Chemical structure of Polypyrrole**

Polyaniline is a conducting polymer that combines electronic and optical properties. Polyaniline exists in 3 stable oxidation states that exhibit different conductivities and colors. Among them, the emeraldine state presents the highest conductivity in its doped state. Polyaniline has advantages such as stability at room temperature, ease of synthesis and transparency. The chemical structure of Polyaniline is presented in the following figure (figure 1.13)
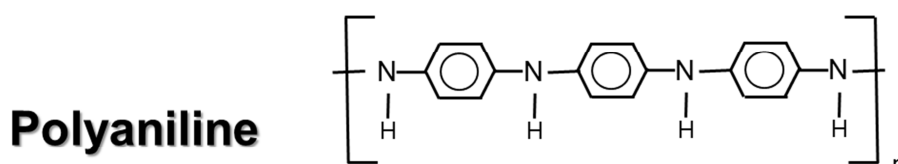
Polyaniline

Figure 1.13 **Chemical structure of Polyaniline**

Companies such as Panipol are developing Polyaniline inks compatible with inkjet and others process. This polymer has been studied for applications such as gas sensing [80], especially for ammonia [58,81], combined with graphene for capacitor electrodes [82] and recently for biomedical applications such as biosensors [83,84]. However, this polymer is not compatible with implantable bio-devices[85].

PEDOT:PSS is one of the most promising conducting polymers and has been broadly studied in the last decades. the chemical structure of PEDOT:PSS is shown in figure 1.14. It can be prepared by oxidative chemical or electrochemical polymerization
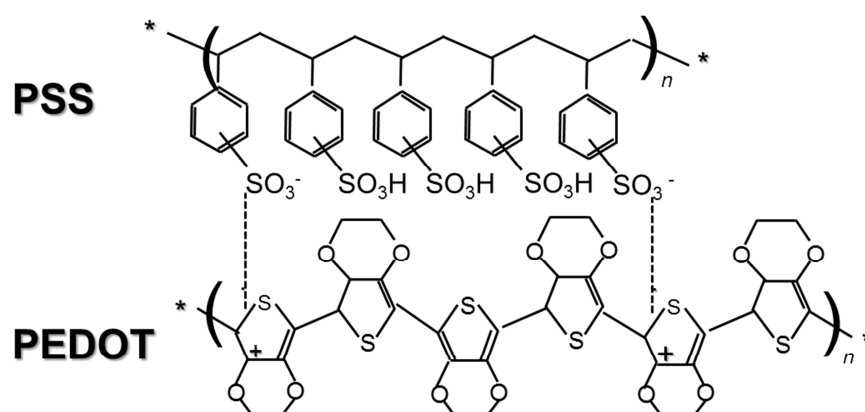
Figure 1.14 **Chemical structure of PEDOT:PSS**

PEDOT in its neutral state is a conducting polymer but remains difficult to process mostly because it is insoluble and rapidly oxidizes in air. In combination with PSS, a water soluble polymer which serves as a charge balancing counterion [86], this complex is stable in solution. In its oxidized state, PEDOT:PSS is a stable polymer and it is one of the most studied polymers currently used for printing transparent electrodes [87] or hole transport layers[16] in applications such as solar cells and Organic Light-Emitting Diode (OLEDs). These results pave the way for substituting ITO (Indium tin oxide) as transparent electrode for organic solar cells or anode for flexible displays. PEDOT:PSS inks are available commercially in water based formulations from few suppliers such as Heraeus and Agfa (Orgacon) that are compatible with printing technologies such as inkjet process or screen printing. PEDOT:PSS thin films present high transparency, good thermal stability and high conductivity which can be further tuned by doping the polymer with solvents [88]. Recently, PEDOT:PSS has been highlighted as a good candidate for biomedical applications due to its higher electronic and ionic properties combined with its biocompatibility[89,90,91].

1.2.4 Comparison of printing techniques

Screen printing is one of the most advanced and robust technique in terms of research and development for printed electronics. It allows depositing highly viscous inks resulting in thicker layers compared to other printing techniques and can fit many electronic applications.

It is a mature technology that has been already used in industry to date. This prerequisite could be achieved by other techniques like gravure printing by optimizing the size of the engraved cells to reach the micron scale. Both flexography and gravure show promising perspective in electronics but limits still exist such as the manufacturing costs for gravure or the presence of the halo for the flexography. A compromise must be found between thickness and resolution. Aerosol jet printing is a recent versatile technique, and also customizable offering an alternative to other processes as it shows flexibility in terms of compatibility with inks (viscosity). However, this technology requires further developments to compete with actual fabrication processes.

Inkjet is also a promising technique especially at the laboratory scale as it allows the digital fabrication of complete devices with low manufacturing costs. Additionally, the geometry can be customized on demand. This technique is easy to use as well as to evaluate new designs and inks. Today, it is still challenging to integrate inkjet into roll-to-roll processes due to maintenance issues related to nozzle clogging and ink stability. The printed resolution is limited by the rheology of the ink, the characteristics of the printhead, and the physicochemical properties of the substrate.

Table 1.1 gives an overview of the printing techniques by comparing their principle characteristics.

	Gravure	Flexography	Screen Printing	Aerosol jet	Inkjet
Printing form	cylinder engraved	Printing plate	Mesh screen	Digital	Digital
Speed (m/min)	8-100	5-180	30-100	1.2	0.02-0.5
Resolution (µm)	20	50	<100	10	20
Viscosity (cP)	10-500	10-100	500-10000	1-2500	5-20
Thickness(µm)	1-8	1	<10	>0.1	0.1 to 15

Table 1.1 **Comparison of printing techniques.**

Finally, printing technologies can be sheet based or roll to roll techniques enabling the use of flexible plastics or papers as substrates and can operate at high speed. Conventional photolithographic patterning process replacement by these promising techniques can be envisaged for the development of specific applications such as OPV, OLED, biosensors and biomedical devices on different substrate like paper, plastic and recently fabric . In particular in the biomedical field, the compatibility of the functional formulations with a wide range of materials and the solution processable conducting polymers offers new perspectives for the fabrication of innovative tools.

In this thesis, inkjet process is chosen as the printing approach to fabricate diagnostics devices for use in electrophysiological applications. PEDOT:PSS was the conducting material selected for the development of an ink fitting the inkjet requirements. In the next section, recent works conducted on the understanding of the electrical enhancement of PEDOT:PSS and the initial studies on PEDOT:PSS inks formulations are presented.

1.3   PEDOT:PSS: Motivation towards enhancing the electrical properties :

1.3.1 Solution processing of PEDOT:PSS

To improve the electrical properties of PEDOT:PSS, several studies were conducted over the last few years by testing different doping techniques. Some of them focused on the structural effect of incorporating "doping" solvents in PEDOT:PSS dispersion and highlighted the role of these solvents in the conformation change in the conducting polymer chain.

In the work proposed by Kim et al, the authors proposed the enhancement of PEDOT:PSS conductivity by mixing organic solvents with the polymer, for instance, DMSO, THF or DMF and studied the effect on charge transport properties of the polymer[88]. They suggested that adding a solvent with high dielectric constant to PEDOT:PSS, induced a strong screening effect between the positively charged PEDOT and the negatively charged counter ion which results in an increase in the conductivity by a factor 10. Other groups also reported

on a reorientation in PEDOT:PSS chain induced by high temperature after the addition of solvents[92]. In that case, Sorbitol and Glycerol were investigated to enhance the conductivity and characterized as plasticizers.

Another assumption presented comes from morphological changes in the pristine PEDOT:PSS after solvent addition (Sorbitol) such as PSS removal during film formation leading to electrical enhancement in the dry conducting film[93]. Indeed, PSS is an insulator and the electrical conductivity of PEDOT:PSS is lowered up to 10 S/cm when the PEDOT/PSS ratio is 1:2.5. The addition of such solvent resulted in a thinner PSS insulating layer and led to a 3D network of highly conducting PEDOT [94].

Ouyang et al presumed that the presence of two or more polar groups in organic solvents enabled the enhancement of electrical conductivity[95]. They tested the addition of Ethylene Glycol to PEDOT:PSS and assumed the electrical changes they observed were caused by the modification in the conformation of the polymer from a coil to linear or expanded structure, leading to a chain transformation from benzoid to quinoid structure (see figure 1.15) which boosted the delocalization of charges and the charge mobility.

Benzoïd structure   Quinoïd structure
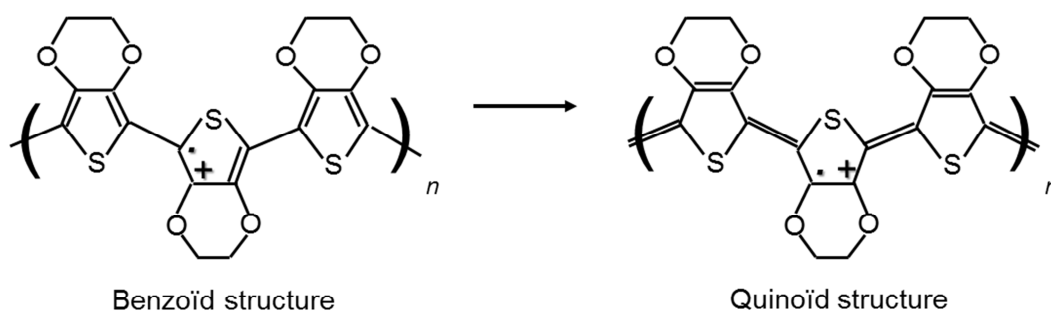
Figure 1.15 **Transformation in the chemical structure of PEDOT PSS from benzoïd to quinoïd**

The origin of conductivity enhancement can be attributed to the interaction between the dipole moments of solvents and PEDOT chains. Particularly, it formed an organic compound and did not play a role in charge screening contrary to Kim et al assumptions which resulted in the creation of hydrogen bonds between organic compounds and PSS[88] . This theory has

also been confirmed recently by Xiong et al [96]. Some polar solvents such as sorbitol or glycerol have been also investigated as additives to PEDOT:PSS solution and the electrical conductivity has been enhanced indeed by several orders of magnitude as explained by Nardes and al [97]. Specifically this is attributed to a self-organization from 3D agglomerates to aligned 1D aggregates thus decreasing distance between PEDOT grains. The length of chains in diols polymers has also been proposed to play a role in conductivity changes. Considering that all these solvents induced conformational changes in the PEDOT:PSS. Fabretto et al also assumed that Diethylene Glycol (DEG) exhibited the highest interchain charge mobility. [98]

1.3.2 Thermal treatment

The influence of thermal treatment on PEDOT:PSS films has also been investigated these last few years [99,100]. Huang and al studied the influence of thermal treatment onto the electrical conductivity of PEDOT:PSS by varying the storage and environmental conditions. They show the effect of thermal treatments when samples are dried in different atmospheric conditions. The optimum conductivity was obtained at 200°C in N2. Xiong studied the influence of temperature on the conductivity during the curing step[101]. They observed a decrease of conductivity of the printed samples above 250°C due to the degradation of the polymer. A maximal conductivity around 82.5 S/cm and 52.4 S/cm was observed after curing at 150°C and 100°C, respectively.

1.3.3 Post treatment of the PEDOT:PSS film

Recent works have studied the effects of post treatments in enhancing the electrical properties of PEDOT:PSS. Kim et al thermally annealed the films and then immersed them in a solution of Ethylene Glycol[102]. This step helped to increase the conductivity up to 1418 S/cm assuming that this increase was coming from the removal of PSS which is the insulating ion.

The addition of inorganic solvents to dried PEDOT:PSS films has as well as led to better conductivity. Xia et al demonstrated that by adding 1M of sulfuric acid in a dried PEDOT:PSS film and then heat it at 160°C several times, the conductivity could reach 3065

S/cm[103]. As proposed by other studies, this increase was due to the removal of PSS and a structural rearrangement of PEDOT in a crystalline 3D nanofibrils network. Finally films treated with 100% H_2SO_4 exhibited conductivity up to 4380 S/cm which remains the best PEDOT:PSS conductivity in literature [104].

1.3.4 PEDOT:PSS and inkjet

Recent studies demonstrated the feasibility to use a commonly-used desktop inkjet setup to print PEDOT:PSS formulations[105,106] or to use specific inkjet printers compatible with electronic inks (Dimatix or sono-microplot) [107] for the fabrication of organic electronic components.

Regarding the ink composition, the major challenges include high electrical conductivity, low viscosity with adequate surface tension, pH neutrality of the solution and stability of the ink in the cartridge and during the printing. As already mentioned, only few suppliers offered PEDOT:PSS water based inks, compatible with inkjet. In all cases the nozzles tend to clog after a while and the formulation cannot be customized. Consequently several groups tested different inks compositions adapted from PEDOT:PSS commercial formulations [104,107,108] and adjusted the viscosity and the surface tension of inks by adding solvents and wetting agents[107,108]. However, problems were encountered when it comes to the stability of PEDOT:PSS such as the choice of solvents. For instance, the addition of Glycerol which presents a poor miscibility with PEDOT:PSS, caused small pits in the printed film observed by Yoshioka et al, who reported the formation of cracks during the solvent evaporation step[104]. Moreover the selection of a wetting agent can also cause micro-features in the film[109].

Resolution of the lines can be controlled by adjusting the substrate surface energy[106]. Another alternative for the patterning was proposed by Ely et al who designed polymer wells using wet photolithography to control PEDOT:PSS deposition[107]. They investigated the effects of surface treatments such as O_2 plasma treatment and (3-Aminopropyl)triethoxysilane APTS deposition onto SU_8 and ITO coated glass. They showed that O_2 plasma improved the uniformity of printed PEDOT:PSS film by adjusting the wetting properties of substrates.

The following table summarizes the different processes used for the deposition of PEDOT:PSS and the corresponding electrical conductivities based on studies by several groups:

Author	Year	Process	Conductivity (S/cm)
Kim[102]	2011	drop cast	80
Yoshioka[105]	2006	Inkjet	24
Srichan[106]	2009	Inkjet	14
Wilson[109]	2012	Spincoat/Inkjet	150
Ummartyotin[108]	2011	Inkjet	15
Xiong[101]	2012	Inkjet	82
Jung[110]	2013	Inkjet	ND

Table 1.2. **Electrical conductivities reported after depositing PEDOT:PSS inks**

During the first year of my PhD, I focused on the development of a conducting ink using a commercially available formulation of PEDOT:PSS (Clevios PH1000) tested for electrophysiological recording applications. Although the exact formulation is not described and discussed in this thesis for confidentiality reason (Patent under preparation), I present in the next chapters, the relevant work I conducted with the new PEDOT:PSS printed ink for the fabrication and characterization of biomedical devices such as ECG and EMG recordings and for further applications related to biosensing applications.

1.4   References

1   Das, R. & Harrop, P. Printed, organic & flexible electronics: forecasts, players & opportunities 2009–2029. *Cambridge: IDTechEx* (2013).

2   Pudas, M., Hagberg, J. & Leppävuori, S. Gravure offset printing of polymer inks for conductors. *Progress in Organic Coatings* **49**, 324-335, doi:http://dx.doi.org/10.1016/j.porgcoat.2003.09.013 (2004).

3   Voigt, M. M. *et al.* Polymer Field-Effect Transistors Fabricated by the Sequential Gravure Printing of Polythiophene, Two Insulator Layers, and a Metal Ink Gate. *Advanced Functional Materials* **20**, 239-246, doi:10.1002/adfm.200901597 (2010).

4   Kopola, P. *et al.* Gravure printed flexible organic photovoltaic modules. *Solar Energy Materials and Solar Cells* **95**, 1344-1347, doi:http://dx.doi.org/10.1016/j.solmat.2010.12.020 (2011).

5   Hübler, A. *et al.* Printed Paper Photovoltaic Cells. *Advanced Energy Materials* **1**, 1018-1022, doi:10.1002/aenm.201100394 (2011).

6   Ding, J. M., de la Fuente Vornbrock, A., Ting, C. & Subramanian, V. Patternable polymer bulk heterojunction photovoltaic cells on plastic by rotogravure printing. *Solar Energy Materials and Solar Cells* **93**, 459-464, doi:http://dx.doi.org/10.1016/j.solmat.2008.12.003 (2009).

7   Yang, J. *et al.* Organic photovoltaic modules fabricated by an industrial gravure printing proofer. *Solar Energy Materials and Solar Cells* **109**, 47-55 (2013).

8   Reddy, A. S. G. *et al.* Gravure Printed Electrochemical Biosensor. *Procedia Engineering* **25**, 956-959, doi:http://dx.doi.org/10.1016/j.proeng.2011.12.235 (2011).

9   Mäkelä, T., Haatainen, T., Majander, P. & Ahopelto, J. Continuous roll to roll nanoimprinting of inherently conducting polyaniline. *Microelectronic Engineering* **84**, 877-879, doi:http://dx.doi.org/10.1016/j.mee.2007.01.131 (2007).

10   Søndergaard, R. R., Hösel, M. & Krebs, F. C. Roll-to-Roll fabrication of large area functional organic materials. *Journal of Polymer Science Part B: Polymer Physics* **51**, 16-34, doi:10.1002/polb.23192 (2013).

11   Hübler, A. C. *et al.* Three-dimensional integrated circuit using printed electronics. *Organic Electronics* **12**, 419-423, doi:http://dx.doi.org/10.1016/j.orgel.2010.12.010 (2011).

12   Krebs, F. C., Fyenbo, J. & Jørgensen, M. Product integration of compact roll-to-roll processed polymer solar cell modules: methods and manufacture using flexographic printing, slot-die coating and rotary screen printing. *Journal of Materials Chemistry* **20**, 8994-9001 (2010).

13   Yu, J.-S. *et al.* Silver front electrode grids for ITO-free all printed polymer solar cells with embedded and raised topographies, prepared by thermal imprint, flexographic and inkjet roll-to-roll processes. *Nanoscale* **4**, 6032-6040 (2012).

14   Kamholz, R. *Andy Warhol and His Process*, <http://www.sothebys.com/en/news-video/blogs/all-blogs/21-days-of-andy-warhol/2013/11/andy-warhol-and-his-process.html> (2013).

15   Shaheen, S. E., Radspinner, R., Peyghambarian, N. & Jabbour, G. E. Fabrication of bulk heterojunction plastic solar cells by screen printing. *Applied physics letters* **79**, 2996-2998, doi:doi:http://dx.doi.org/10.1063/1.1413501 (2001).

16   Krebs, F. C. *et al.* A complete process for production of flexible large area polymer solar cells entirely using screen printing—First public demonstration. *Solar Energy*

Materials and Solar Cells **93**, 422-441, doi:http://dx.doi.org/10.1016/j.solmat.2008.12.001 (2009).

17   Krebs, F. C. All solution roll-to-roll processed polymer solar cells free from indium-tin-oxide and vacuum coating steps. *Organic Electronics* **10**, 761-768, doi:http://dx.doi.org/10.1016/j.orgel.2009.03.009 (2009).

18   Gray, C., Wang, J., Duthaler, G., Ritenour, A. & Drzaic, P. S.   89-94.

19   Pardo, D. A., Jabbour, G. E. & Peyghambarian, N. Application of Screen Printing in the Fabrication of Organic Light-Emitting Devices. *Advanced Materials* **12**, 1249-1252, doi:10.1002/1521-4095(200009)12:17<1249::aid-adma1249>3.0.co;2-y (2000).

20   Jabbour, G. E., Radspinner, R. & Peyghambarian, N. Screen printing for the fabrication of organic light-emitting devices. *Selected Topics in Quantum Electronics, IEEE Journal of* **7**, 769-773 (2001).

21   Lee, D.-H., Choi, J., Chae, H., Chung, C.-H. & Cho, S. Single-layer organic-light-emitting devices fabricated by screen printing method. *Korean J. Chem. Eng.* **25**, 176-180, doi:10.1007/s11814-008-0032-3 (2008).

22   Tudorache, M. & Bala, C. Biosensors based on screen-printing technology, and their applications in environmental and food analysis. *Anal Bioanal Chem* **388**, 565-578, doi:10.1007/s00216-007-1293-0 (2007).

23   O'Halloran, M. P., Pravda, M. & Guilbault, G. G. Prussian Blue bulk modified screen-printed electrodes for H 2 O 2 detection and for biosensors. *Talanta* **55**, 605-611 (2001).

24   Albareda-Sirvent, M., Merkoçi, A. & Alegret, S. Configurations used in the design of screen-printed enzymatic biosensors. A review. *Sensors and Actuators B: Chemical* **69**, 153-163, doi:http://dx.doi.org/10.1016/S0925-4005(00)00536-0 (2000).

25   Hill, H. A. O., Higgins, I. J., McCann, J. M. & Davis, G.   (Google Patents, 1998).

26   Hill, H. A. O., Higgins, I. J., McCann, J. M. & Davis, G.   (Google Patents, 1996).

27   Su, C. S., Chang, C. W., Hung, M. L., Cheng, W. J. & Wu, T. G.   (Google Patents, 2006).

28   Krebs, F. C. Fabrication and processing of polymer solar cells: a review of printing and coating techniques. *Solar Energy Materials and Solar Cells* **93**, 394-412 (2009).

29   Kopola, P. *et al.* Aerosol jet printed grid for ITO-free inverted organic solar cells. *Solar Energy Materials and Solar Cells* **107**, 252-258, doi:http://dx.doi.org/10.1016/j.solmat.2012.06.042 (2012).

30   Girotto, C., Rand, B. P., Genoe, J. & Heremans, P. Exploring spray coating as a deposition technique for the fabrication of solution-processed solar cells. *Solar Energy Materials and Solar Cells* **93**, 454-458 (2009).

31   Cho, J. H. *et al.* Printable ion-gel gate dielectrics for low-voltage polymer thin-film transistors on plastic. *Nature materials* **7**, 900-906 (2008).

32   Ingo, G. *et al.* Surface biofunctionalization and production of miniaturized sensor structures using aerosol printing technologies. *Biofabrication* **2**, 014106 (2010).

33   Strutt, J. W. & Rayleigh, L. On the instability of jets. *Proc. London Math. Soc* **10**, 4-13 (1878).

34   Rune, E.   (Google Patents, 1951).

35   Sweet, R. G. High frequency recording with electrostatically deflected ink jets. *Review of Scientific Instruments* **36**, 131-136 (1965).

36   Zoltan, S. I.   (Google Patents, 1972).

37   Kyser, E. L. & Sears, S. B.   (Google Patents, 1976).

38   Donald, D. K., Lee, M. J. & Vaught, J. L.   (Google Patents, 1982).

39   Endo, I., Sato, Y., Saito, S., Nakagiri, T. & Ohno, S.   (Google Patents, 1988).

40   Setti, L. *et al.* Thermal inkjet technology for the microdeposition of biological molecules as a viable route for the realization of biosensors. *Analytical letters* **37**, 1559-1570 (2004).

41   Setti, L. *et al.* An HRP-based amperometric biosensor fabricated by thermal inkjet printing. *Sensors and Actuators B: Chemical* **126**, 252-257, doi:http://dx.doi.org/10.1016/j.snb.2006.12.015 (2007).

42   Setti, L. *et al.* An amperometric glucose biosensor prototype fabricated by thermal inkjet printing. *Biosensors and Bioelectronics* **20**, 2019-2026, doi:http://dx.doi.org/10.1016/j.bios.2004.09.022 (2005).

43   Arias, A. *et al.* All jet-printed polymer thin-film transistor active-matrix backplanes. *Applied physics letters* **85**, 3304-3306 (2004).

44   Sirringhaus, H., Kawase, T. & Friend, R. H. High-Resolution Ink-Jet Printing of All-Polymer Transistor Circuits. *MRS Bulletin* **26**, 539-543 (2001).

45   Hebner, T. R., Wu, C. C., Marcy, D., Lu, M. H. & Sturm, J. C. Ink-jet printing of doped polymers for organic light emitting devices. *Applied physics letters* **72**, 519-521, doi:doi:http://dx.doi.org/10.1063/1.120807 (1998).

46   Shimoda, T., Morii, K., Seki, S. & Kiguchi, H. Inkjet printing of light-emitting polymer displays. *MRS Bulletin* **28**, 821-827 (2003).

47   Aernouts, T., Aleksandrov, T., Girotto, C., Genoe, J. & Poortmans, J. Polymer based organic solar cells using ink-jet printed active layers. *Applied physics letters* **92**, 033306, doi:doi:http://dx.doi.org/10.1063/1.2833185 (2008).

48   Eom, S. H. *et al.* Polymer solar cells based on inkjet-printed PEDOT:PSS layer. *Organic Electronics* **10**, 536-542, doi:http://dx.doi.org/10.1016/j.orgel.2009.01.015 (2009).

49   Hoth, C. N., Choulis, S. A., Schilinsky, P. & Brabec, C. J. High Photovoltaic Performance of Inkjet Printed Polymer:Fullerene Blends. *Advanced Materials* **19**, 3973-3978, doi:10.1002/adma.200700911 (2007).

50   Abe, K., Suzuki, K. & Citterio, D. Inkjet-printed microfluidic multianalyte chemical sensing paper. *Analytical chemistry* **80**, 6928-6934 (2008).

51   Sirringhaus, H. *et al.* High-Resolution Inkjet Printing of All-Polymer Transistor Circuits. *Science* **290**, 2123-2126, doi:10.1126/science.290.5499.2123 (2000).

52   Kawase, T., Shimoda, T., Newsome, C., Sirringhaus, H. & Friend, R. H. Inkjet printing of polymer thin film transistors. *Thin Solid Films* **438–439**, 279-287, doi:http://dx.doi.org/10.1016/S0040-6090(03)00801-0 (2003).

53   Wang, J. Z., Zheng, Z. H., Li, H. W., Huck, W. T. S. & Sirringhaus, H. Dewetting of conducting polymer inkjet droplets on patterned surfaces. *Nat Mater* **3**, 171-176 (2004).

54   Bharathan, J. & Yang, Y. Polymer electroluminescent devices processed by inkjet printing: I. Polymer light-emitting logo. *Applied physics letters* **72**, 2660-2662, doi:doi:http://dx.doi.org/10.1063/1.121090 (1998).

55   Steirer, K. X. *et al.* Ultrasonically sprayed and inkjet printed thin film electrodes for organic solar cells. *Thin Solid Films* **517**, 2781-2786, doi:http://dx.doi.org/10.1016/j.tsf.2008.10.124 (2009).

56   Hoth, C. N., Schilinsky, P., Choulis, S. A. & Brabec, C. J. Printing highly efficient organic solar cells. *Nano letters* **8**, 2806-2813 (2008).

57   Jang, J., Ha, J. & Cho, J. Fabrication of Water-Dispersible Polyaniline-Poly(4-styrenesulfonate) Nanoparticles For Inkjet-Printed Chemical-Sensor Applications. *Advanced Materials* **19**, 1772-1775, doi:10.1002/adma.200602127 (2007).

58   Crowley, K. *et al.* Fabrication of an ammonia gas sensor using inkjet-printed polyaniline nanoparticles. *Talanta* **77**, 710-717, doi:http://dx.doi.org/10.1016/j.talanta.2008.07.022 (2008).

59   Fromm, J. E. Numerical calculation of the fluid dynamics of drop-on-demand jets. *IBM Journal of Research and Development* **28**, 322-333 (1984).

60   Reis, N. & Derby, B. Ink Jet Deposition of Ceramic Suspensions: Modeling and Experiments of Droplet Formation. *MRS Online Proceedings Library* **625**, null-null, doi:doi:10.1557/PROC-625-117 (2000).

61   Derby, B. Inkjet printing of functional and structural materials: fluid property requirements, feature stability, and resolution. *Annual Review of Materials Research* **40**, 395-414 (2010).

62   Denneulin, A., Bras, J., Carcone, F., Neuman, C. & Blayo, A. Impact of ink formulation on carbon nanotube network organization within inkjet printed conductive films. *Carbon* **49**, 2603-2614 (2011).

63   Angelo, P. D. & Farnood, R. R. Poly (3, 4-ethylenedioxythiophene): poly (styrene sulfonate) inkjet inks doped with carbon nanotubes and a polar solvent: the effect of formulation and adhesion on conductivity. *Journal of Adhesion Science and Technology* **24**, 643-659 (2010).

64   Aleeva, Y. & Pignataro, B. Recent advances in upscalable wet methods and ink formulations for printed electronics. *Journal of Materials Chemistry C* **2**, 6436-6453 (2014).

65   Grouchko, M. & Magdassi, S.   (Google Patents, 2013).

66   Park, B. K., Kim, D., Jeong, S., Moon, J. & Kim, J. S. Direct writing of copper conductive patterns by ink-jet printing. *Thin Solid Films* **515**, 7706-7711, doi:http://dx.doi.org/10.1016/j.tsf.2006.11.142 (2007).

67   Perelaer, J., de Gans, B.-J. & Schubert, U. S. Ink-jet printing and microwave sintering of conductive silver tracks. *ADVANCED MATERIALS-DEERFIELD BEACH THEN WEINHEIM-* **18**, 2101 (2006).

68   Seung, H. K. *et al.* All-inkjet-printed flexible electronics fabrication on a polymer substrate by low-temperature high-resolution selective laser sintering of metal nanoparticles. *Nanotechnology* **18**, 345202 (2007).

69   Kim, H.-S., Dhage, S. R., Shim, D.-E. & Hahn, H. T. Intense pulsed light sintering of copper nanoink for printed electronics. *Applied Physics A* **97**, 791-798 (2009).

70   Dick, K., Dhanasekaran, T., Zhang, Z. & Meisel, D. Size-dependent melting of silica-encapsulated gold nanoparticles. *Journal of the American Chemical Society* **124**, 2312-2317 (2002).

71   Go, E. C. *Effects of oligomer-to-monomer ratio on ink film properties of white UV-curable gravure ink for printing on biaxially oriented polypropylene (BOPP).* (Rochester Institute of Technology, 2009).

72   Shirakawa, H., Louis, E. J., MacDiarmid, A. G., Chiang, C. K. & Heeger, A. J. Synthesis of electrically conducting organic polymers: halogen derivatives of polyacetylene,(CH) x. *J. Chem. Soc., Chem. Commun.*, 578-580 (1977).

73   McCullough, R. D., Lowe, R. D., Jayaraman, M. & Anderson, D. L. Design, synthesis, and control of conducting polymer architectures: structurally homogeneous poly (3-alkylthiophenes). *The Journal of Organic Chemistry* **58**, 904-912 (1993).

74   Beck, F. & Oberst, M. Electrocatalytic deposition of polypyrrole in the presence of bromide. *Journal of applied electrochemistry* **22**, 332-340 (1992).

75   Li, C., Sun, C., Chen, W. & Pan, L. Electrochemical thin film deposition of polypyrrole on different substrates. *Surface and Coatings Technology* **198**, 474-477 (2005).

76   Muthulakshmi, B., Kalpana, D., Pitchumani, S. & Renganathan, N. Electrochemical deposition of polypyrrole for symmetric supercapacitors. *Journal of Power Sources* **158**, 1533-1537 (2006).

77   Ramanavičius, A., Ramanavičienė, A. & Malinauskas, A. Electrochemical sensors based on conducting polymer—polypyrrole. *Electrochimica Acta* **51**, 6025-6037, doi:http://dx.doi.org/10.1016/j.electacta.2005.11.052 (2006).

78   Mabrook, M. F., Pearson, C. & Petty, M. C. Inkjet-printed polypyrrole thin films for vapour sensing. *Sensors and Actuators B: Chemical* **115**, 547-551, doi:http://dx.doi.org/10.1016/j.snb.2005.10.019 (2006).

79   Gangopadhyay, R. & Molla, M. R. Polypyrrole–polyvinyl alcohol stable nanodispersion: a prospective conducting black ink. *Journal of Polymer Science Part B: Polymer Physics* **49**, 792-800 (2011).

80   Loffredo, F., Burrasca, G., Quercia, L. & Sala, D. D. in *Macromolecular Symposia.* 357-363 (Wiley Online Library) (2007).

81   Hibbard, T., Crowley, K. & Killard, A. J. Direct measurement of ammonia in simulated human breath using an inkjet-printed polyaniline nanoparticle sensor. *Analytica Chimica Acta* **779**, 56-63 (2013).

82   Xu, Y. *et al.* Screen-Printable Thin Film Supercapacitor Device Utilizing Graphene/Polyaniline Inks. *Advanced Energy Materials* **3**, 1035-1040, doi:10.1002/aenm.201300184 (2013).

83   Morrin, A. *et al.* Novel biosensor fabrication methodology based on processable conducting polyaniline nanoparticles. *Electrochemistry Communications* **7**, 317-322 (2005).

84   Dionisi, A., Borghetti, M., Sardini, E. & Serpelloni, M. in *Instrumentation and Measurement Technology Conference (I2MTC) Proceedings, 2014 IEEE International.* 1629-1633 (IEEE).

85   Huang, L. *et al.* Synthesis of biodegradable and electroactive multiblock polylactide and aniline pentamer copolymer for tissue engineering applications. *Biomacromolecules* **9**, 850-858 (2008).

86   Skotheim, T. A. & Reynolds, J. *Conjugated Polymers: Theory, Synthesis, Properties, and Characterization.* (Taylor & Francis, 2006).

87   Cho, C.-K. *et al.* Mechanical flexibility of transparent PEDOT:PSS electrodes prepared by gravure printing for flexible organic solar cells. *Solar Energy Materials and Solar Cells* **95**, 3269-3275, doi:http://dx.doi.org/10.1016/j.solmat.2011.07.009 (2011).

88   Kim, J. Y., Jung, J. H., Lee, D. E. & Joo, J. Enhancement of electrical conductivity of poly(3,4-ethylenedioxythiophene)/poly(4-styrenesulfonate) by a change of solvents. *Synthetic Metals* **126**, 311-316, doi:http://dx.doi.org/10.1016/S0379-6779(01)00576-8 (2002).

89   Leleux, P. *et al.* Conducting Polymer Electrodes for Electroencephalography. *Advanced healthcare materials* **3**, 490-493, doi:10.1002/adhm.201300311 (2014).

90   Khodagholy, D. *et al.* In vivo recordings of brain activity using organic transistors. *Nat Commun* **4**, 1575,

doi:http://www.nature.com/ncomms/journal/v4/n3/suppinfo/ncomms2573_S1.html (2013).

91   Berggren, M. & Richter-Dahlfors, A. Organic Bioelectronics. *Advanced Materials* **19**, 3201-3213, doi:10.1002/adma.200700419 (2007).

92   GHOSH *et al. Nano-structured conducting polymer network based on PEDOT-PSS*. (Elsevier, 2001).

93   Jönsson, S. K. M. *et al.* The effects of solvents on the morphology and sheet resistance in poly(3,4-ethylenedioxythiophene)–polystyrenesulfonic acid (PEDOT–PSS) films. *Synthetic Metals* **139**, 1-10, doi:http://dx.doi.org/10.1016/S0379-6779(02)01259-6 (2003).

94   Crispin, X. *et al.* Conductivity, morphology, interfacial chemistry, and stability of poly(3,4-ethylene dioxythiophene)–poly(styrene sulfonate): A photoelectron spectroscopy study. *Journal of Polymer Science Part B: Polymer Physics* **41**, 2561-2583, doi:10.1002/polb.10659 (2003).

95   Ouyang, J. *et al.* On the mechanism of conductivity enhancement in poly(3,4-ethylenedioxythiophene):poly(styrene sulfonate) film through solvent treatment. *Polymer* **45**, 8443-8450, doi:http://dx.doi.org/10.1016/j.polymer.2004.10.001 (2004).

96   Xiong, S., Zhang, L. & Lu, X. Conductivities enhancement of poly(3,4-ethylenedioxythiophene)/poly(styrene sulfonate) transparent electrodes with diol additives. *Polym. Bull.* **70**, 237-247, doi:10.1007/s00289-012-0833-8 (2013).

97   Nardes, A. M., Janssen, R. A. J. & Kemerink, M. A Morphological Model for the Solvent-Enhanced Conductivity of PEDOT:PSS Thin Films. *Advanced Functional Materials* **18**, 865-871, doi:10.1002/adfm.200700796 (2008).

98   Fabretto, M. *et al.* The mechanism of conductivity enhancement in poly(3,4-ethylenedioxythiophene)–poly(styrenesulfonic) acid using linear-diol additives: Its effect on electrochromic performance. *Thin Solid Films* **516**, 7828-7835, doi:http://dx.doi.org/10.1016/j.tsf.2008.04.099 (2008).

99   Vitoratos, E. *et al.* Thermal degradation mechanisms of PEDOT: PSS. *Organic Electronics* **10**, 61-66 (2009).

100   Huang, J., Miller, P. F., de Mello, J. C., de Mello, A. J. & Bradley, D. D. C. Influence of thermal treatment on the conductivity and morphology of PEDOT/PSS films. *Synthetic Metals* **139**, 569-572, doi:http://dx.doi.org/10.1016/S0379-6779(03)00280-7 (2003).

101   Xiong, Z. & Liu, C. Optimization of inkjet printed PEDOT:PSS thin films through annealing processes. *Organic Electronics* **13**, 1532-1540, doi:http://dx.doi.org/10.1016/j.orgel.2012.05.005 (2012).

102   Kim, Y. H. *et al.* Highly Conductive PEDOT:PSS Electrode with Optimized Solvent and Thermal Post-Treatment for ITO-Free Organic Solar Cells. *Advanced Functional Materials* **21**, 1076-1081, doi:10.1002/adfm.201002290 (2011).

103   Xia, Y., Sun, K. & Ouyang, J. Solution-Processed Metallic Conducting Polymer Films as Transparent Electrode of Optoelectronic Devices. *Advanced Materials* **24**, 2436-2440, doi:10.1002/adma.201104795 (2012).

104   Kim, N. *et al.* Highly Conductive PEDOT:PSS Nanofibrils Induced by Solution-Processed Crystallization. *Advanced Materials* **26**, 2268-2272, doi:10.1002/adma.201304611 (2014).

105   Yoshioka, Y. & Jabbour, G. E. Desktop inkjet printer as a tool to print conducting polymers. *Synthetic Metals* **156**, 779-783, doi:http://dx.doi.org/10.1016/j.synthmet.2006.03.013 (2006).

106 Srichan, C. *et al.* in *Electrical Engineering/Electronics, Computer, Telecommunications and Information Technology, 2009. ECTI-CON 2009. 6th International Conference on.* 465-468.

107 Ely, F. *et al.* Patterning quality control of inkjet printed PEDOT:PSS films by wetting properties. *Synthetic Metals* **161**, 2129-2134, doi:http://dx.doi.org/10.1016/j.synthmet.2011.08.014 (2011).

108 Ummartyotin, S., Juntaro, J., Wu, C., Sain, M. & Manuspiya, H. Deposition of PEDOT: PSS Nanoparticles as a Conductive Microlayer Anode in OLEDs Device by Desktop Inkjet Printer. *Journal of Nanomaterials* **2011**, 7, doi:10.1155/2011/606714 (2011).

109 Wilson, P., Lekakou, C. & Watts, J. F. A comparative assessment of surface microstructure and electrical conductivity dependence on co-solvent addition in spin coated and inkjet printed poly(3,4-ethylenedioxythiophene):polystyrene sulphonate (PEDOT:PSS). *Organic Electronics* **13**, 409-418, doi:http://dx.doi.org/10.1016/j.orgel.2011.11.011 (2012).

110 Jung, S., Sou, A., Gili, E. & Sirringhaus, H. Inkjet-printed resistors with a wide resistance range for printed read-only memory applications. *Organic Electronics* **14**, 699-702, doi:http://dx.doi.org/10.1016/j.orgel.2012.12.034 (2013).

Chapter 2

Introduction to biomedical electrodes for electrophysiological recordings

The discovery of conducting polymers led to the rise of organic bioelectronics enabling the development of new diagnosis tools such as new cutaneous devices for electrophysiology, paving the way to technological progress in the arena of disease detection and treatment.

In this chapter, I will introduce the principles of electrophysiological recordings especially ECG and EMG which were the signals studied with the printed tools developed in this PhD. I introduce basic notions of biopotentials electrodes used in electrophysiology. I will give a brief overview of the different types of electrodes used for medical and research applications with a loop on the innovations regarding the fabrication of electrodes in research for health monitoring.

2.1 Electrophysiology

Electrophysiology is the study that covers the electrical mechanism and activity of living tissues and cells. The signal is generated through the local activity of ions in the cell membrane or in a bigger scale from organs such as the heart. In neuroscience, it concerns the recording of electrical activity of neurons generated by action potentials. For neuroscientists, the study of these recordings enables the establishment of diagnostics tools.

In the next paragraph, I will give a brief overview of the two electrical activities recorded by the biomedical devices fabricated during my thesis, ElectroCardioGram (ECG) and ElectroMyoGram (EMG).

2.1.1 Electrocardiogram

- Principle

ECG is the graphic representation of the electrical activity of the heart muscle. It comes from the contraction of the cardiac muscle in response to the electrical depolarization of the cardiac cells. The cardiac cells called pacemakers are specific cells which generate automatic action potentials and propagated them to other cardiac cells.

The first ECG acquisition system has been developed by Einthoven[30] in the beginning of the 20th century with the invention of the string galvanometer. Nowadays and to observe the cardiac activity, conventionally, an ECG with 12-lead recording is used. In that configuration, 10 electrodes are placed in specified areas on the patient's body. To interpret signals acquired from the ECG, according to the placement in the body, spatial information is revealed about the heart activity.

The ECG signal is in the millivolt range and the frequency range of interest varies from 0.1 to 100 Hz. Distinct entities can be distinguished in atypical ECG : a P wave, a QRS complex and a T and U waves. They represent atrial depolarization, ventricular depolarization, ventricular repolarization, and papillary muscle repolarization, respectively. A representation of a classic ECG signal is shown figure 2.1.

.
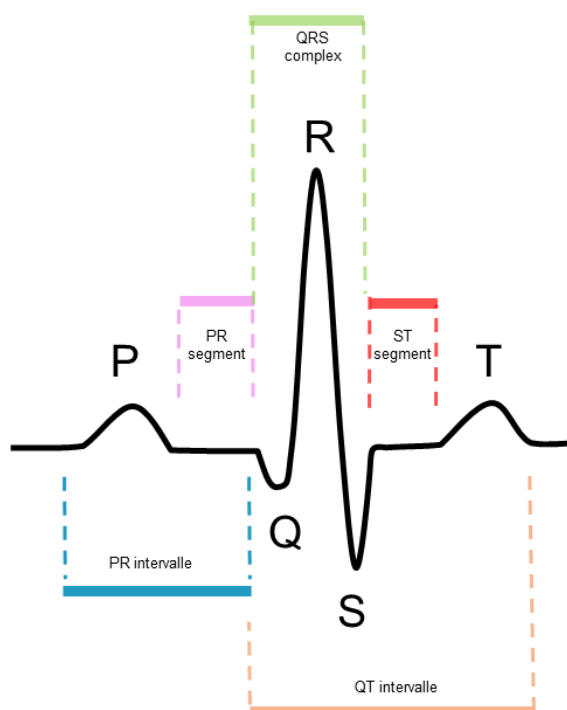
Figure 2.1.**Schematic of a normal ECG**

Many cardiovascular diseases can be detected by the analysis and interpretation of the ECG signal such as arrhythmia, tachycardia, bradycardia, pericarditis, myocardial infections and others.

2.1.2 Electromyogram

- **Principle**

EMG is a technique which consists in the recording, the analysis and the interpretation of the myoelectric signals which can be voluntary or unvoluntary. Luigi Galvani, in the 18th century, revolutionized the field of bioelectronics with his famous discovery of generating muscle contractions under an electrical current.

EMG signals originate from the neuromuscular activation of muscles under stimulation of muscle membranes. Action potentials generated at the muscle fiber membrane result from the depolarization and repolarization of motor neuron. The Motor units (MUs) are the

functional units which implement muscular contraction[31]. They can comprise of 3-2000 muscle fibers. Summation of these action potentials of Motor Units is called Motor Unit Action Potential (MUAP). EMG spikes can be detected by electrodes and the voltage vary from few µV to few mV[32]. The frequency range of interest varies from 10 to 1000 Hz. An example of EMG is shown in figure 2.2 after recording the biosignal from a biceps after long and short contractions.
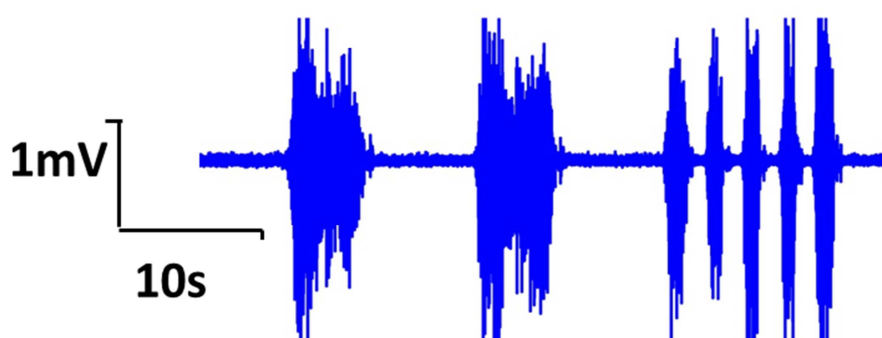
Figure 2.2 **Representation of a normal EMG recorded by Ag/AgCl electrodes after 2 long contractions (5s) and 5 short contractions (1s) of the biceps**

EMG is a tool used in clinical, kinesiological and research applications. This method permits to localize and identify the damages in muscle tissue, nerves, detect paralysis, to verify the treatment efficiency.

2.2   Biopotential electrodes

The detection and analysis of electrical activity of the different organs is a key factor for early diagnostics. To evaluate the organs activities (heart, brain, muscles, or eyes) biological signals acquisition is usually made through the measurement of electronic potentials on the surface of living tissue. The detection of ionic current flow in the body is usually accomplished using biopotential electrodes.[1] Generally a pair of electrodes is placed on the surface of the tissue and acts as a transducer to convert ionic potentials

generated through the body to electronic potentials recorded by the electronic system[2]. The potentials measured, are analyzed and amplified by an electronic system.

Ionic current is generated in the body when excitable cells are stimulated. This phenomenon provokes membrane potential to vary. The cell membrane is permeable to the passage of specific ions, Na^+ and K^+ Cl^- ions, involved in this mechanism. When a cell is stimulated, the concentrations of these ions are modified. Then the specific ions are pumped through the membrane modifying the cell membrane potential. This membrane potential comes from the difference between electrical potential from outside and inside of the cell. These ions concentration gradients generate specific electric potential, the half-cell potential which can be calculated, based on Nernst equation potential.

$$E = -\frac{RT}{nF} \ln(\frac{a_1}{a_2}) \quad (1)$$

Where a_1 and a_2 are the activities of the ions from both side of the membrane, R is the universal gas constant (J/mol/K), F the faraday constant (C/mol), n the valence of ions, T the absolute temperature (K)

The stimulation of the cells provokes action potentials responsible for the contraction of muscle cells such as cardiac cells. Then the electrodes allow the measurement of the ionic flow on the surface of the skin coming from these contractions. Depending on their configuration, electrodes can be either polarizable (no charge can pass through the electrode/electrolyte interface and they are usually modeled as a capacitor (i.e. Platinum electrode) or non-polarizable (the current can cross freely among the electrode/electrolyte interface with no overpotential, they can be modeled as a resistor (such as Ag/AgCl electrodes that are close to non-polarizable electrodes). Biopotential electrodes can be thus used either for recording or for stimulation depending on the desired application.

Common problem regarding the signal quality is the interferences generated by the acquisition system. For instance, computers or cellular phones are sources of noise. The dominant frequency for the ambient noise is 50 Hz (A/C power supply). Additionally, stretching of the skin, muscle movements are also source of noise which can affect the

signal. Skin impedance variations can induce fluctuations in the signal. To minimize such effects, standard skin preparation protocols such as cleaning and hair removal can improve the signal quality by a factor of 10^3.

Electrodes allow the detection of critical electrophysiological signals such as electrocardiogram (ECG), electromyogram (EMG), or electroencephalogram (EEG). Electrodes can be either invasive (implanted) or noninvasive (cutaneous) depending on the activity of the target organ analyzed. For instance to record neural activity, usually micro-electrode arrays are fabricated using photolithography technology[4]. Besides, OECTs based on conducting polymers have emerged as well as exhibit promising future for the recording of brain activity and the detection of neural diseases such as epilepsy. During my PhD, I focused on the development of noninvasive printed electrodes for ECG and EMG cutaneous recordings.

2.2.1 Categories of electrodes

The cutaneous electrodes can be distinguished in 2 categories: the gelled and the dry electrodes. The dry electrodes are designed to operate without electrolyte since the electrolyte is provided by the sweat generated by the skin at the interface between the conducting material and the skin. The dry electrodes present advantages for long term use and show more patient compliance than gelled electrodes. However one of their main drawbacks is their generally higher skin-electrode impedance. The gelled electrodes comprise a piece of conducting material and a layer of ionic liquid gel. They exhibit good signal quality, low skin-electrode impedance and a good adhesion to skin. A classic example of gelled electrode is the Ag/AgCl electrode.

The electrical model of the electrode-skin interface is presented figure 2.3 based on the model proposed by Meziane et al[6].
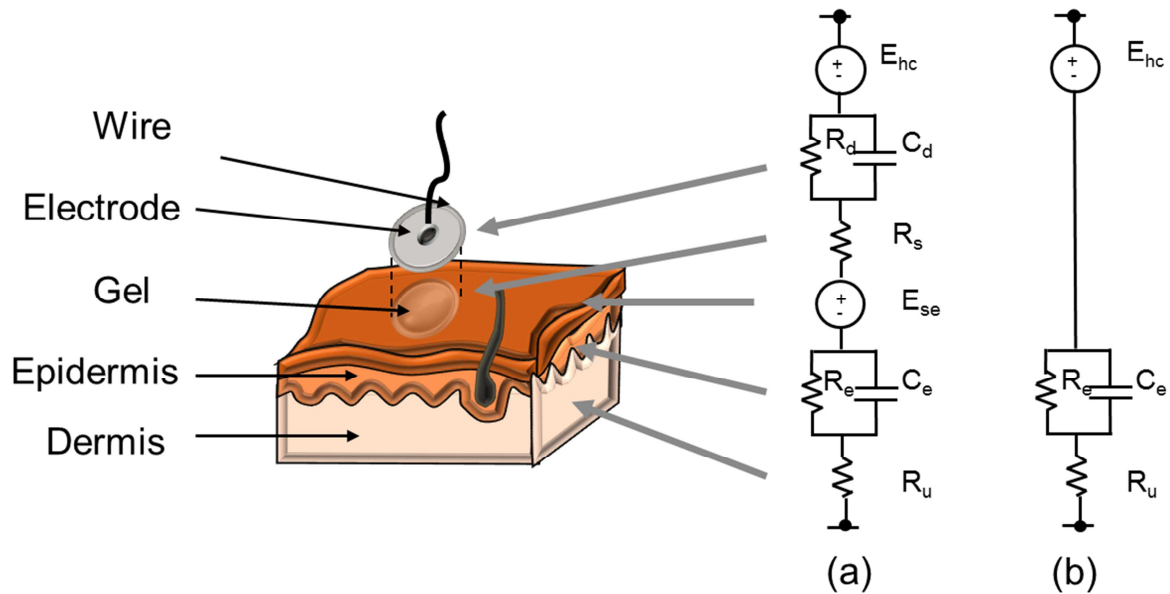
Figure 2.3 **Schematic and electrical model of biomedical (a) wet electrode, (b) dry electrode**

Where E_{hc} is the half-cell potential of the contact between the electrode and the skin/gel (V), C_d and R_d are the capacitance (F) and the resistance (Ω) associated to the epidermal layer respectively, R_s is the resistance (Ω) associated with the interface effects from the gel between electrode and skin , E_{se} is the half-cell potential created by the semipermabilility of the stratum corneum (V), C_e and R_e are the capacitance (F) and resistance (Ω) of epidermis respectively, R_u is the resistance of dermis (Ω).

A brief overview of the electrodes used in this thesis is proposed in the next paragraph

- **Ag/AgCl electrodes**

    Ag/AgCl electrodes are electrodes commonly used in electrochemical measurements as well as in clinical and medical applications. They consist of a metallic conductor (silver) and an electrolyte gel containing chloride ions which allows the free move of ions. The ionic charges are carried through the electrolyte, then converted in electrical current and then read by the electronic system. They can be modeled as non polarizable electrodes since they present a low half-cell potential[7] (220mV) which renders them interesting for biomedical applications. An adhesive is typically used to ensure good contact between electrodes and the skin. These electrodes record good signal quality but have proven to be

inconvenient for patients since they cause irritation or allergies after long term measurements. Also the drying of the gel, can result in loss of the signal during motion[8].

- **Wearable electrodes**

Smart clothes are attracting a great deal of interest in healthcare industry. Indeed there is a great ongoing demand for the development of innovative fabric electrodes for electrophysiological applications which could exhibit the same performance than the state of the art Ag/AgCl electrodes for long-term use. Integration of electrical system into clothes would be more comfortable solution for daily use. The smart textiles are either fabricated by direct integration of conducting yarns[9–11] into a standard fabric or by the deposition of materials using different additive techniques such as coating[12,13], dip coating[14], as well as a technique inspired by the Japanese kimono dyeing method[15] or with printing technologies such as screen printing[16,17] or inkjet printing[18–20]. The materials investigated are either metals and carbon nanoparticles[21] or conducting polymers. In particular, PEDOT:PSS has shown promising characterisitics as it is biocompatible and easy to process and thus has been widely used for the development of intelligent textiles to create new biopotential electrodes.

To improve the contact between the electrode and the skin interface, groups recently explored the possibility to depose biocompatible gels on top of the dry conducting material [22,23]and reduce the effects of motion artifacts during the signal acquisition.

- **E-skin electrodes**

A new generation of electrodes mimicking temporary tattoos is currently raising a lot of interest following the work led by John Rogers group, pioneer for the development of ultrathin and conformable skin-like platforms [24–26] combining multiple applications such as biosensing and monitoring of neural activities. The ultra-conformability of the tattoo improved the contact between the electronics and the skin rendering nonessential the use of conductive gel. Studies are currently conducted focusing on the integration of conducting polymers in the circuits to pattern the active material. PEDOT:PSS or carbon are

investigated using technologies such as screen printing[27] or subtractive inkjet[28] or coating[29].

There is a growing demand for the development of new diagnostics tools for the detection and the analysis of electrophysiological signals and many studies propose alternatives to the Ag/AgCl electrodes. In the next chapters, I present the work conducted on the cutaneous electrodes I fabricated using inkjet technique. The electrodes showed in figure 2.4 are electrodes printed using a PEDOT:PSS ink formulated during the first year of my PhD, They are conceived on low cost and disposable substrates (i.e. paper and tattoos) and as well as wearable and stretchable substrates (textiles) paving the way for easy recording methods of ECG and EMG.
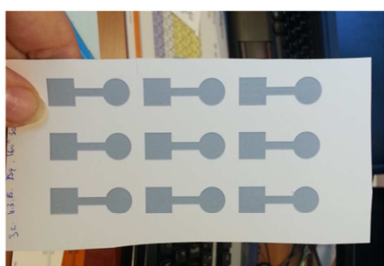
(a)   (b)

(c)   (d)

Figure 2.4 **Photographs of electrodes printed on (a) paper, textile i.e. (b) ribbon, (c) tight and (d) tattoo paper**

2.3   References

1.   Chapter 48 - Biopotential Electrodes - apnt_134_5.pdf. Available at: http://www.fis.uc.pt/data/20062007/apontamentos/apnt_134_5.pdf. (Accessed: 22nd October 2016)

2.   notes2.pdf. Available at: https://www.robots.ox.ac.uk/~neil/teaching/lectures/med_elec/notes2.pdf. (Accessed: 22nd October 2016)

3.   Merletti, R. & Migliorini, M. Surface EMG electrode noise and contact impedance. in (1998).

4.   Kipke, D. R. *et al.* Advanced Neurotechnologies for Chronic Neural Interfaces: New Horizons and Clinical Opportunities. *J. Neurosci.* **28,** 11830–11838 (2008).

5.   Khodagholy, D. *et al.* In vivo recordings of brain activity using organic transistors. *Nat Commun* **4,** 1575 (2013).

6.   N Meziane and J G Webster and M Attari and A J Nimunkar. Dry electrodes for electrocardiography. *Physiol. Meas.* **34,** R47 (2013).

7.   Analog Devices : Biopotential Electrode Sensors in ECG/EEG/EMG Systems - ECG-EEG-EMG_FINAL.pdf. Available at: http://www.analog.com/media/en/technical-documentation/white-papers/ECG-EEG-EMG_FINAL.pdf. (Accessed: 22nd October 2016)

8.   Searle, A. & Kirkup, L. A direct comparison of wet, dry and insulating bioelectric recording electrodes. *Physiol. Meas.* **21,** 271 (2000).

9.   Magill, A. & Remy, M. A. *Health monitoring garment*. (2003).

10.   Linz, T., Kallmayer, C., Aschenbrenner, R. & Reichl, H. Fully untegrated EKG shirt based on embroidered electrical interconnections with conductive yarn and miniaturized flexible electronics. in 4 pp.-pp.26 (2006). doi:10.1109/bsn.2006.26

11.   Rattfält, L., Lindén, M., Hult, P., Berglin, L. & Ask, P. Electrical characteristics of conductive yarns and textile electrodes for medical applications. *Med. Biol. Eng. Comput.* **45,** 1251–1257 (2007).

12.   Kang, I., Schulz, M. J., Kim, J. H., Shanov, V. & Shi, D. A carbon nanotube strain sensor for structural health monitoring. *Smart Mater. Struct.* **15,** 737–748 (2006).

13.   Shim, B. S., Chen, W., Doty, C., Xu, C. & Kotov, N. A. Smart Electronic Yarns and Wearable Fabrics for Human Biomonitoring made by Carbon Nanotube Coating with Polyelectrolytes. *Nano Lett.* **8,** 4151–4157 (2008).

14.   Pani, D. *et al.* Fully textile, PEDOT: PSS based electrodes for wearable ECG monitoring systems. *IEEE Trans. Biomed. Eng.* **63,** 540–549 (2016).

15.   Takamatsu, S. *et al.* Direct patterning of organic conductors on knitted textiles for long-term electrocardiography. *Sci. Rep.* **5,** (2015).

16.   Matsuhisa, N. *et al.* Printable elastic conductors with a high conductivity for electronic textile applications. *Nat Commun* **6,** (2015).

17.   Yang, K., Freeman, C., Torah, R., Beeby, S. & Tudor, J. Screen printed fabric electrode array for wearable functional electrical stimulation. *Sens. Actuators Phys.* **213,** 108–115 (2014).

18. Li, Y., Torah, R., Beeby, S. & Tudor, J. An all-inkjet printed flexible capacitor for wearable applications. in *Design, Test, Integration and Packaging of MEMS/MOEMS (DTIP), 2012 Symposium on* 192–195 (IEEE, 2012).

19. Roberts, T. *et al.* Flexible Inkjet-Printed Multielectrode Arrays for Neuromuscular Cartography. *Adv. Healthc. Mater.* **5,** 1462–1470 (2016).

20. Alves, A. P. *et al.* Experimental Study and Evaluation of Paper-based Inkjet Electrodes for ECG Signal Acquisition. in 275–281 (2014).

21. Jung, H. C. *et al.* CNT/PDMS Composite Flexible Dry Electrodesfor Long-Term ECG Monitoring. *IEEE Trans. Biomed. Eng.* **59,** 1472–1479 (2012).

22. Leleux, P. *et al.* Conducting Polymer Electrodes for Electroencephalography. *Adv. Healthc. Mater.* **3,** 490–493 (2014).

23. Isik, M. *et al.* Cholinium-based ion gels as solid electrolytes for long-term cutaneous electrophysiology. *J. Mater. Chem. C* **3,** 8942–8948 (2015).

24. Kim, D.-H. *et al.* Epidermal Electronics. *Science* **333,** 838–843 (2011).

25. Yeo, W.-H. *et al.* Multifunctional Epidermal Electronics Printed Directly Onto the Skin. *Adv. Mater.* **25,** 2773–2778 (2013).

26. Huang, X. *et al.* Materials and Designs for Wireless Epidermal Sensors of Hydration and Strain. *Adv. Funct. Mater.* **24,** 3846–3854 (2014).

27. Bareket, L. *et al.* Temporary-tattoo for long-term high fidelity biopotential recordings. *Sci. Rep.* **6,** 25727 (2016).

28. Zucca, A. *et al.* Tattoo Conductive Polymer Nanosheets for Skin-Contact Applications. *Adv. Healthc. Mater.* **4,** 983–990 (2015).

29. Zucca, A. *et al.* Roll to roll processing of ultraconformable conducting polymer nanosheets. *J. Mater. Chem. C* **3,** 6539–6548 (2015).

30. Rivera-Ruiz, M., Cajavilca, C. & Varon, J. Einthoven's String Galvanometer: The First Electrocardiograph. *Tex. Heart Inst. J.* **35,** 174 (2008).

31. Microsoft Word - The EMG Booklet 27.doc - ABC-EMG-ISBN.pdf. Available at: http://www.noraxon.com/wp-content/uploads/2014/12/ABC-EMG-ISBN.pdf. (Accessed: 27th October 2016)

32. Basmajian, J. & Deluca, C. Muscle Alives. (1985).

Chapter 3

Printed PEDOT:PSS electrodes on paper

This chapter is based on the following publication:

"Inkjet printed PEDOT:PSS electrodes for ECG measurements on paper"

Eloïse Bihar†, Timothée Roberts†, Mohamed Saadaoui, Thierry Hervé, Jozina B. De Graaf, and George Malliaras*, Advanced healthcare materials, 2017, doi: 10.1002/adhm.20160116.

In this chapter, I report the fabrication of biopotential electrodes by the recording of electrophysiological signals such as electrocardiography via a simple finger to electrode contact.

The ink used was the PEDOT:PSS formulation optimized during my first year of PhD. I selected a commercial paper as a substrate as it is ecofriendly and recyclable and can be integrated in biomedical devices for single or multiple uses. I investigated the performances of PEDOT:PSS printed electrodes for a 3 months period. I present the results obtained during this period and show that these paper electrodes exhibit a good quality signal with no

deterioration after multiple uses. These paper electrodes are compatible with the development of the next generation of low cost and convenient-to-use healthcare monitoring devices.

3.1   Introduction

Cardiovascular diseases (CVDs) are the leading cause of deaths, with more than 610,000 cases per year in the United States alone, and are responsible for over 30% of the deaths in the world.[1] These illnesses are worldwide problems that concern both industrialized and developing countries. From 2010 to 2030, the associated medical costs are predicted to increase by a factor 3.[2] This problem is compounded by other factors such as tobacco, alcohol or obesity, which increase the risks of developing CVDs. In many cases, early detection could prevent fatality but in many countries CVDs are detected late as a result of difficult access to preventative healthcare programs. Therefore, low cost, easy-to-use detection methods are of tremendous value in identifying early diseases such as heart failure. Currently, the detection of electrophysiological signals, including those stemming from cardiac activity, in clinical and research applications is realized using conventional electrodes. There are mostly made of Ag/AgCl layer, coated with conducting gel that is used to reduce the impedance at the electrode/skin interface. These electrodes are disposable, lead to a good recorded signal quality, but present several limitations.[3–5] For instance, the irritation coming from the adhesive used to ensure a good contact between the electrode and the skin can induce allergies/intolerances. Moreover, these electrodes exhibit poor performance in long term monitoring mostly due to the drying of the gel. Finally, even the use of a gel does not adequately prevent motion artifacts in some applications.

Several works have focused on the development of dry electrodes that avoid problems associated with the drying of the gel.[4–7] These studies explored the feasibility of long term measurements of cutaneous electrophysiological signals without inducing skin irritation,[4] and with a minimal influence from motion artifacts.[6] Other studies explored the feasibility of integrating conducting materials into textiles to fabricate wearable electrodes for electrocardiography (ECG) or electromyography (EMG).[8–10] Various technologies were used to pattern the conducting layer such as printing of metallic inks,[7,8] or a technique inspired by the dying of kimonos to deposit organic conductors.[9] Indeed, conducting polymers such as

poly(3,4-ethylenedioxythiophene) doped with poly(styrene sulfonate) (PEDOT:PSS) are being widely studied these last few years for applications in bioelectronics due to their ease of processing, mixed electronic/ionic conductivity and biocompatibility.[10-11]. PEDOT:PSS, in particular, has been receiving a great deal of attention as a promising material for advanced transducers for cutaneous electrophysiology.[12-13]

Recently, the use of inkjet printing to make electrodes for ECG acquisition was reported.[14,15] These studies showed encouraging results using electrodes printed from metallic inks, opening new perspectives for printed electronics applications. Indeed, inkjet printing is an additive technology, which does not require the use of masks or additional manufacturing steps, and minimizes materials waste. It combines the possibilities to easily customize the printed pattern and to tune layer thickness by the deposition of single or multiple layers. In this paper we report the fabrication of fully inkjet-printed, metal-free electrodes using a commercial paper as an eco-friendly and recyclable substrate, and a biocompatible conducting polymer, PEDOT:PSS, as the active material. We show that printing a single layer of PEDOT:PSS ink on a commercial paper allows the measurement of ECG from a human volunteer by simply contacting the electrodes with his/her fingers. We compared the performance of electrodes consisting of 1, 2 and 3 printed layers in terms of recording quality over a period of 3 months, and in terms of electrochemical impedance to the skin. This work paves the way for the development of economical, ecological and convenient-to-use ECG-based diagnostics.

3.2   Results and discussion

We selected a commercial paper (Powercoat HD, Arjowiggins) as the substrate for the electrode, as it is eco-friendly and recyclable and presents a surface roughness (Ra) estimated at 60nm. Three electrodes, consisting of 1, 2 and 3 layers of the conducting polymer PEDOT:PSS, were deposited side-by-side on a piece of paper as shown in Figure 3.1.a without variation in the surface roughness of the printed paper. Each electrode consisted of a disk with a diameter of 1 cm (similar to the dimensions of a conventional Ag/AgCl electrode), connected to a $1 \times 1 cm^2$ contact pad area, as shown in Figure 3.2.
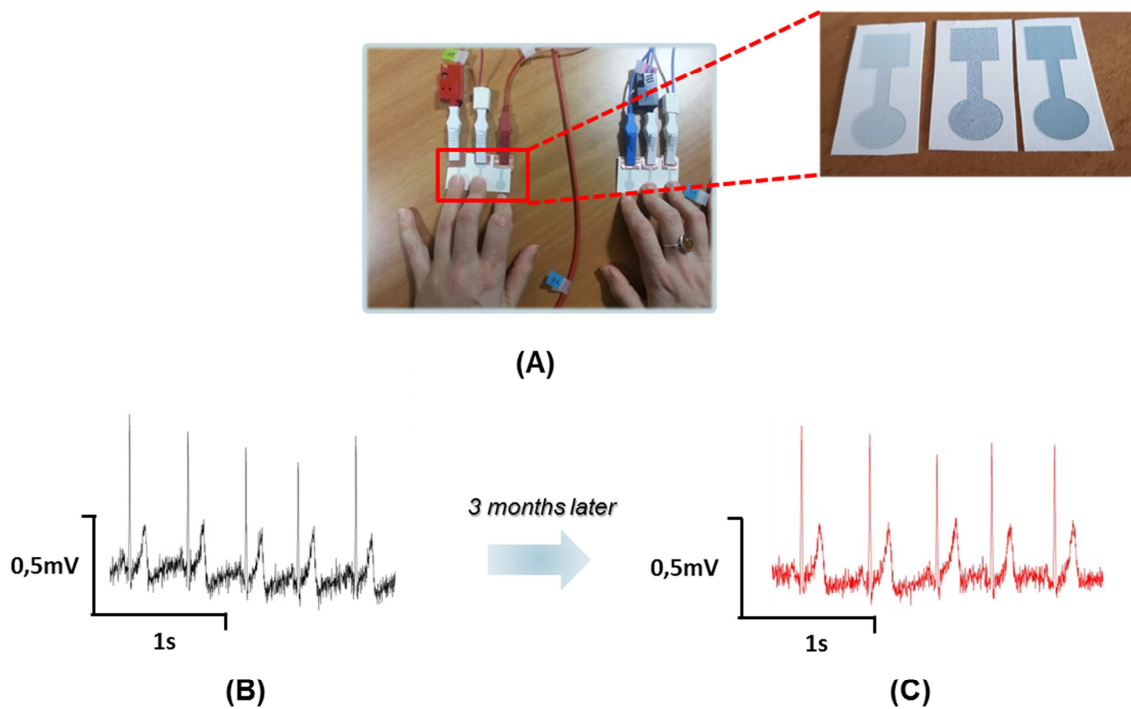
Figure 3.1 **(A) Photograph of printed PEDOT:PSS electrodes** on a commercial paper with a zoom on individual electrodes consisting of 1 to 3 layers. Associated ECG measurements for a printed electrode (1 layer) soon after fabrication (B) and after 3 months (C).

The electrodes were connected to the acquisition system using toothless alligator clips and copper foil. A volunteer placed his/her hands on two pieces of paper containing electrodes, establishing contact with electrodes consisting of 1 layer with his/her ring fingers, electrodes consisting of 2 layers with his/her middle fingers, and electrodes consisting of 3 layers with his/her index fingers. Figure 3.1.b shows the signal measured from a set of electrodes consisting of 1 printed layer (ring fingers), allowing to distinguishing clearly the specific electrical waves of the heartbeat such as the QT intervals. This signal is of adequate quality to detect CVD related anomalies such as arrhythmias. A measurement repeated 3 months later is displayed in Fig. 3.1.c, showing no visible signal deterioration during this period.
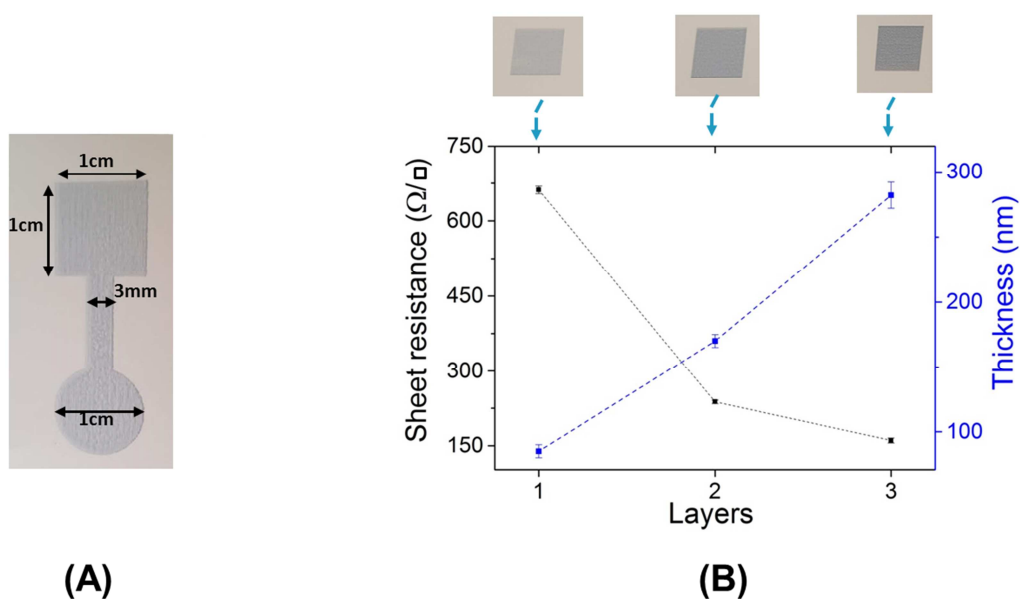
Figure 3.2 **(A) Photograph showing the dimensions of the PEDOT:PSS electrode (B)** Sheet resistance of printed PEDOT:PSS electrodes on paper consisting of 1, 2 and 3 layers, n=3

In order to better quantify the stability the electrodes, measurements were repeated approximately once a week for a period of 3 months. Three simultaneous recordings were conducted for each type of electrode (1, 2, 3 layers) and repeated twice per session. In total, 6 ECG acquisitions of 1 minute per electrode types were run every week. Figure 3.3 shows the evolution of the mean signal-to-noise ratio (SNR) per electrode type. The data shows that the signal quality stays contrast as a function of time. At the same time, no visible changes to the electrodes were detected. The data also shows that SNR increases slightly with the number of depositions used to make the recording electrodes. Indeed, the mean SNR values that corresponds to all measurements obtained within a 3 months period by the electrode consisting of 1 layer was 10.28 ± 0.62 dB. This value increases to 10.79 ± 0.61 dB and to 11.01 ± 0.41 dB, for recordings obtained by electrodes consisting of 2 and 3 layers, respectively.
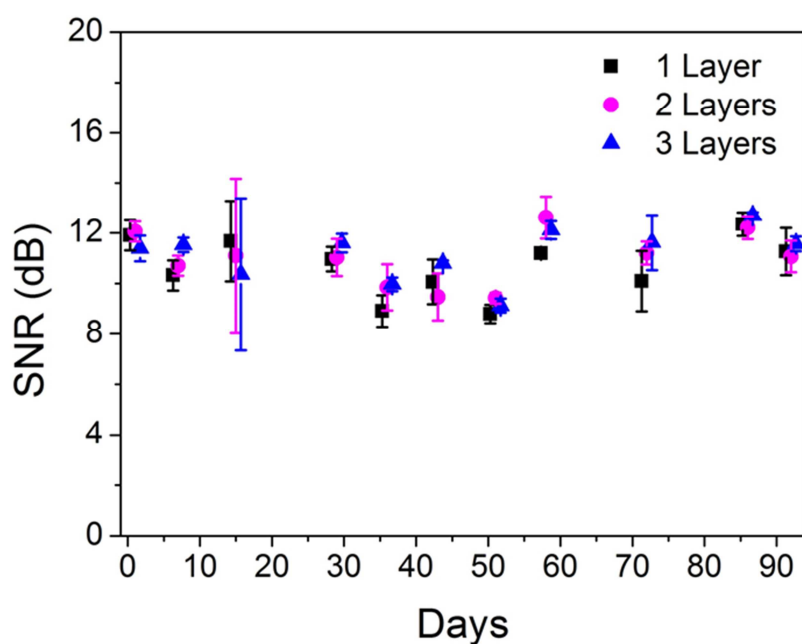
Figure 3.3 **Mean signal-to-noise ratio (SNR) of ECG signals over time for PEDOT:PSS electrodes consisting of 1, 2, and 3 layers, n=6.**

In order to understand this increase we performed electrochemical impedance spectroscopy measurements and characterize the contact between electrode and skin. We placed the electrodes on the arm of the volunteer as drawn in Figure 3.4. The printed electrode was used as the working electrode, while commercial wet Ag/AgCl electrodes were used as counter and reference electrodes.
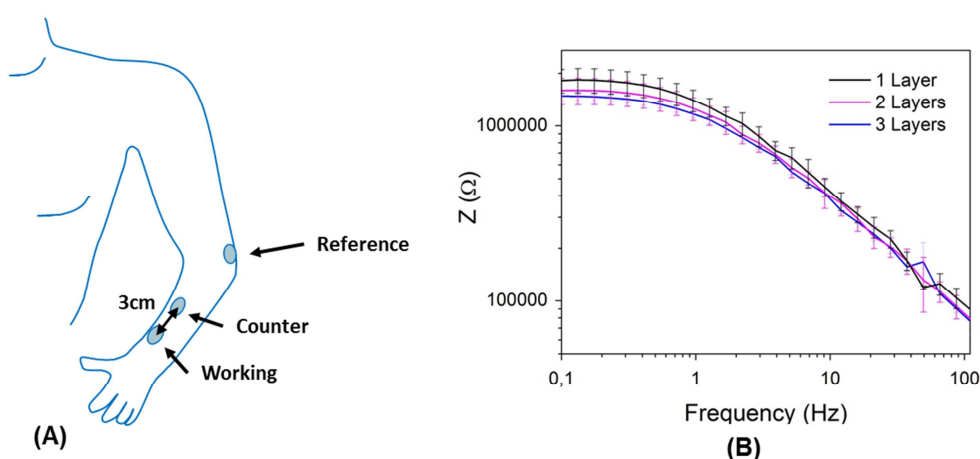
Figure 3.4 (**A**) **Schematic of the experiment for electrode/skin impedance measurements. (B) Electrochemical impedance spectra measured from printed PEDOT:PSS electrodes consisting of 1, 2 and 3 layers, n=3.**

The data shows that the electrode/skin impedance decreases slightly with the number of layers printed. For example, at 1 Hz, the impedance drops from 1.40×10^6 Ohm for a 1-layer electrode, to 1.26×10^6 Ohm for a 2-layer electrode, to 1.17×10^6 Ohm for a 3-layer electrode. This decrease is consistent with the decrease of the sheet resistance of the PEDOT:PSS layer with thickness (Figure 3.2). Compared to commercial and state-of-the-art textile electrodes reported in literature, the printed electrodes show an impedance that is approximately one order of magnitude higher (at 1 Hz).[9] This can be attributed to a combination of a lower conductivity, and poorer mechanical and electrical contact due to the limited flexibility of the paper substrate and the absence of a gel. Despite their high impedance, the electrodes provide high quality ECG recordings in a convenient testing format.

In addition to applications in the diagnosis of CVDs, various other physiological phenomena/conditions can be extracted from the analysis of electrocardiograms. One example is breathing. This is done by monitoring variations in the RS amplitude, which increases and decreases during inhalation and exhalation, respectively.[16] Using the same electrodes and experimental setup, we lengthened the acquisition time to two minutes and asked the volunteer to stabilize his/her breathing. Typical data are displayed in Figure 3.5, showing the variation of the RS amplitude and of the corresponding signal envelope. Breathing is easily noticeable and shows that data obtained from the printed electrodes are of high enough quality to allow analysis of RS amplitudes.
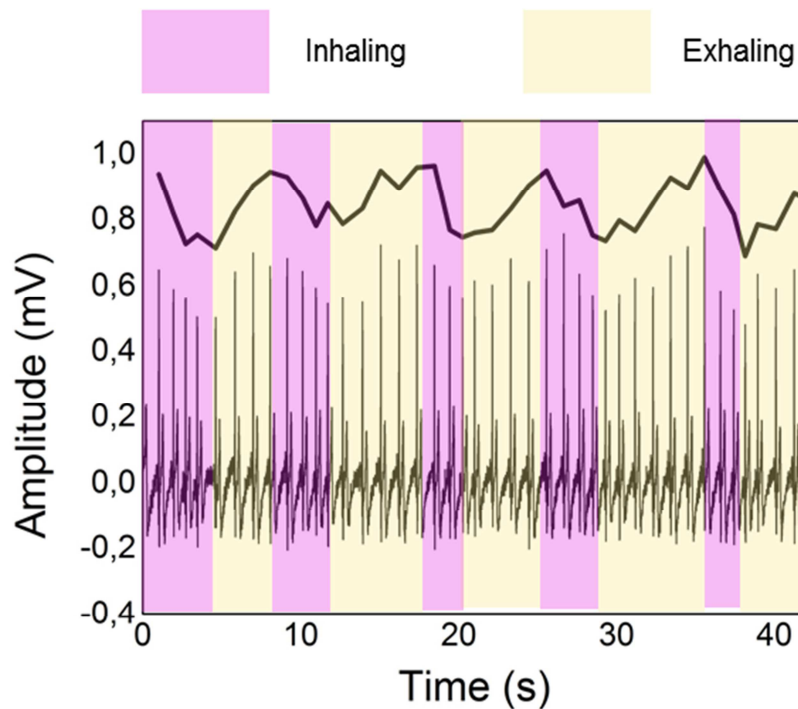
Figure 3.5. **Breathing detection from ECG measurement using PEDOT:PSS electrodes consisting of 1 layer.**

The electrodes described here could be easily used with an external device such as a smartphone to obtain electrophysiological signals. Their performance makes them suitable for a single or multiple uses. Being paper-based and metal-free, they could be easily integrated in a recycling process with a limited impact on the environment. Finally, a potential application of ECG that is currently receiving a great deal of attention is authentication.[17] Indeed, features extracted from electrocardiograms were shown to be independent of electrode location, invariant to the individual's anxiety state, and unique to the individual.[18] One, for example, can envision printing electrodes on a smart credit card that authenticating the owner based on the recorded ECG. Experiments that demonstrate this concept are ongoing.

3.3   Conclusions

In this work we demonstrate inkjet-printed conducting polymer electrodes on paper for applications in electrocardiography. Electrocardiograms were obtained by simply placing two fingers on the electrodes. The recordings exhibited good signal quality, which remained stable over a period of 3 months. This work paves the way for the facile and cost-effective fabrication of metal-free medical electrodes on paper with a reduced number of manufacturing steps. As a result, it may help deliver convenient-to-use and inexpensive tools for the prevention of cardiovascular diseases.

3.4   Experimental Section

PEDOT:PSS ink: The PEDOT:PSS ink was formulated from a commercially available PEDOT:PSS (Heraeus, Clevios PH1000) dispersion, with the addition of 20 wt% ethylene glycol (Sigma Aldrich) and organic solvents. 0.8 wt% glycidoxypropyltrimethoxysilane (GOPS, Sigma Aldrich) and 0.3% proprietary surfactants were added to the ink to avoid delamination and to match the rheological requirements of the ink with the inkjet printer.

Inkjet printing: A Dimatix DMP-2800 inkjet printer was used to print the electrodes onto a coated paper (Powercoat HD by Arjo-wiggins, Inc.). We printed, one, two and three layers of PEDOT:PSS and we cured the samples in a conventional oven for 30 min at 160°C. The dimensions of the electrodes are shown in Figure 3.2. The thickness of 1, 2 and 3 layers was measured by using a mechanical profilometer (Ambios technology).The roughness of the printed

Electrochemical impedance spectroscopy: Impedance measurements were performed using an Autolab potentiostat (Metrohm Autolab B.V.), and the associated software NOVA. No constant differential voltage was applied. A sinusoidal signal of 10 mV was used with a range of frequency between 0.1 and 100 Hz. The working and counter electrodes were placed 3 cm apart on the forearm. The reference electrode was placed on the elbow. The printed electrode was the working electrode while wet Ag/AgCl electrodes (Ambu Blue Sensor N, N-00-S/25, 0.95 cm diameter contact area) were used as counter and reference electrodes.

Physiological data acquisition: All volunteers (3) provided informed signed consent to participate in this study. ECG data were acquired using a RHD2216 chip from Intan Technologies. The signals were sampled at 1.1 kHz at 16 bits. A first order high pass at 0.1Hz and a third order low pass at 100 Hz analog filters were used. 3 bipolar channels were used during the experiments, each channel connecting to with 2 electrodes of the same type (1, 2 or 3 layers). A ground electrode was placed on the right leg. All measurements were carried out while the volunteer was not moving.

Data post-processing: All post-processing was carried out using National Instrument's LabVIEW software. The ECG data were first filtered using a forth order Butterworth band pass, high passed at 0.5 Hz and low passed at 100 Hz, and a forth order notch filter at 50 Hz. The signal-to-noise ratio (SNR) was then calculated for each measurement using the equation:

$$SNR(Sr) = 20 * \log\left(\sqrt{\frac{\sum_i Sf_i^2}{\sum_i (Sr_i - Sf_i)^2}}\right)$$, Sr being the raw signal and Sf the filtered signal. The

average value and its standard deviation were then calculated for the devices during periodic experiments. Breathing analysis was obtained using a simple algorithm that isolated the amplitudes of each RS complex of the ECG signal and then looked for a decrease or an increase in those amplitudes.

3.5 References

[1]   J. Xu, S. L.Murphy, K. D. Kochanek, B. A. Bastian, National Vital Statisctics Reports, **2016**, 64, 2

[2]   P. A. Heidenreich, P. A., Trogdon, et. al., *Circulation*, **2011,** *123*, 933.

[3]   A. Searle, L. Kirkup, *Physiol. Meas.* **2000**, *21*, 271.

[4]   J.-Y. Baek, J.-H. An, J.-M. Choi, K.-S. Park, S.-H. Lee, *Sens. Actuators Phys.* **2008**, *143*, 423.

[5]   K. P. Hoffmann, R. Ruff, *IEEE Eng Med Biol Soc.* **2007**, pp. 5739–5742.

[6]   C.-T. Lin, L.-D. Liao, Y.-H. Liu, I.-J. Wang, B.-S. Lin, J.-Y. Chang, *IEEE Trans Biomed Eng.* **2011**, *58*, 1200.

[7]   T. Roberts, J. B. De Graaf, C. Nicol, T. Hervé, M. Fiocchi, S. Sanaur, *Adv. Healthc. Mater.***2016**, DOI 10.1002/adhm.201600108.

[8]   N. Matsuhisa, M. Kaltenbrunner, T. Yokota, H. Jinno, K. Kuribara, T. Sekitani, T. Someya, *Nat Commun* **2015**, *6*.

[9]   S. Takamatsu, T. Lonjaret, D. Crisp, J.-M. Badier, G. G. Malliaras, E. Ismailova, *Sci. Rep.* **2015**, *5*.

[10]   J. Rivnay, R. M. Owens, G. G. Malliaras, *Chem. Mater.* **2013**, *26*, 679.

[11]   M. Berggren, A. Richter-Dahlfors, *Adv. Mater.* **2007**, *19*, 3201.

[12]   A. Campana, T. Cramer, D.T. Simon, M. Berggren, F. Biscarini, *Adv. Mater.* **2014**, *26*, 3874.

[13]   P. Leleux, J.-M. Badier, J. Rivnay, C. Bénar, T. Hervé, P. Chauvel, G. G. Malliaras, *Adv. Healthc. Mater.* **2014**, *3*, 490.

[14]   A. P. Alves, J. Martins, H. P. da Silva, A. Lourenço, A. L. Fred, H. Ferreira, *Proceedings of the International Conference on Physiological Computing Systems* **2014**, pp. 275–281.

[15]   J. C. Batchelor, A. J. Casson, *IEEE Eng Med Biol Soc.* **2015**, pp. 4013–4016.

[16]   George B. Moody, Roger G. Mark, Andrea Zoccola, Sara Mantero, *Comput. Cardiol.* **1985**, *12*, 113.

[17]   https://www.washingtonpost.com/news/innovations/wp/2014/11/21/the-heartbeat-vs-the-fingerprint-in-the-battle-for-biometric-authentication/

[18]   S.A. Israel, J.M. Irvine, A. Cheng, M.D. Wiederhold, B.K. Wiederhold, *Pattern Recognition* **2005**, *38*, 133.

Chapter 4

Printed textile electrodes

This chapter is based on the following publication:

"Fully printed electrodes on stretchable textiles for long-term electrophysiological measurements"

Eloïse Bihar†, Timothée Roberts†, Esma Ismailova, Mohamed Saadaoui, Mehmet Isik, Ana Belen Sanchez, David Mecerreyes, Thierry Hervé, Jozina B. De Graaf, and George Malliaras* , Advanced materials technology, 2017, doi: 10.1002/admt.201600251.

In this chapter, fully-printed electrodes consisting of a conducting polymer and an ionic liquid gel fabricated on a stretchable textile were shown to record cardiac activity while the wearer was moving and for long periods of time.

The mechanical and electrical properties of the printed polymer on the stretchable textile were tested. The performances of the textile electrodes during this period were analyzed. We compared dry and gelled electrodes ECG signal acquisitions by printing an additional layer of iongel composed by a biocompatible IL polymer (cholinium lactacte and 2-cholinium lactate methacrylate monomer) on top of the active area of the PEDOT:PSS electrode.

4.1   Introduction

Cutaneous devices for health monitoring are attracting a great deal of interest in both industry and academia. Recent advances on the deposition of electronic materials onto textiles are generating a considerable effort focused on the integration of electrical health monitoring systems into clothing.[1–3] Such autonomous, wearable monitoring systems allow a better patient comfort during daily use. They aim to provide early diagnosis of cardiovascular diseases (CVDs) such as arrhythmias and can be used for prevention of heart-related problems. For instance, early detection of people presenting high cardiovascular risks could prevent fatal issues by providing adequate medical care.[4].

Existing commercial devices for infant and adult health monitoring use wet (gel-assisted) Ag/AgCl electrodes but these electrodes cause discomfort, and in some cases, skin irritation and allergic reactions from the adhesive used to fix them on the skin.[5] They are also not suitable for long-term measurements due to the drying of the gel.[6] To find alternatives, many studies explored electrodes embedded in or deposited on textiles.[7] Textile electrodes can be fabricated by integrating conducting yarns into the textile,[8,9] by dip-coating the fibers,[10] or by deposition of conducting materials on the textile.[11] The latter approach, coupled with a direct deposition technique such as inkjet printing, offers great versatility and has the potential to lead to customizable electrodes for health monitoring. To date, however, only a few studies reported the use of inkjet for the fabrication of wearable electrodes for health monitoring.[12,13] Inkjet technology is an additive technology which permits to design customizable electrodes with reduced manufacturing costs. It offers many advantages such as compatibility with a wide range of substrates, small number of fabrication steps, low materials waste, and the possibility to integrate this technique in a roll-to-roll process, making production efficient and inexpensive.

In this work we report the fabrication fully-printed, wearable electrodes using inkjet technology by printing the conducting polymer poly(3,4-ethylenedioxythiophene) doped with poly(styrene sulfonate) (PEDOT:PSS) on a commercial stretchable textile. A commercially available pantyhose (100% wt. polyamide) was chosen as the substrate, at it offers a high level of stretchability. We chose PEDOT:PSS as the conducting layer due to its biocompatibility,[14] and its mixed ionic/electronic conductivity, which yields high quality

cutaneous contacts.[15] We further printed an ionic liquid gel to improve the contact between the conducting polymer and skin, as such gels have been shown to lead to high quality contacts with excellent long-term stability.[16] We record electrocardiograms (ECG) from a volunteer and demonstrate recordings that are stable and rather insensitive to motion artifacts, paving the way for the fabrication of low cost, customizable electrodes for cutaneous electrophysiology.

4.2   Results and discussion

The printed electrode geometry (Figure 4.1) consists of a round disk with a diameter of 1 cm, similar to that of a commercial Ag/AgCl electrode, connected to a square contact pad with area of 1 cm^2.

(a)   (b)
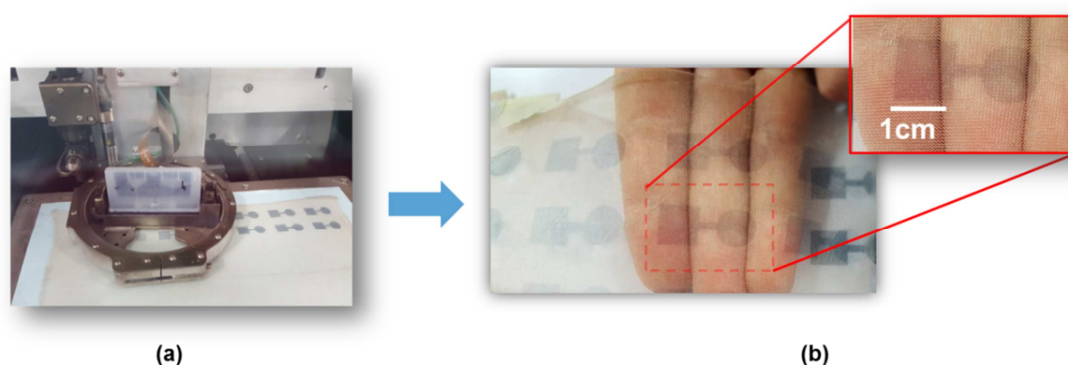
Figure 4.1 (a) Photograph of the inkjet printing process. (b) Photograph of printed electrodes on a commercial textile with a zoom on an individual electrode.

We inkjet-printed several layers of the conducting ink (Figure 4.2) and obtained electrodes with a color that became more apparent as the quantity of conducting material added onto the textile increased. As seen in Figure 4.2.b, the electrical resistance of a 1 cm^2 PEDOT:PSS square decreased with the number of printed layers, reaching a plateau at 8 layers.

Mechanical deformation tests showed that PEDOT:PSS rigidified slightly the textile, yet the electrodes could be stretched at least up to 200% (Figure 4.3). The resistance of electrodes consisting of 4, 6, 8, and 10 layers increased only by a factor of 6.02, 2.66, 1.38 and 1.48 times, respectively, at 100% strain (Figure 4.2.c). Compared to literature, these values are close to the state-of-the-art and validate the choice of textile as a substrate.[17–19]. Figure 4.2.d shows that after a slight initial increase, resistance remains constant after 50 cycles at 30% strain, proving the stability of the printed polymer electrical properties under mechanical stress.
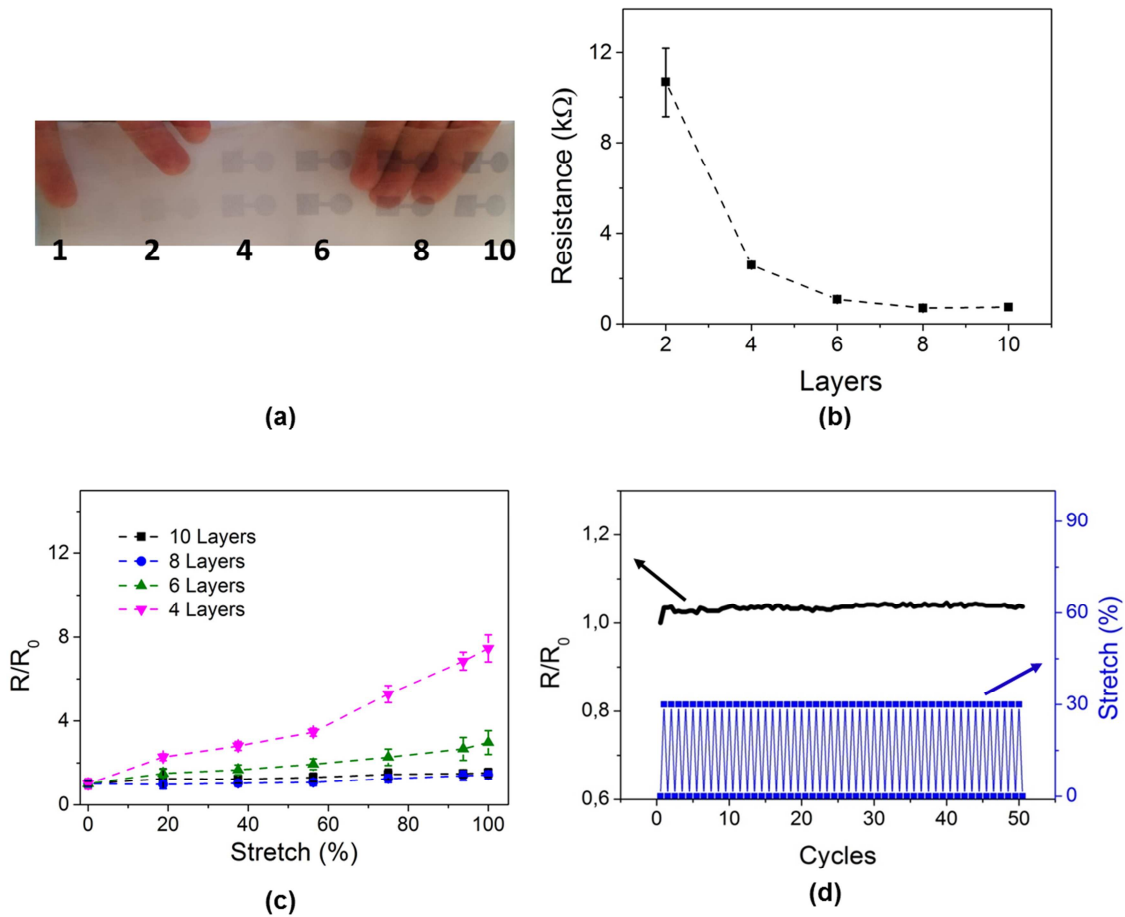

(a)

(b)

(c)

(d)

Figure 4.2 (a) Photograph of electrodes with a different number of printed layers (1, 2, 4, 6, 8, 10). **(b)** Resistance of a printed square (1×1 cm^2). **(c)** Normalized resistance (R/R_0) of printed squares as a function of stretching. **(d)** Normalized resistance (R/R_0) during stretching cycles (n=3).

Based on the results above, electrodes consisting of 8 printed layers of PEDOT:PSS were chosen for further investigation. When taken up to 200% strain, their resistance increased by a factor of 3.48 (Figure 4.3.c).
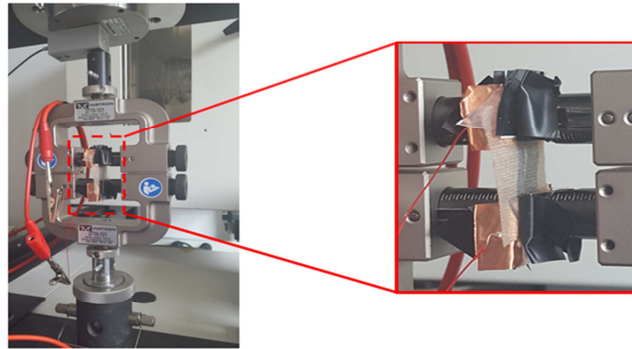
(a)
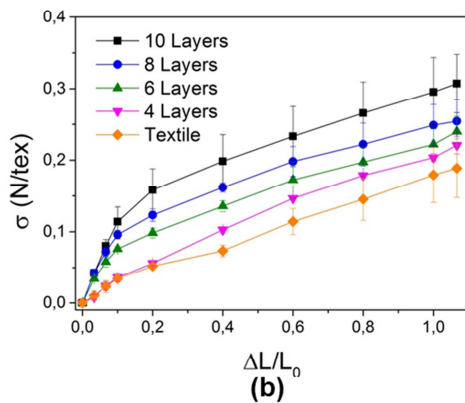
(b)
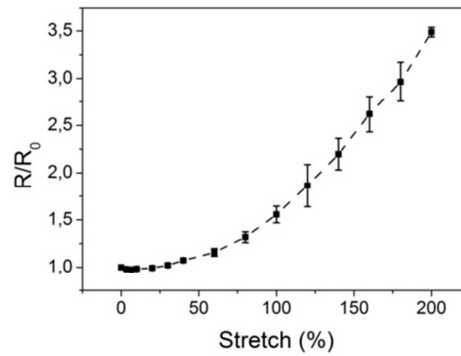
(c)

Figure 4.3(**a**) Setup of the mechanical properties testing experiment with a zoom on the printed textile. (**b**) Stress-strain curve of a virgin textile and a textile with a different number of PEDOT:PSS layers (4, 6, 8, 10). The increase in the slope of the load extension curve (from 0 to 15%) shows that the textile is rigidified by the PEDOT:PSS. (**c**) Normalized resistance (R/R_0) of a PEDOT:PSS textile electrode consisting of 8 printed layers versus stretch

The high degree of stretchability is consistent with recent work from the Bao group that shows that surfactants allow changes of conformation of PEDOT:PSS chains during stretching [18]. Such high excursions, though, were found to cause delamination of PEDOT:PSS (Figure 4.4).

At 0% strain   **At 200% stretch**   **After 50 cycles at 30% stretch**
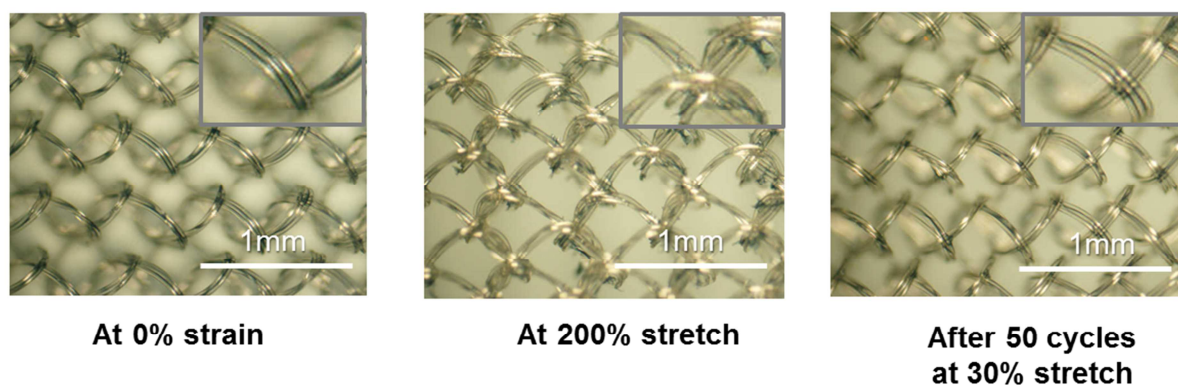
Figure 4.4 (a) Micrograph of a PEDOT:PSS electrode consisting of 8 layers on textile at no stretch, at 200% stretch, and after 50 cycles at 30% stretch, with a zoom on the yarn.

Thus, cyclic tests were performed at lower values of strain in order to evaluate durability during repetitive deformation. Figure 4.2.d shows that after a slight initial increase, resistance remains constant after 50 cycles at 30% strain, proving the stability of the printed polymer electrical properties under mechanical stress. Micrographs of the film after the experiment provided no evidence of cracking or delamination (Figure 4.4).

In order to improve the contact between the skin and the dry electrode interface, we used a gel formulation based on the biocompatible cholinium lactate ionic liquid.[19] We printed the ionic liquid ink on the PEDOT:PSS active electrode area and photopolymerized it as discussed in the experimental section. The ink penetrated directly into the yarns to form a thin transparent encapsulation layer around PEDOT:PSS coated fibers (Figure 4.5).

Textile   **Textile + 8 layers PEDOT:PSS**   **Textile + 8 layers PEDOT:PSS + 5 layers ionic liquid gel**
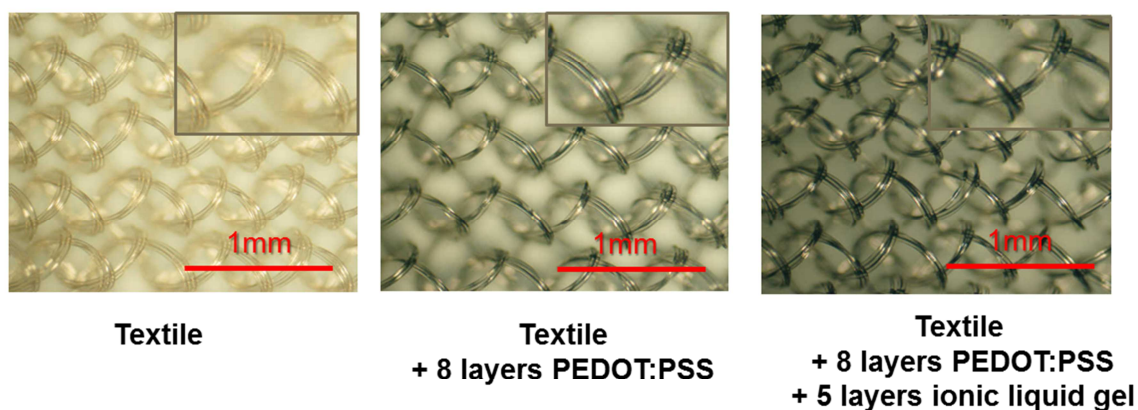
Figure 4.5 **Images of the virgin textile, the textile with 8 layers of PEDOT:PSS, and the textile with 8 layers of PEDOT:PSS and 5 layers of ionic liquid gel.**

Electrochemical impedance measurements of the electrode/skin interface were performed on a volunteer, as shown in Figure 4.6, using the textile one as the working electrode, and wet Ag/AgCl electrodes as counter and reference. The data shows that the addition of the ionic liquid gel lowers impedance, as expected due to the extended contact with skin.
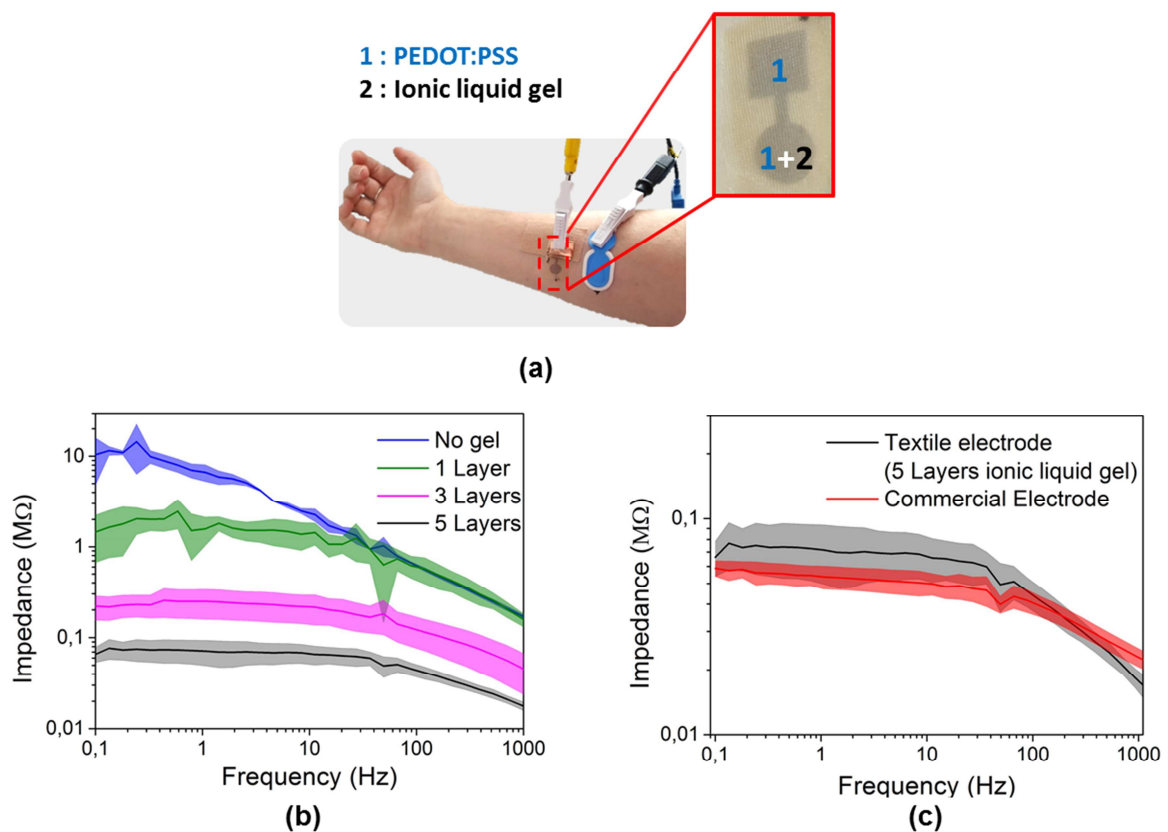
Figure 4.6 **(a)** Photograph showing the electrode configuration for the impedance measurements. **(b)** Impedance spectra measured from a PEDOT:PSS electrodes made of 8 printed layers with and without an ionic liquid gel consisting of various number of layers. **(c)** Impedance spectra of a commercial electrode and a printed electrode consisting of 8 layers of PEDOT:PSS and 5 layers of ionic liquid gel (n=3).

The addition of five layers of ionic liquid gel decreases impedance by 2 orders of magnitude in the frequency range of 0.1 to 10 Hz, and one order of magnitude in the range of 10 to 1000 Hz (Figure 4.6.b). Indeed, the gel-assisted textile electrode with 5 layers of ionic liquid gel shows an impedance spectrum that is similar to that of a commercial wet Ag/AgCl electrode (Figure 4.6.c). A coating consisting of 5 printed layers of ionic liquid gel was, therefore, selected and used to make gel-assisted PEDOT:PSS textile electrodes for the remainder of this study.

In order to validate the use of the textile electrodes in electrophysiology we measured the ECG of a volunteer. ECG signals were simultaneously acquired with the three electrode types: dry and gel-assisted textile electrodes and commercial wet Ag/AgCl electrodes. Measurements were conducted between the two forearms, over a period of 40 days at four different times: t_0, t_0+4h, t_0+8h, t_0+24h, and t_0+40 days. Typical ECG recordings at t_0 and t_0+40 days are shown in **Figure 4.7**.
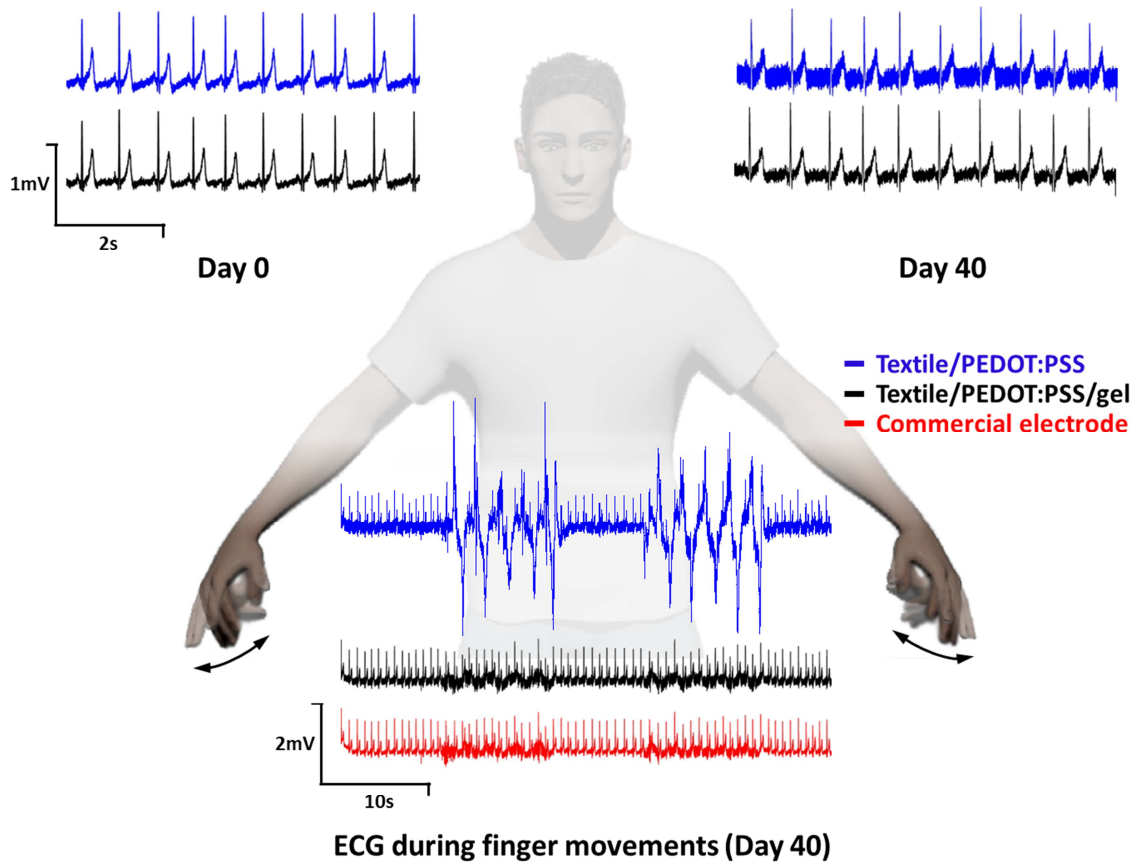
Figure 4.7 **ECG data acquired under different conditions: (i) static recoding at t_0 in the**

top left corner, (ii) static recording at t_0+40 days in the top right corner, (iii) dynamic recording under repeated hand motion at t_0+40 days in the bottom center.

The characteristic waves of ECG, essential to establish CVD diagnostics, are clearly recorded by both the dry and the gel-assisted textile electrodes. The mean signal-to-noise ratio (SNR), calculated at t_0 for 3 different recordings, was 12.93±0.80dB and 13.75±0.26dB, for the dry and the gel-assisted electrodes, respectively, and remained constant for the first 24 hours of recording (Figure 4.8).
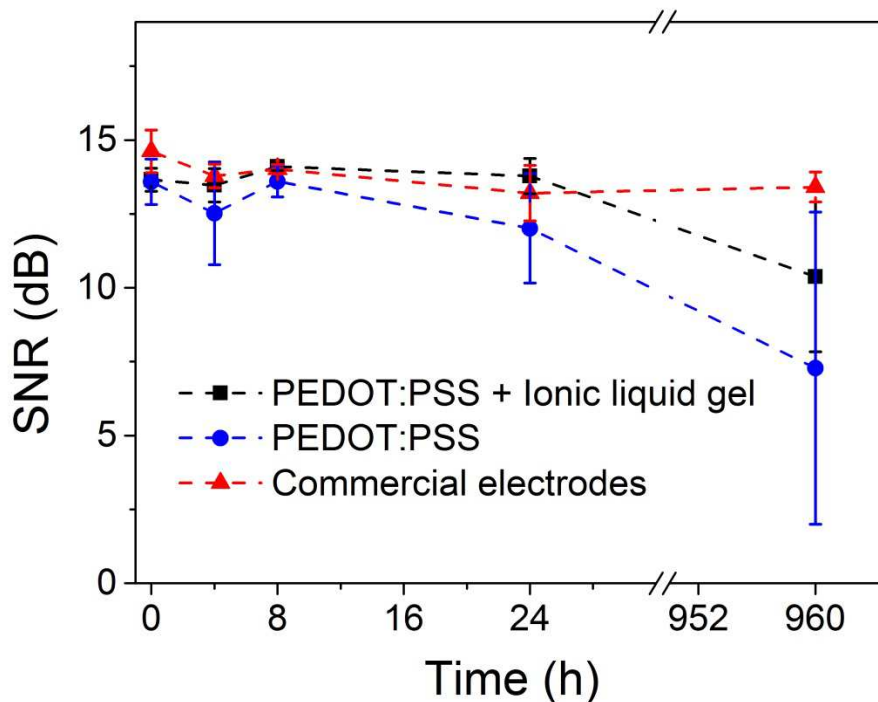
Figure 4.8 **Mean signal-to-noise ratio (SNR) over time (40 days) for commercial wet Ag/AgCl electrode and textile electrodes with 8 layers of PEDOT:PSS and 5 layers of ionic liquid gel (n=6). A fresh Ag/AgCl electrode was used for every measurement**.

40 days later, the performance of the printed electrodes exhibited signs of slight degradation, characterized by a decrease in SNR to 7.28±5.28 dB and 10.37±2.53 dB, for the dry the gel-assisted electrodes, respectively.

To evaluate the impact of motion artifact generated on the ECG signals, we asked the volunteer to repeatedly open and close his/her hands to induce movement artifacts on the

recordings. Figure 4.7 shows typical recordings for each electrode type. While the signal was clearly affected on the dry textile electrodes, it was affected considerably less on both the gel-assisted textile and the commercial electrodes. During movement, the ECG complex recorded by these two electrodes was still detectable, while in recordings from the dry textile electrode, the characteristic peaks were indiscernible. The advantage of the gel-assisted textile electrode, compared to the commercial one, is that it does not dry out. Indeed, the commercial electrode lost its ability to record after approximately 12 hours. Therefore, the use of an ionic liquid gel printed on textile electrodes improved the signal stability over time and under motion.

4.3   Conclusions

We used inkjet printing to make electrodes from PEDOT:PSS on a commercial stretchable textile. Contact with the skin was improved by the addition of a cholinium lactate-based ionic liquid gel that was also inkjet-printed directly on the textile. These gel-assisted electrodes made low impedance contacts to the skin and yielded recordings that were of comparable quality that those of commercial wet Ag/AgCl electrodes, but without drying and using a format that is more compatible with wearable diagnostics. As such, they pave the way for the fabrication of customizable health monitoring devices for cutaneous applications.

4.4   Experimental section

Ink formulations: To formulate the conducting ink, we added in a commercially available dispersion (Heraeus, Clevios PH1000) 20% of ethylene glycol (Sigma Aldrich) and other organic solvents to enhance electrical conductivity, 0.8 wt% of glycidoxypropyltrimethoxysilane (GOPS, Sigma Aldrich) to prevent delamination, and 0.3% of surfactants to achieve suitable rheological properties for inkjet printing. To create the ionic liquid ink, we mixed a solution containing cholinium lactate and 2-cholinium lactate

methacrylate monomer with the crosslinker (ethyleneglycol dimethacrylate) and a photoinitiator [19]. We added ethanol to achieve adequate viscosity for inkjet printing.

Inkjet printing: We used a Dimatix DMP-2800 inkjet printer to fabricate the electrodes. We printed successively 1, 2, 4, 6, 8 and 10 layers of PEDOT:PSS ink on a commercial, stretchable polyamide textile (Dim, knee highs) and cured the samples 60min at 110°C in a conventional oven. To crosslink the ionic liquid gel, we placed the samples in the oven for 10 min (100°C) for solvent evaporation, and exposed the printed textiles to UV light (from a UVGL-58 hand-held UV lamp).

Electrical characterization: Electrical tests during stretching were performed using an Instron tabletop model 3665. The studied samples consisting of printed rectangles (1.5×3 cm^2) on textile. We connected the conducting textile via a copper tape attached to the Instron's jaws and measured resistance using a multimeter (Fluke 175).

Electrochemical impedance spectroscopy: We used an Autolab potentiostat (Metrohm Autolab B.V.), and the associated software NOVA to perform the impedance measurements using the fabricated and commercial electrodes placed on the skin of a volunteer. The frequency range was between 0.1 and 100 Hz and the sinusoidal signal was 10 mV. We placed the reference electrode on the elbow. The working and counter electrodes were placed on the forearm, 3 cm apart. The working electrode was the electrode under study, while the reference and counter electrodes were wet Ag/AgCl electrodes (Ambu Blue Sensor N, N-00-S/25, 0.95 cm diameter contact area).

Physiological data acquisition: Informed consent was signed by the volunteer. A RHD2216 amplifier chip from Intan Technologies was used to record the ECG signal. The chip was configured to use a high-pass filter at 0.1 Hz and a low-pass filter at 100 Hz. After filtering, the signals were sampled on 16 bits at 1.1 KHz. ECGs were recorded between the two forearms with a ground electrode on the right leg. The textile electrodes were attached halfway on the forearm of the participants with a sports bracelet. They were then connected to the recording electronics using a copper tape and a metal wire.

Data post-processing: Labview software from National Instrument was used to process the signal. The "raw" ECG signal (Sr) were obtained by filtering the output of the RHD2216 using a fourth-order Butterworth band-pass filter. The high- and low-pass frequencies were 0.5 and 100 Hz, respectively. A 50 Hz Notch filter was added to obtain the filtered signal (Sf).

The signal-to-noise ratio (SNR) was then calculated for each measurement using the following equation:

$$SNR(Sr) = 20 * \log\left(\frac{RMS(Sf)}{RMS(Sr - Sf)}\right).$$

4.6 References

[1]   S. Park, S. Jayaraman, *MRS Bull.* **2003**, *28*, 585.

[2]   D. Marculescu, R. Marculescu, N. H. Zamora, P. Stanley-Marbell, P. K. Khosla, S. Park, S. Jayaraman, S. Jung, C. Lauterbach, W. Weber, T. Kirstein, D. Cottet, J. Grzyb, G. Troster, M. Jones, T. Martin, Z. Nakad, *Proc. IEEE* **2003**, *91*, 1995.

[3]   P. Lukowicz, T. Kirstein, G. Troster, *Methods Inf. Med.-Method. Inf. Med.* **2004**, *43*, 232.

[4]   "WHO | Cardiovascular diseases (CVDs)," http://www.who.int/mediacentre/factsheets/fs317/en/, accessed: October 2016.

[5]   N, Mazzaro, Risk of skin reaction when using ECG electrodes, http://www.ambu.es/files/billeder/es/micro/cardiologia/the_risk_of_skin_reactions_using_ecg_electrodes_0711.pdf, accessed: July, 2016.

[6]   A. Gruetzmann, S. Hansen, J. Müller, *Physiol. Meas.* **2007**, *28*, 1375.

[7]   M. Catrysse, R. Puers, C. Hertleer, L. Van Langenhove, H. van Egmond, D. Matthys, *Sens. Actuators Phys.* **2004**, *114*, 302.

[8] M. S. Lebby, K. E. Jachimowicz (Motorola Inc), US 5906004 A, 1998.

[9] L. Hu, M. Pasta, F. L. Mantia, L. Cui, S. Jeong, H. D. Deshazer, J. W. Choi, S. M. Han, Y. Cui, Nano Lett. 2010, 10, 708.

[10]   D. Pani, A. Dessì, J. F. Saenz-Cogollo, G. Barabino, B. Fraboni, A. Bonfiglio, *IEEE Trans. Biomed. Eng.* **2016**, *63*, 540.

[11]   S. Takamatsu, T. Lonjaret, D. Crisp, J.-M. Badier, G. G. Malliaras, E. Ismailova, Sci. Rep., 2015, 5, 15003.

[12]   Y. Li, R. Torah, S. Beeby, J. Tudor, in *Des. Test Integr. Packag. MEMSMOEMS DTIP 2012 Symp. On*, IEEE, **2012**, pp. 192–195.

[13]   T. Roberts, J. B. De Graaf, C. Nicol, T. Hervé, M. Fiocchi, S. Sanaur, Adv. Healthc. Mater. 2016, 12, 1462.

[14]   M. Berggren, A. Richter-Dahlfors, *Adv. Mater.* **2007**, *19*, 3201.

[15]   S. Takamatsu, T. Lonjaret, E. Ismailova, A. Masuda, T. Itoh, G. G. Malliaras, *Adv. Mater.* **2016**, *28*, 4485.

[16]   D. J. Lipomi, J. A. Lee, M. Vosgueritchian, B. C.-K. Tee, J. A. Bolander, Z. Bao, *Chem. Mater.* **2012**, *24*, 373.

[17]   T. S. Hansen, K. West, O. Hassager, N. B. Larsen, *Adv. Funct. Mater.* **2007**, *17*, 3069.

[18]   M. Vosgueritchian, D. J. Lipomi, Z. Bao, *Adv. Funct. Mater.* **2012**, *22*, 421.

[19]   M. Isik, T. Lonjaret, H. Sardon, R. Marcilla, T. Herve, G. G. Malliaras, E. Ismailova, D. Mecerreyes, *J. Mater. Chem. C* **2015**, *3*, 8942.

Chapter 5

Printed PEDOT:PSS electrodes on tattoo

This chapter is based on the following publication:

"Customizable printed Tattoo-Textile electrodes for ElectroMyoGraphy"

Eloïse Bihar†, Timothée Roberts†, Mohamed Saadaoui, Esma Ismailova, Thierry Hervé, Jozina B. De Graaf,and George Malliaras*, *in Preparation*

To date, conventional electromyography (EMG) methods suffer from limitations in long-term applications due to patient discomfort related to issues such as chronic skin irritation. In this chapter, we present a simple and customizable method to detect EMG non-invasively and with long-term stability. For that, inkjet printed conformable tattoo electrodes based on the conducting polymer poly(3,4-ethylenedioxythiophene) polystyrene sulfonate (PEDOT:PSS) were employed as the transducing element on the skin/electrode interface. Interestingly, to enable a reliable connection of the tattoo with the electronic acquisition system, the conventional wiring was replaced by a simple contact between the tattoo and a similarly ink-jet printed textile electrode. We show that our tattoo-textile electrode system was able to detect the biceps activity during muscle contraction for a period of seven hours. Combining the tattoo electrode with an electronic textile, constitutes a versatile and easy-to-use method for the integration of electrodes in critical electrophysiological applications such as myo-controlled prosthesis or muscle injury prevention and detection, paving the way to next generation electronic skin devices.

5.1   Introduction

Currently, a great deal of attention is paid to create novel intelligent systems for medical diagnosis tools. Progresses have been made for the development of cutaneous conformable, flexible and stretchable sensors with a minimally invasive effect on the skin-electrode interface. Wet Ag/AgCl electrodes are standardly used for muscle activity detection but these electrodes demonstrate several limitations such as allergies or irritation[1] and the fact they can't be used for long-term application because of the drying of the gel. To avoid discomfort, the development of innovative biomedical devices such as smart textiles[2–4] or electronic skin[5–7] have gained a lot of interest to improve the daily life quality of patients. New dry electrodes have been conceived such as textile electrodes or recently e-skin /tattoo electrodes. Recently, intelligent electronic systems[6,8,9] mimicking the temporary commercial tattoos have been reported, integrating different sensors and the materials required to compose a fully autonomous system. They showed a good conformation to skin and resistance to deformation with no irritation to the skin and were able to detect electrophysiological signals. Electrodes with electronics embedded in textiles have been tested to record muscle electrical activity such as Electrocardiography[10] (ECG) or Electromyography[4] [11](EMG). Several techniques allow the electronic patterning of the textiles such as the integration of conducting yarns[12,13] into the fabrics or by coating[14,15]. These textiles demonstrate great potential for long-term monitoring of electrophysiological signals.

New smart devices using conducting polymers instead of inorganic conductors are investigated for bioelectronics. For instance, PEDOT:PSS is a biocompatible[16] conducting polymer widely studied this last decade for its combined ionic and electronic properties. It shows a great conformation on the skin. Recently PEDOT:PSS has been highlighted as a promising candidate to produce conducting tattoos[17,18] for EMGs recordings[19,20] or a combined with carbon to create tattoo electrodes for oculography[21].These new tools contribute to the prevention or early detection of cardiovascular diseases but can also be used for electrical stimulation or the myo-electric control of prosthetics. Indeed, there is a global need to develop prosthetics easy to handle, adaptable for each patient and financially affordable[22]. Emergent technologies such as inkjet[23] or screen printing[24] are considered as cost-effective approaches with reduced number of manufacturing steps. Inkjet technology is a

simple non contact technique which allows the fabrication of customizable designs. The patterns could be easily modified on demand. Inkjet could be used to manufacture low cost biomedical devices such as biosensors[25] and industrialized via integration in roll to roll processes.

In this work, we present a simple method to fabricate intelligent devices using inkjet technology and for interconnecting the skin-tattoo electrodes to smart textile for EMG acquisition. We connected the tattoo electrodes by replacing conventional electrical wires with a simple direct contact with dry printed textile electrodes. The conducting material used was PEDOT:PSS. We proved the proper functioning and stability of the proposed tattoo-textile system by measuring its electrochemical impedance (EIS) and though the acquisitions of biceps EMG signal.

5.2   Results

We first selected a commercial temporary tattoo paper for the fabrication of the tattoo electrode. We printed 1 layer of PEDOT:PSS ink (Figure 5.1). The dimension of the active area of the electrode is $1x1cm^2$ square and 1 layer represents 100nm thickness.
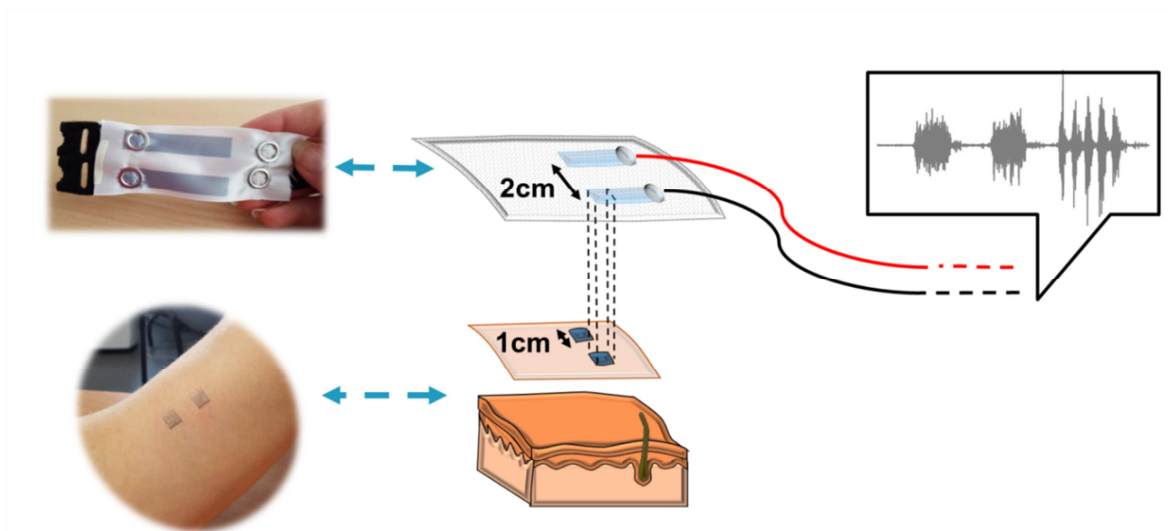

Figure 5.1**Schematic of the textile-Tattoo electrodes.** The printed tattoo is deposed on the skin after humidification with water. Printed textile electrodes are placed on top of the tattoo

replacing the wires to connect the tattoo with the electronic system allowing detection of EMG.

The conductivity of the ink printed on the thin film is 240S/cm. The printed conducting polymer tattoo was then deposited on the skin after when moisture is applied to the tattoo transfer paper with a perfect skin on the skin surface. To record electrophysiological activity, the tattoo electrodes were connected to the acquisition system through PEDOT:PSS textile electrodes by applying a simple contact pressure between the tattoo and textile electrodes. To optimize the electrical performance of the conducting textile, we investigated the impact of the PEDOT:PSS layers on the resistance of printed square ($1,5x1,5$ cm^2). We printed 2, 4, 6 layers of the ink and observed the resistance decreased accordingly to the increasing conducting polymer thickness up to reach a plateau after 6 layers of printing PEDOT:PSS (Figure 5.2) which we attribute to correspond to a complete impregnation of the fabric by the conducting polymer.
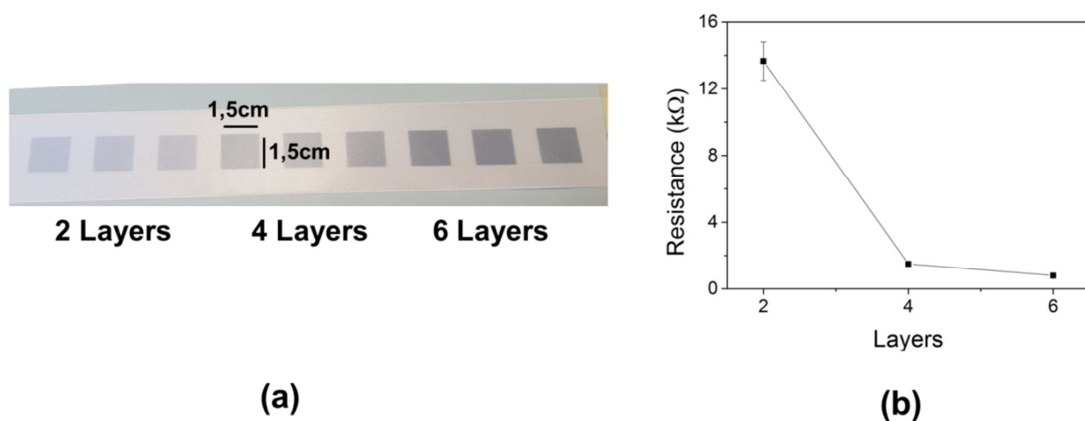
Figure 5.2 **Electrical characteristics of the printed textile.** (a) Photograph of the ribbon with 2, 4, 6 layers of PEDOT:PSS printed on the fabric, (b) Electrical resistance of the printed squares ($1,5x1,5$cm^2) (n=9)

Then we compared the electrode-skin impedances of the tattoo-textile electrodes, textile electrodes and wet Ag/AgCl electrodes (Figure 5.3.a). We observed that the textile electrode presented higher impedance than tattoo-textile electrode in the frequency range for EMG

study with a distinguishable peak at 50 Hz (frequency of ambient noise interferences) showing that fabric electrodes present a higher sensitivity to external noise than the tattoo-textile ones.
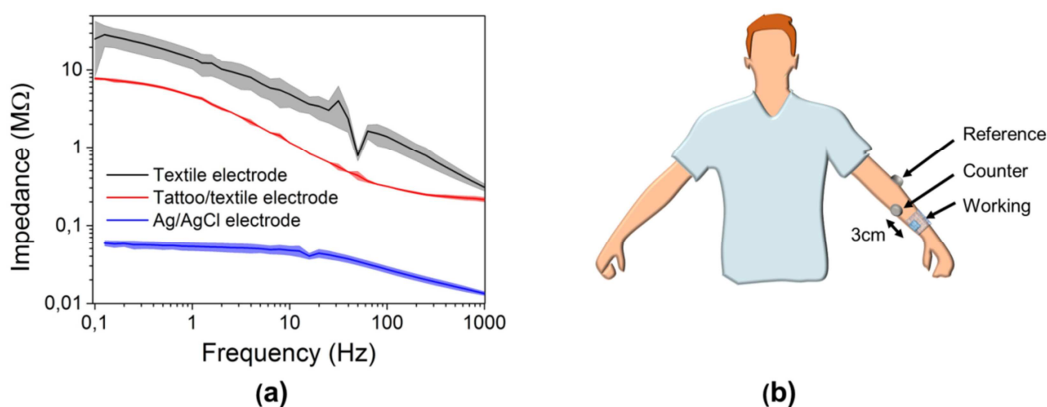
Figure 5.3 (**a**) **EIS Spectra measured from the textile electrodes, (b) Schematic of the experiment**

We also observed that the tattoo-textiles electrodes exhibited a better stability during the signal acquisition with a narrow error bar. The electrodes were placed on a volunteer as presented Figure 5.3.b. In comparison with the wet Ag/AgCl electrodes, the commercial electrodes displayed impedance values 2 orders of magnitude lower than tattoo electrodes for low frequencies (from 0,1Hz to 100 Hz) and 1 order of magnitude lower for higher frequencies (from 0,1Hz to 100 Hz) This difference could be explained by the presence of gel electrolyte in the wet Ag/AgCl electrodes which facilitate the transduction of ionic current into electronic current[26].

We observed the degradation of the tattoo film deposited on the skin in ambient environment for a period of 7 hours (Figure 5.4.a). The samples did not show visible deterioration of the film during the first 3 hours showing the stability of the tattoo over time. Then, we started to distinguish few cracks in the conducting film, which became clearly visible at T0+6h corresponding to the deterioration of the tattoo film/foil while exposed to ambient environment.

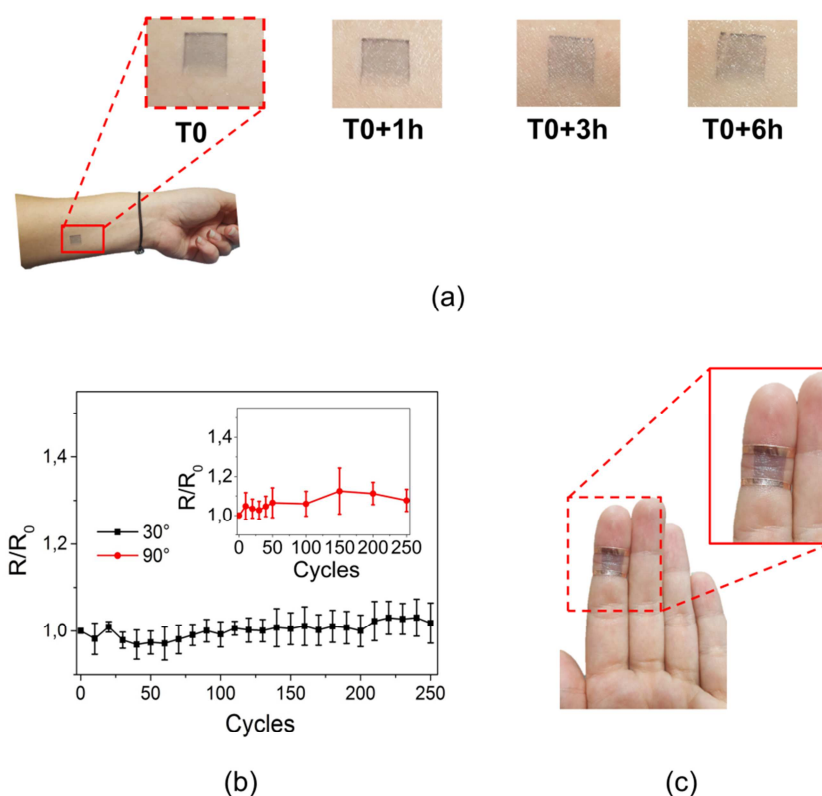Figure 5.4 **Evaluation of the functionality of the tattoo on the skin.** (a) Photographs of the printed tattoo on the forearm right after the deposition (T0), after 1h, (T1h), after 3h, (T3h), and after 6h, (T6h), (b) Variation of the electrical resistance of the printed tattoo after repeated contractions of the index at 30° and 90°, (c) Photograph of the flexion experiment

To evaluate the mechanical resistance of the tattoo, we measured its electrical resistance under repetitive flexions/extensions and compared it with the initial resistance value (Figure 5.4.b). We deposed a tattoo between the digital and intermediate phalanges or the index finger, and connected it with copper adhesives placed underneath it, on the edge of the conducting film (Figure 5.4.c). We recorded the electrical resistance of the PEDOT:PSS film after running multiple cycling tests while applying difference angles of bending (30° and 90°). We did not notice any significant variation in the electrical resistance at flexion 30° while there was a slight increase up to 20% for flexion 90° mostly attributed to the deterioration of the polymer film at the interface with thicker copper adhesive. This hypothesis, similar to the one proposed by Zucca et al [20], was confirmed by the observation of cracks formation at the adhesive-tattoo interface. In parallel, we verified the electrical properties of the textile

electrode by measuring the resistance of the printed textile before and after wearing the fabric for a period of 7 hours. We did not observed a fluctuation in the conducting polymer conductivity proving the stability of the textile electrodes over time.

To validate the use of our tattoo-textile system for physiological applications, we acquired ElectroMyoGraphy (EMG) on a volunteer, connecting the tattoo electrode to the acquisition system by a simple pressure contact through an electronic textile electrode (Figure 4.a). The electrodes have been positioned 2cm apart, on the lower part of the left arm biceps. We recorded EMG signals every 3 hours in 7 hour intervals (Figure 5.5).

Figure 5.5 **EMG recordings of the biceps contraction on a volunteer.** Comparison between the EMG signals measured from the textile electrodes, tattoo-textile electrodes and for wet Ag/AgCl electrodes after 2 long contractions (10s) and 5 short contractions (1s) at T0

Recordings used for SNR calculation, consisted of 10 seconds of resting and 10 seconds of contraction where the patient was asked to lift a 1Kg weight with an elbow angle around 90°. These experiments have been repeated 6 times for each interval. We compared the signals acquired from the tattoo electrodes with those acquired from textiles electrodes and the state of the art wet Ag/AgCl electrodes (Figure 5.6).
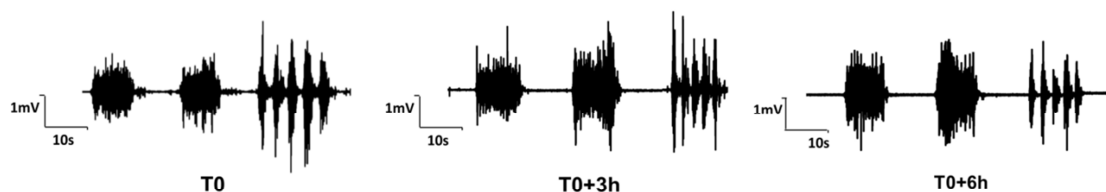
Figure 5.6 **EMG recordings of the biceps contraction on a volunteer.** Comparison between the EMG signals measured tattoo-textile electrodes after 2 long contractions (10s) and 5 short contractions (1s) at T0, at T0+3h and finally at T0+6h.

The latter have been position on the right arm. The Signal to Noise Ratio (SNR) has been calculated from these recordings.

The tattoos-textiles electrodes were able to detect biceps activity both short (1s) and long (10s) voluntary muscle contractions during 7 hours (Figure 5.5). The tattoo electrodes exhibited at T0 a mean SNR of 10.96±1.69dB versus 29.13±0.69dB and 18.21±1.55dB for wet Ag/AgCl electrodes and for textile electrodes respectively. After the deposition of the tattoo, we observed a substantial amelioration in the signal quality of the EMG recordings which we attributed to the moistening of the skin. This assumption was confirmed by the increase in the mean SNR extracted from the signals measured 3 hours later, e.g. 26.27±1.97dB against 25.10±1.35dB for the wet Ag/AgCl electrodes. In comparison, the dry textiles electrodes recordings exhibited a consistent quality of the signal acquisition during the day with a mean SNR value of 18.21±1.55dB lower than the tattoo-textile one after 3 hours.
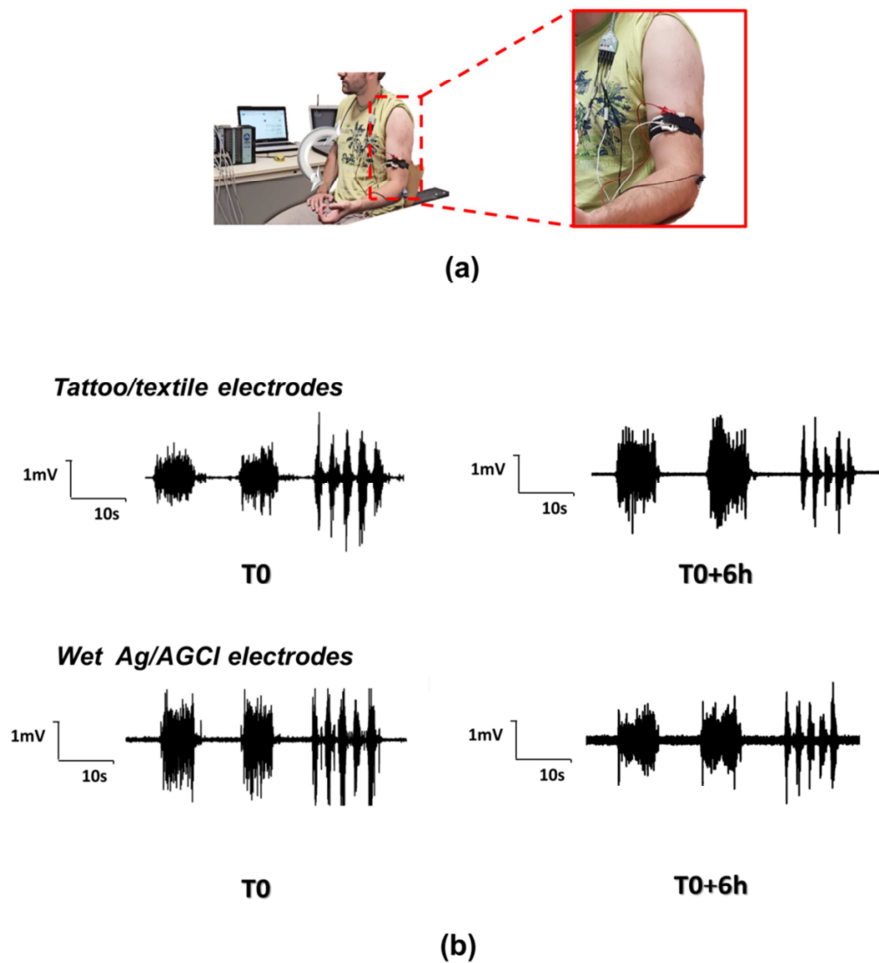
Figure 5.7. **EMG recordings of the biceps contraction on a volunteer.** (a) Photograph of the EMG experiment with a loop on the electrodes connection on the arm, (b) EMG signal measured at T0 and T0+6h for tattoo-textile electrodes and for wet Ag/AgCl electrodes after 2 long contractions (10s) and 5 short contractions (1s)

Interestingly, 6 hours after the first recordings, we did not notice visible deterioration of the tattoo deposited on the skin, we supposed that the moistening coming from the prolonged contact between the tattoo-skin interface and the textile prevented the apparition of cracks at the surface. Indeed, the tattoo-textile electrodes displayed similar performance than the wet Ag/AgCl electrodes with a mean SNR of 20.94±1.50dB and 19.71±4.62dB for the tattoo-textile and wet Ag/AgCl electrodes respectively at T0+6h demonstrating the stability of the tattoo-textile electrodes.

5.3   Discussion and Conclusions

In conclusion, we fabricated inkjet printed tattoo-textile electrodes mimicking commercial temporary tattoos using a biocompatible conducting polymer, PEDOT:PSS, as the transducer and we recorded neuro muscular activity such as EMG. The tattoo electrode, a low cost and noninvasive biomedical device, showed good conformation to the skin with no irritation or allergies. One of the major challenges for the advance for e-skin devices for the development of new health monitoring systems is to realize a smart interface connection between the data acquisition system and the electrophysiological signal measured on the skin without damaging the tattoo. Here, we presented a simple reliable method to connect the tattoo to the acquisition system using printed dry PEDOT:PSS textiles replacing traditional wires. This connection is done through a simple cutaneous contact with printed conducting textile with no degradation of the tattoo and successfully registered EMG on a volunteer. Our system was able to measure the signal from a biceps contraction for a period of 7 hours proving the stability and functionality of the system we proposed in this work. Performances of the tattoo-textile electrodes challenged the conventional wet Ag/AgCl electrodes for long term recordings. These results pave the way for an easy and low cost fabrication of e-skin and for a smart connection for electronic skin through smart clothes which could be further developed for embedded applications, for instance, for the integration in a myo-controlled prosthesis or for the detection of muscle injury.

5.4   Materials and methods

PEDOT:PSS ink: To formulate the PEDOT:PSS ink we prepared a solution including PEDOT:PSS (Heraeus, Clevios PH1000) dispersion, 20 wt% ethylene glycol (Sigma Aldrich) and 0.8 wt% glycidoxypropyltrimethoxysilane (GOPS, Sigma Aldrich) to prevent any delamination of the conductive pattern during the tattoo deposition on skin. We added 0.3% surfactants to adjust the surface tension of the ink (29 mN/m). We added a combination of organic solvents to fit the ink with the rheological requirements for inkjet process.

Ink-jet printing: We used a Dimatix DMP-2800 inkjet printer to fabricate the device. We respectively printed up to 6 layers of PEDOT:PSS on a commercial satin ribbon (Ideatiss). The dimensions are shown in figure S1. Then we printed 1 layer of a $1cm^2$ square of PEDOT:PSS on a commercial tattoo paper (Tattoo 2.1 the Magic Touch, 123 Applications). The drop spacing was 15 µm. The samples have been cured for 60 min at 110°C in a conventional oven. . The thickness of 1 PEDOT:PSS layer printed on the tattoo substrate was measured by using a mechanical profilometer (Ambios technology).The electrical characterization of a $1cm^2$ printed PEDOT:PSS square was conducted using a four point probe system (Jandel).

Electro-Chemical Impedance Spectroscopy: We performed the EIS measurements on a volunteer using a potentiostat (Metrohm Autolab B.V.) and it software NOVA. We did not apply any constant differential voltage. The experiments were conducted by applying a sinusoidal signal of 10 mV. The range of frequency selected was varying from 0.1Hz to 1000Hz. The working and counter electrodes were respectively placed 3cm apart from each other on a forearm of a volunteer and the reference was placed in the elbow. The electrodes we characterized during EIS measurements were the working electrodes while the counter and the reference have been kept fixed (e.g. wet Ag/AgCl electrodes).

Mechanical characterization: We evaluated the mechanical resistance of the tattoo by measuring its resistance after multiple flexion/extension of a finger. The tattoo was placed across the distal phalange of the index finger. The connection was made by two copper tapes underlying the printed PEDOT:PSS square on opposite edge. The flexion/extension was repeated 250 times at 30° and at 90° angle of closure. The resistance was measured every 10 repetitions.

EMG Data Acquisition: Informed consents have been signed by volunteers participating in the study. A RHD2216 chip from Intan Technologies has been used to acquire EMG data. The data were encoded on 16 bits at 1.1 kHz per channels. The on-chip filters were set as follow: the first order high pass was set at 10 Hz and the third order low pass filter was set at 300Hz. 2 EMG were recorded at the same time. Two tattoo electrodes were placed two

centimeter apart at the center of the biceps of the left arm. Textile electrodes were placed on top of these tattoos in order to connect them. The second recording was done on the biceps of the right arm thanks to two wet Ag/AgCl electrodes. In order to have comparable signals, two weight of 1Kg were used during the experiment. A ground electrode was placed on the right leg. Each recording has been repeated at least 6 times at t0, t0+3h and t0+6h.

Data Post-processing: Labview software was used to filter and calculate signal-to-noise-ratio (SNR) from the recorded signal. A first order Butterworth band-pass, from 10Hz to 300Hz, was applied to all recording. Then the SNR value of each signal was calculated using the following equation: $SNR(Sr) = 20 * \log\left(\sqrt{\dfrac{\sum_i Sc_i^2}{\sum_i Sr_i^2}}\right)$, where Sc is a portion of 5 seconds of the signal during a contraction and Sr is a portion of 5 seconds of the signal during a resting position.

All protocols and procedure were approved by the direction of research of the Ecole des Mines de St. Etienne. All volunteers provided informed signed consent to participate in the study.

5.5   References and Notes

1.   N, Mazzaro. Risk of skin reaction when using ECG electrodes. (2016). Available at: http://www.ambu.es/files/billeder/es/micro/cardiologia/the_risk_of_skin_reactions_using_ecg_electrodes_0711.pdf. (Accessed: 22nd July 2016)

2.   Tao, X. M. *Smart Fibres, Fabrics and Clothing: Fundamentals and Applications*. (Elsevier, 2001).

3.   Park, S. & Jayaraman, S. Smart textiles: Wearable electronic systems. *MRS Bull.* **28,** 585–591 (2003).

4.   Matsuhisa, N. *et al.* Printable elastic conductors with a high conductivity for electronic textile applications. *Nat Commun* **6,** (2015).

5.   Wagner, S. *et al.* Electronic skin: architecture and components. *Phys. E Low-Dimens. Syst. Nanostructures* **25,** 326–334 (2004).

6.   Kim, D.-H. *et al.* Epidermal Electronics. *Science* **333,** 838–843 (2011).

7.   Tee, B. C.-K., Wang, C., Allen, R. & Bao, Z. An electrically and mechanically self-healing composite with pressure- and flexion-sensitive properties for electronic skin applications. *Nat. Nanotechnol.* **7,** 825–832 (2012).

8.   Yeo, W.-H. *et al.* Multifunctional Epidermal Electronics Printed Directly Onto the Skin. *Adv. Mater.* **25,** 2773–2778 (2013).

9.   Huang, X. *et al.* Materials and Designs for Wireless Epidermal Sensors of Hydration and Strain. *Adv. Funct. Mater.* **24,** 3846–3854 (2014).

10.   Takamatsu, S. *et al.* Direct patterning of organic conductors on knitted textiles for long-term electrocardiography. *Sci. Rep.* **5,** (2015).

11.   Papaiordanidou, M. *et al.* Cutaneous Recording and Stimulation of Muscles Using Organic Electronic Textiles. *Adv. Healthc. Mater.* **5,** 2001–2006 (2016).

12.   Rattfält, L., Lindén, M., Hult, P., Berglin, L. & Ask, P. Electrical characteristics of conductive yarns and textile electrodes for medical applications. *Med. Biol. Eng. Comput.* **45,** 1251–1257 (2007).

13.   Magill, A. & Remy, M. A. *Health monitoring garment*. (2003).

14.   Kang, I., Schulz, M. J., Kim, J. H., Shanov, V. & Shi, D. A carbon nanotube strain sensor for structural health monitoring. *Smart Mater. Struct.* **15,** 737–748 (2006).

15.   Shim, B. S., Chen, W., Doty, C., Xu, C. & Kotov, N. A. Smart Electronic Yarns and Wearable Fabrics for Human Biomonitoring made by Carbon Nanotube Coating with Polyelectrolytes. *Nano Lett.* **8,** 4151–4157 (2008).

16.   Berggren, M. & Richter-Dahlfors, A. Organic Bioelectronics. *Adv. Mater.* **19,** 3201–3213 (2007).

17.   Greco, F. *et al.* Ultra-thin conductive free-standing PEDOT/PSS nanofilms. *Soft Matter* **7,** 10642 (2011).

18.   Greco, F., Zucca, A., Taccola, S., Mazzolai, B. & Mattoli, V. Patterned Free-Standing Conductive Nanofilms for Ultraconformable Circuits and Smart Interfaces. *ACS Appl. Mater. Interfaces* **5,** 9461–9469 (2013).

19. Zucca, A. *et al.* Tattoo Conductive Polymer Nanosheets for Skin‐Contact Applications. *Adv. Healthc. Mater.* **4,** 983–990 (2015).

20. Zucca, A. *et al.* Roll to roll processing of ultraconformable conducting polymer nanosheets. *J. Mater. Chem. C* **3,** 6539–6548 (2015).

21. Bareket, L. *et al.* Temporary-tattoo for long-term high fidelity biopotential recordings. *Sci. Rep.* **6,** 25727 (2016).

22. Limb Loss Awareness Month | Amputee Coalition.

23. Roberts, T. *et al.* Flexible Inkjet-Printed Multielectrode Arrays for Neuromuscular Cartography. *Adv. Healthc. Mater.* **5,** 1462–1470 (2016).

24. Scheiblin, G. *et al.* Screen-printed organic electrochemical transistors for metabolite sensing. *MRS Commun.* 1–5 doi:10.1557/mrc.2015.52

25. Bihar, E. *et al.* A Disposable paper breathalyzer with an alcohol sensing organic electrochemical transistor. *Sci. Rep.* **6,** 27582 (2016).

26. Searle, A. & Kirkup, L. A direct comparison of wet, dry and insulating bioelectric recording electrodes. *Physiol. Meas.* **21,** 271 (2000).

Chapter 6

Introduction to OECTs for biosensing

Organic electrochemical transistors (OECTs) recently demonstrated their high potential for biomedical applications especially in the case when PEDOT:PSS is used as the active material for transducing the biological signal in electronic current. OECTs present inherent signal amplification properties which render them ideal for implementation in the field of biosensing such as the detection of specific analytes in the physiological milieu.

In this chapter, I introduced the basic principles about transistors and especially OECTs as transducers for biosensing applications.

6.1   Bioelectronics and biosensing

Bioelectronics is a field of research where the combination of electronic and ionic conductivity of conducting polymers allows to efficiently link the abiotic world of electronics, where the dominant charge carriers are the electrons, with the ionic biological milieu. Based on that, biomedical devices with new and outstanding functionalities emerge, aiming to effectively interface the abiotic/biotic environment and thus provide solutions to unmet clinical needs.

6.2   Organic transistor

Since the first patent of the Field effect transistor (FET) in 1925 by J. E. Lilienfeld, FETs dominated the microelectronics market industry as a fundamental building block for the fabrication of electronic circuits such as amplifiers and microprocessors. . However the FETs silicon based technology requires manufacturing processes that involve high temperature and sophisticated photolithographic patterning methods which render it non compatible with the development of disposable and low cost sensors on flexible substrate.

The new generation of transistors called Organic Thin Film Transistors (OTFTs), firstly described in 1986, and which established the use of organic semiconductors offered an alternative pathway to novel applications such as e-paper, sensors etc. The use of organic semiconductors led to a remarkable progress in the transistors fabrication avoiding the use of high temperature and low pressure, and thus enabled their integration in large area and low cost substrates such as plastics, glass or papers. To this end, OTFTs have attracted a lot of attention in the last decades for their potential as sensing devices allowing for new electronics with low manufacturing costs.

As for traditional transistors, OTFTs are three terminal electrical devices. The current between 2 electrodes (the source and the drain) is modulated by the gate voltage or current. OTFTs can be distinguished in different sub-classes.

6.3   Organic electrochemical transistor (OECT)

In particular, organic electrochemical transistors (OECTs) have emerged as especially promising organic electronic devices. The OECT was first reported by White et al.[1]. Their mechanism is based on the oxidation or reduction reaction occurring at the conjugated polymer which is doped or dedoped. In a similar three terminal device configuration, the source and the drain electrodes are connected via a (semi)conducting channel, and a gate electrode via an ionic electrolyte. In Particular, for PEDOT:PSS, the application of a gate bias (V_G), results in the modulation of the channel current, through the electrolyte which pushed cations in the channel, changing its doping state and thus its conductivity[2] which reduces the

drain current (I_D). Figure 7.1 shows a schematic cross-section of a typical OECT configuration comprised of a Ag/AgCl gate electrode and a PEDOT:PSS channel as well as the equivalent ionic circuit of the OECT.
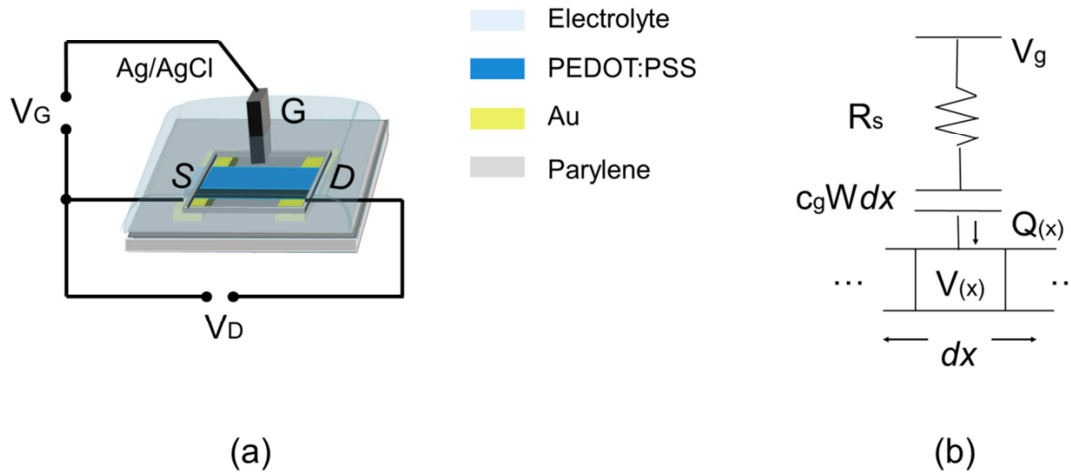

Figure 6.1**The OECT:** a. Schematic cross-section of an OECT, b. Ionic equivalent circuit of OECT

Being the electrolyte an integral part of the device, as in the case of OECTs, makes the devices compatible with aqueous solution thus enabling a direct interface between the biological media and the electronics. Apart from OECTs, Electrolyte Gated Organic Field Effect Transistors (EGOFETs) are also gated through an electrolyte thus enabling such interface as well and have been extensively used for biological applications[3–5]. Electrolyte gated transistors (both OECTs and EGOFETs) offer also the advantage of low bias operation. The main difference between the two aforementioned device configurations lies in the charge transport dimensionality at the electrolyte/semiconductor interface. In particular, in the case of a field effect operation (EGOFETs), electrostatic charges accumulate at the interface, whereas in an OECT, ions penetrate into the bulk of the channel thus volumetrically doping it[6].

A significant advantage of the OECT versus its electrolyte gated counterparts is the efficiency of the ionic signal transduction, in other words the transconductance. Indeed, OECTs have proven to exhibit the highest transconductance (g_m) defined as $g_m = \partial I_D/\partial V_G$ among electrolyte-gated transistors of comparable geometry, owing to the volumetric

capacitance of the conducting channel[7]. In the case of biosensing aplications, transconductance can be undoubtedly considered the figure of merit, since it sensitively quantifies the magnitude of the I_D, in response to a change in the V_G. It was also recently shown by Rivnay et al. that the value of the transconductance of an OECT can be customized by not only changing the channel geometry but also the conducting polymer film thickness, owing to its volumetric capacitance[6]. In general, it was proven that by tuning the device geometry there is a trade-off between fast response and high currents thus leading to different device characteristics depending on the application of interest.

6.4   Applications of the OECT

Arguably, the amplification properties of OECTs have led to their successful implementation in the field of biosensing, exhibiting excellent analytical sensor characteristics such as sensitivities. PEDOT:PSS represents to date the champion material of organic bioelectronics and has been typically employed as the active layer of OECTs and used for various biosensing applications. Some examples of PEDOT:PSS based OECT biosensors include ion selective sensors[8], cell-based sensors [9,10] and when coupled with redox enzymes, as biocatalytic sensors for the detection of human metabolites such as glucose and lactate[11–13].Metabolite sensing (usually using enzymatic determination) holds great potential for point of care (POC) diagnostics. Recently, a POC biosensing platform comprised of a photolithographically fabricated PEDOT:PSS based OECT array was demonstrated, for the simultaneous detection of three critical metabolites, glucose, lactate and cholesterol[14] This multiplatform allowed for direct metabolite detection from human saliva samples, using only one drop of saliva. The planar device configuration (source, drain gate in the planar) allowed for the implementation of a microfluidic to facilitate the sample distribution and thus render the process more controllable as well as automated.

Apart from high sensitivity and multiplexing, the need for low cost and stable biosensors requires the use of alternative fabrication techniques. The solution processability of the organic materials like PEDOT:PSS allows for scalable and high throughput production toward cost effective, automated, rapid and portable next generation devices.

To this end, printing techniques emerge as a viable alternative to the conventional photolithographic approaches. For instance, screen printing was studied for its convenience to use different materials, and its feasibility for multiple biological applications such as metabolite sensing [15,16] Lately, OECTs onto textile were fabricated via a screen printing approach and the proposed platform served for chemical sensing showing potential for further integration in wearable devices[17].

Other additives printing techniques have been instigated to generate active layers of circuits such as electrochemical diodes and transistors[18]. Inkjet process is an ideal alternative to photolithography for the deposition of a wide range of inks. Mannerbro et al were the first to realize an all inkjet printed OECT in 2008 [19,20]. They implemented the transistor and also simple electrochemical circuitry was demonstrated on flexible substrates. For the fabrication of those first printed OECTs a low cost desktop thermal inkjet printer was used. Recent studies[21] have also explored the possibilities to use inkjet technology to realize OECTs for applications in biosensors. Basirico et al [20] have reported on the fabrication of an all-organic printed electrochemical transistor made from PEDOT:PSS with enhanced conductivity by using a post treatment. Moreover they studied the effects of tuning the device geometry (i.e. varying the ratio between the gate and channel area to the OECT performance.

Recently, we inkjet print OECTs on paper and we use them for the enzymatic determination of alcohol in human breath[22]. Particularly, by the immobilization of the alcohol dehydrogenase enzyme and its cofactor both embedded in a electrolyte gel which immobilized onto the OECT, the determination of alcohol could be achieved. The enzymatic reaction was found to result in a decrease of the OECT source-drain current in a way which is proportional to the alcohol concentration. This work is described in the following chapter.

Overall, OECTs possess numerous advantages for biosensing and particularly enzymatic sensing including a wide electrochemical window of operation, high ionic strength, low evaporation rates, and versatility in the biofunctionalization scheme, that render them especially promising devices for POC diagnostics. . In combination with printing technology they show promising possibilities

6.5   First printed OECTs characterizations

In this section, I present the preliminary work conducted on the fabrication of inkjet printed OECTs. At first I focused on to validating the functionality of the PEDOT:PSS ink through the fabrication and characterization of functional OECT devices on glass substrates.

To evaluate the electrical performance of the devices, a comparison of OECTs made by spincoated PEDOT:PSS formulation[13,14] already described in literature (e.g. Clevios PH100, 5%wt of ethylene glycol, 1%wt of GOPs and DBSA) and inkjet printed OECTs of identical dimensions using my optimized ink was conducted.

For the deposition and patterning of the channel, a traditional spin coater (Laurell Technologies) and a polyimide mask were used. For an accurate comparison, the speed (1000RPM, 30s) was selected accordingly to achieve similar thickness with the one obtained for 2 printed layers (i.e.190nm). Both samples were cured using a traditional oven for 30min at 160°C.

To estimate the conductivity of the ink, electrical measurements were carried with a 4 point probes equipment (Jandel). The sheet resistance was measured on test vehicles of a 1cm x 1cm square and the conductivity was calculated using the following formulas:

$$\rho = R_{sheet} \text{ x } e \quad (1)$$

$$\sigma \quad = \frac{1}{\rho} \quad (2)$$

Where ρ is the resistivity of the material (Ω.m), R_{sheet} is the measured sheet resistance (Ω./sq), e the thickness (m) of the layer measured using mechanical profiler (Ambios technology), and σ is the conductivity of the material (S/m).

The electrical properties of both formulations showed comparable conductivities: 350S/cm for the spin coated formulation and 420S/cm for the inkjet printed one.

Following printed OECTs were realized that consist of PEDOT:PSS channel, and a Ag/AgCl gate electrode. The electrical contacts to connect the device with the acquisition system were consisted of a 100 nm thick layer of Au deposited using evaporation technique.   Gold is

preferred as it ensure an ohmic contact with PEDOT:PSS and thus a sufficient carrier injection. A standard Phosphate Buffer Saline solution (PBS, 0.1M) was used as the electrolyte of the OECT. A PDMS "donut shape" wall was used to confine the electrolyte in the active area of the transistor. The channel was printed or spin coated onto glass slide (figure 6.2). For the printing parameters, a drop spacing of 25µm was used and 2 layers of PEDOT:PSS were printed for the fabrication of the devices. The spin coating parameters and curing conditions were similar to the ones selected for the test vehicles used for electrical resistance measurements. The dimensions of the PEDOT:PSS channel were 5mm x 5mm x 190nm (W x L x e). Before the spin coating, a plasma treatment (120W, 2min) was realized on the substrate to ensure a better wettability of the spin coated formulation. Note that no prior surface treatment was applied for the inkjet deposition. (The surface tension measured by a goniometer was 71mN/m for the spin coated ink against 29mN/m for the inkjet ink).
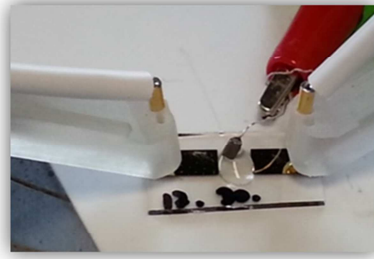
(a)
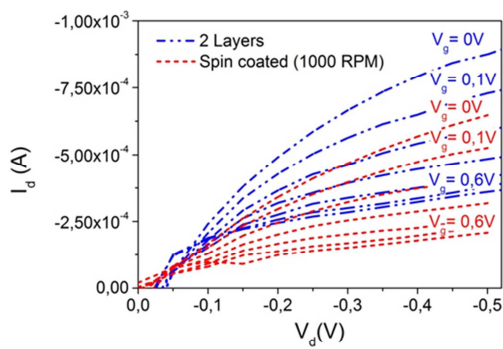
(b)
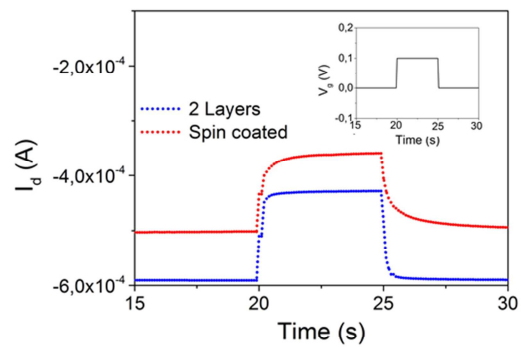
(c)

Figure 6.2 (a) Photograph of the inkjet printed OECT, (b). Comparative electrical response of the OECTs made by spin coating and inkjet printing OECTs (c) Transient

response of the drain current to a square pulse (0,1V) at the gate for 5s for the spin coat and inkjet printed OECTs

Figure 6.2 shows the typical curves (I_d vs. V_d) for both inkjet-printed and spin coated devices. The optimum transconductance $g_m = \partial I_D/\partial V_G$ calculated at V_d=-0,5V was found to be 1,22 mS vs. 1,63 mS while the response time was found to be 190ms vs. 175ms for the spin coated and the printed devices, respectively. The ink formulated exhibits comparable and even better characteristics than the one already used in literature

For the fabrication of printed biosensors, the Ag/AgCl gate was replaced by a printed PEDOT:PSS gate to realize an OECT with a planar configuration. This allows automation and miniaturization. Moreover it allows future integration of micro-fluidics thus enabling the construction of highly integrated platforms. The PEDOT:PSS ink was successfully tested and printed on different substrates such as polyimide (125µm), Polyester (50µm), a commercial glossy paper and a textile (ribbon) (Figure 6.3). The dimension of the gate was 5mm x 2mm and for the channel was 5mm x 500µm.
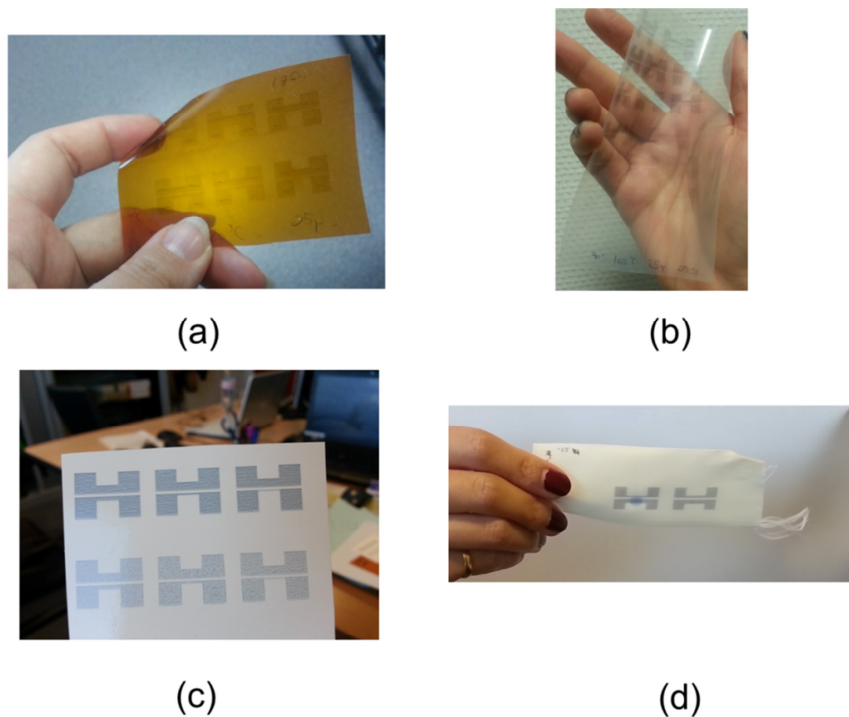

(a)

(b)

(c)

(d)

Figure 6.3 **Inkjet-Printed OECTs on different substrates:** (a) kapton, (b) polyester, (c) paper, (d) textile

The substrate selected for the case of biosensing application was the commercial coated paper (Arjowiggins, REF) since it is a disposable, biodegradable, low cost substrate and perfect for single use applications. The output characteristics of OECTs on this paper substrate were compared with the ones of the conventional plastic substrates (Polyimide and Polyester) and demonstrated transconductance in the same range (Figure 6.4) e.g. 0.13mS vs. 0.31mS and 0.20mS for paper, polyester, and kapton respectively
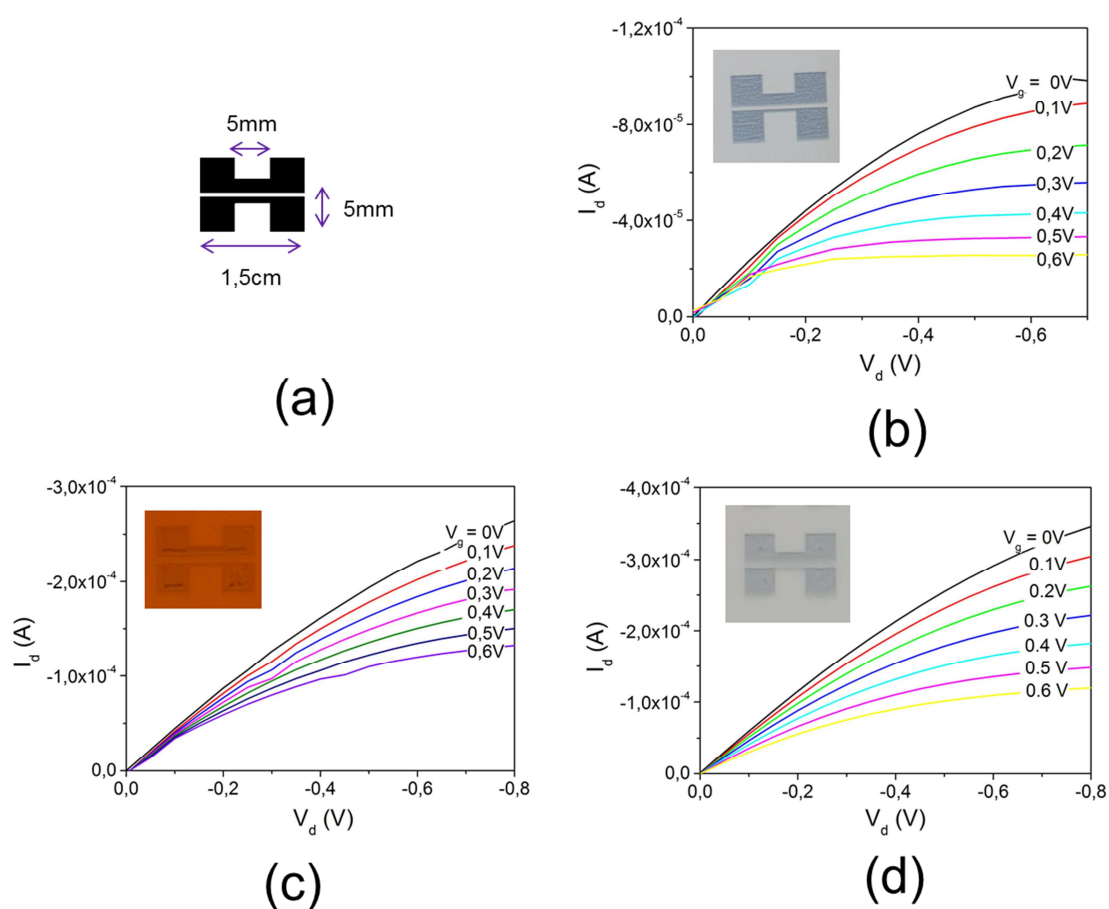

Figure 6.4 **The schematic of OECT:** (a). Schematic the printed OECT, Id versus Vd for OECTs printed on (b) paper, (c) kapton, (d) polyester

The response time of the device was estimated at 50ms (figure 7.5) which is suitable for the applications targeted during this PhD such as alcohol sensing presented in the following chapter.
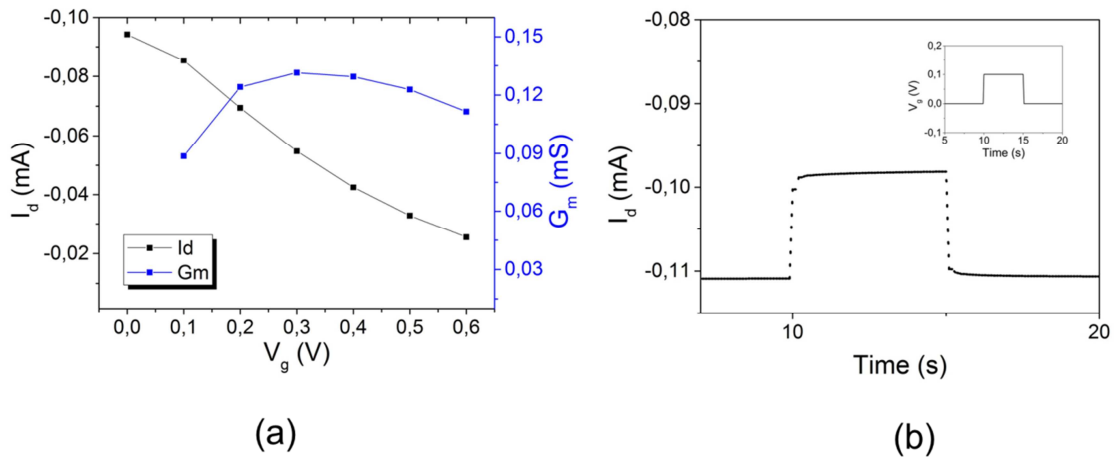
Figure 6.5 **Characteristics of the printed OECT on paper (2Layers)** (a) Transfer and transconductance curves for Vd=-0.6V (b) Transient response of the drain current to a square pulse (0,1V) at the gate for 5s.

6.6 References

1.   White, H. S., Kittlesen, G. P. & Wrighton, M. S. Chemical derivatization of an array of three gold microelectrodes with polypyrrole: fabrication of a molecule-based transistor. *J. Am. Chem. Soc.* **106,** 5375–5377 (1984).

2.   Strakosas, X., Bongo, M. & Owens, R. M. The organic electrochemical transistor for biological applications. *J. Appl. Polym. Sci.* **132,** (2015).

3.   Marinelli, F. *et al.* An organic field effect transistor as a selective NO x sensor operated at room temperature. *Sens. Actuators B Chem.* **140,** 445–450 (2009).

4.   Torsi, L., Magliulo, M., Manoli, K. & Palazzo, G. Organic field-effect transistor sensors: a tutorial review. *Chem. Soc. Rev.* **42,** 8612–8628 (2013).

5.   Schmoltner, K., Kofler, J., Klug, A. & List-Kratochvil, E. J. Electrolyte-Gated Organic Field-Effect Transistor for Selective Reversible Ion Detection. *Adv. Mater.* **25,** 6895–6899 (2013).

6.   Rivnay, J. *et al.* High-performance transistors for bioelectronics through tuning of channel thickness. *Sci. Adv.* **1,** (2015).

7.   Khodagholy, D. *et al.* High transconductance organic electrochemical transistors. *Nat Commun* **4,** (2013).

8.   Sessolo, M., Rivnay, J., Bandiello, E., Malliaras, G. G. & Bolink, H. J. Ion-Selective Organic Electrochemical Transistors. *Adv. Mater.* **26,** 4803–4807 (2014).

9.   Jimison, L. H. *et al.* Measurement of Barrier Tissue Integrity with an Organic Electrochemical Transistor. *Adv. Mater.* **24,** 5919–5923 (2012).

10. Rivnay, J. *et al.* Organic electrochemical transistors for cell-based impedance sensing. *Appl. Phys. Lett.* **106,** 43301 (2015).

11. Tang, H., Yan, F., Lin, P., Xu, J. & Chan, H. L. W. Highly Sensitive Glucose Biosensors Based on Organic Electrochemical Transistors Using Platinum Gate Electrodes Modified with Enzyme and Nanomaterials. *Adv. Funct. Mater.* **21,** 2264–2272 (2011).

12. Khodagholy, D. *et al.* Organic electrochemical transistor incorporating an ionogel as a solid state electrolyte for lactate sensing. *J. Mater. Chem.* **22,** 4440 (2012).

13. Strakosas, X. *et al.* Catalytically enhanced organic transistors for in vitro toxicology monitoring through hydrogel entrapment of enzymes. *J. Appl. Polym. Sci.* (2016).

14. Pappa, A. *et al.* Organic Transistor Arrays Integrated with Finger-Powered Microfluidics for Multianalyte Saliva Testing. *Adv. Healthc. Mater.* **5,** 2295–2302 (2016).

15. Scheiblin, G. *et al.* Screen-printed organic electrochemical transistors for metabolite sensing. *MRS Commun.* 1–5 doi:10.1557/mrc.2015.52

16. Scheiblin, G. *et al.* Fully printed metabolite sensor using organic electrochemical transistor. in **9568,** 95681E–95681E–6 (2015).

17. Gualandi, I. *et al.* Textile Organic Electrochemical Transistors as a Platform for Wearable Biosensors. *Sci. Rep.* **6,** 33637 (2016).

18. Chen, M. Printed Electrochemical Devices Using Conducting Polymers as Active Materials on Flexible Substrates. *Proc. IEEE* **93,** 1339–1347 (2005).

19. Mannerbro, R., Ranlöf, M., Robinson, N. & Forchheimer, R. Inkjet printed electrochemical organic electronics. *Synth. Met.* **158,** 556–560 (2008).

20.	Basiricò, L. *et al.* Electrical characteristics of ink-jet printed, all-polymer electrochemical transistors. *Org. Electron.* **13,** 244–248 (2012).

21.	Andersson Ersman, P., Nilsson, D., Kawahara, J., Gustafsson, G. & Berggren, M. Fast-switching all-printed organic electrochemical transistors. *Org. Electron.* **14,** 1276–1280 (2013).

22.	Bihar, E. *et al.* A Disposable paper breathalyzer with an alcohol sensing organic electrochemical transistor. *Sci. Rep.* **6,** 27582 (2016).

Chapter 7

A case on study : alcohol sensor

This chapter is based on the following publication:

"A Disposable paper breathalyzer with an alcohol sensing organic electrochemical transistor"

Eloïse Bihar, *† Yingxin Deng, † Takeo Miyake, Mohamed Saadaoui, George G. Malliaras, and Marco Rolandi, Scientific reports, 2016, doi:10.1038/srep27582.*

In this chapter, we demonstrate a proof-of-concept disposable breathalyzer using an organic electrochemical transistor (OECT) modified with alcohol dehydrogenase (ADH) as the sensor. The OECT is made with the conducting polymer poly(3,4-ethylenedioxythiophene):poly(styrenesulfonate) (PEDOT:PSS), and is printed on paper. ADH and its cofactor nicotinamide adenine dinucleotide (NAD^+) are immobilized onto the OECT with an electrolyte gel. When the OECT-breathalyzer is exposed to ethanol vapor, the enzymatic reaction of ADH and ethanol transforms NAD^+ into NADH, which causes a decrease in the OECT source drain current. In this fashion, the OECT-breathalyzer easily detects ethanol in the breath equivalent to BAC from 0.01% to 0.2%. The use of a printed OECT may contribute to the development of breathalyzers that are disposable, ecofriendly, and integrated with wearable devices for real-time BAC monitoring.

7.1   Introduction

The euphoria from drinking alcoholic beverages makes them popular worldwide. Abuse in alcohol (ethanol) consumption leads to dependence, behavioral problems, and fatal accidents[1]. In 2013, 10,076 people lost their lives in alcohol-related-driving accidents in the United States alone, accounting for nearly 31% of all traffic related deaths[1]. Driving under the influence is illegal and the maximum allowed blood alcohol concentration (BAC) is 0.05-0.08%, in most countries [2]. A breathalyzer measures the concentration of ethanol in the breath to estimate the BAC of an individual. The first generation of breathalyzers uses a liquid dye sensitive to ethanol exposure, potassium dichromate, and a photodetector[3]. Reliability of these detectors is a challenge and potassium dichromate is environmentally toxic[3]. A new generation of breathalyzers uses the ethanol in the breath to power a fuel cell whose output is proportional to the ethanol concentration[4]. These breathalyzers are connected directly to smart phones to test one's alcohol level before attempting to drive. However, these breathalyzers are still impractical because they require constant recalibration[4]. To-date the most reliable BAC tests and the only one that is admissible in court is the blood test, which is difficult to administer on site or for preventative purposes. A breathalyzer as easy to use as an inexpensive and disposable glucose paper-strip sensor would greatly simplify BAC testing[5].

Organic electrochemical transistors (OECTs) are excellent candidates for disposable biosensors because they are inexpensive, they can be made on flexible substrates, and they can be printed on paper [6,7]. OECTs are typically made with poly(3,4-ethylenedioxythiophene) doped with poly(styrenesulfonate) PEDOT:PSS. PEDOT:PSS is a *p*-type organic semiconductor with several applications in bioelectronics[8,9]. Coupled with enzymes in the electrolyte, PEDOT:PSS OECTs are able to detect micro molar glucose concentration in human blood and sweat[10]. OECTs sensors are amenable to screen-printing[11] and inkjet printing[12] for rapid and inexpensive manufacturing. Here, we demonstrate an early stage proof-of-concept OECT-breathalyzer on paper by integrating a PEDOT:PSS OECT with the enzyme alcohol dehydrogenase.
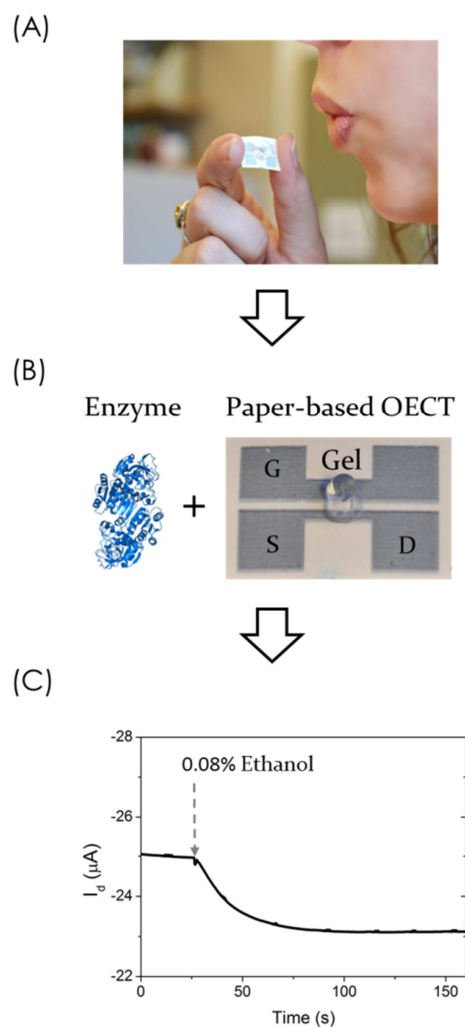
Figure 7.1 **Concept of the OECT-breathalyzer. (A)** Simply breathing on the printed PEDOT:PSS OECT allows for alcohol detection. **(B)** The alcohol dehydrogenase (ADH) enzyme and the OECT are the key components of the sensor. The OECT is printed on paper, and comprises a channel, source (S), drain (D), and gate (G) electrodes made of PEDOT:PSS. The enzyme electrolyte gel is deposited to the OECT bridging the channel and gate. **(C)** I_d response of the OECT upon exposure to ethanol.

This proof-of-concept OECT-breathalyzer may aid the development of a breathalyzer that is easy-to-use, inexpensive, easily calibrated, and can be coupled with a cell-phone or a smart watch for BAC self-testing to reduce alcohol related traffic accidents.

7.2 Results

The OECT is printed on a paper substrate that is approximately 1.5 cm x 1 cm and it is easy to handle. Breathing onto the device enables detection of ethanol concentration in the breath (Figure 7.1.A). The printed OECT on paper has planar geometry with channel, source (S), drain (D), and gate (G) electrodes made of PEDOT:PSS (Figure 7.1.B), a structure that is compatible with rapid, one-step fabrication of the device. We modify commercially available PEDOT:PSS to make it compatible with inkjet printing on paper. A key challenge for the fabrication of an enzyme-based OECT sensor is the immobilization of the enzyme and its cofactor. In this work, the enzyme alcohol dehydrogenase (ADH) and its cofactor nicotinamide adenine dinucleotide (NAD^+) are trapped in a collagen-based gel deposited onto the channel of the OECT (Figure 7.1.B). Exposing the OECT-breathalyzer to ethanol from the breath causes a marked decrease of the source-drain current, I_d, which is used as the output signal for detection (Figure 7.1.C).

The decrease in I_d upon ethanol exposure arises from a series of chemical reactions that oxidize ethanol into acetaldehyde and produce electrons as byproducts, which in turn decrease the conductivity of the OECT channel (Figure 7.2.A).
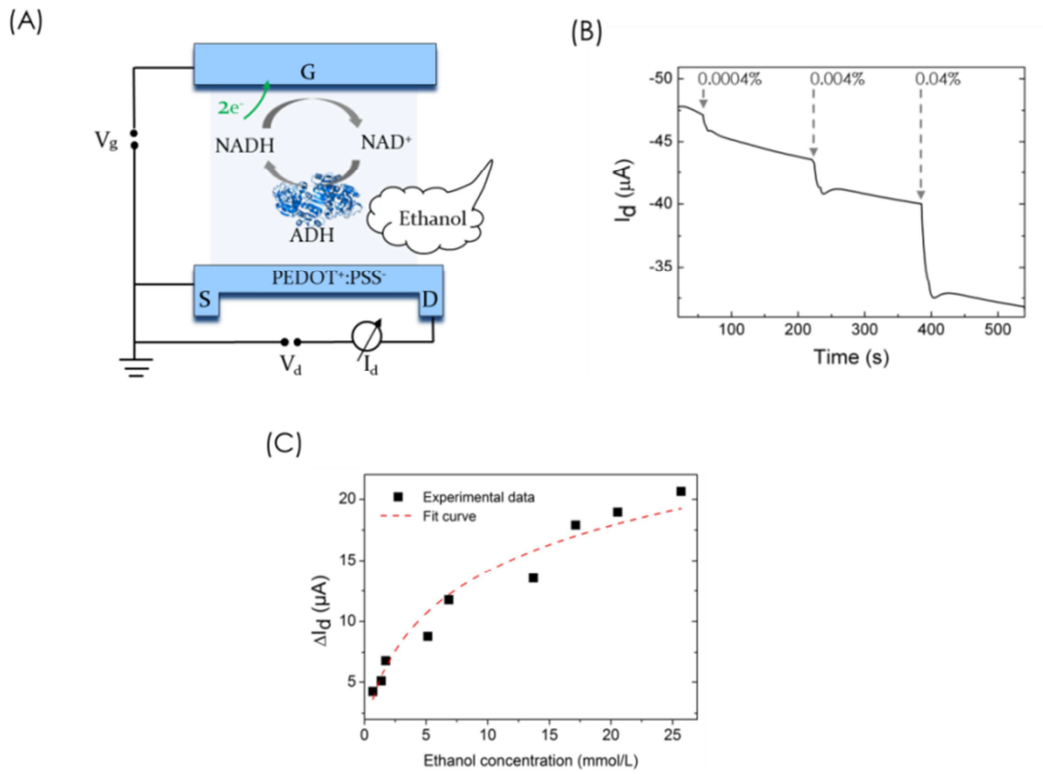
Figure 7.2 **Alcohol detection in solution.** **(A)** Enzymatic reaction of ethanol and ADH in electrolyte solution. Ethanol is oxidized to acetaldehyde, and NAD^+ is reduced to NADH. **(B)** Step change in I_d when adding 0.0004%, 0.004%, and 0.04% ethanol solutions, with $V_g = 0.5$ V, $V_d = -0.7$ V. **(C)** Variation of I_d is plotted at different alcohol concentrations in solution. $\Delta I_d = (I_0 - I_d)$, where I_0 is I_d before exposure to ethanol. The dash line is a fit to equation (3).

First the reaction:

$$CH_3CH_2OH + NAD^+ \overset{ADH}{\longleftrightarrow} CH_3CHO + NADH + H^+ \quad (1)$$

yields the reduced form of nicotinamide adenine dinucleotide (NADH), which itself oxidizes according to [13]:

$$NADH \rightarrow NAD^+ + H^+ + 2e^- \quad (2)$$
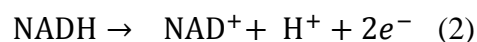
The electrons produced by the NADH oxidation are collected from the gate electrode of the OECT-breathalyzer (Fig. 7.2A), and cause a shift of the applied gate potential to the channel/electrolyte interface, leading to a decrease in I_d [14]. I_d is written as [14]:

$$\Delta I_d \sim g_m \cdot \frac{kT}{2e} \cdot \ln[C] \qquad (3)$$

where g_m is the transconductance of the OECT and C is the concentration of the molecule contributing electrons to the gate (NADH in this case) (Figure 7.3 and Figure 7.4).
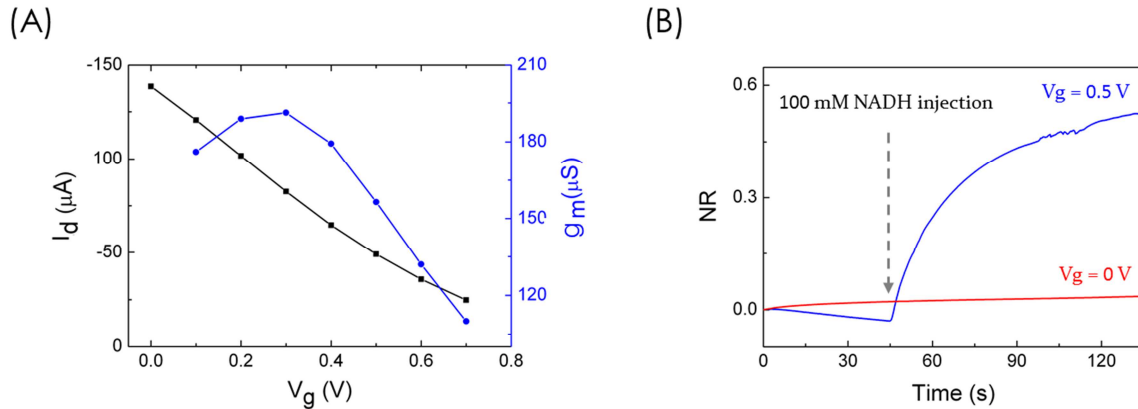

Figure 7.3 **PEDOT:PSS OECT alcohol sensor characteristics. (A)** Transfer curve and resulting transconductance of OECT with 0.2wt% bovine gel at $V_d = -0.7$ V. **(B)** Normalized response (NR) of I_d is plotted at $V_g = 0$ V and $V_g = 0.5$ V. Arrows indicate the addition of 100 mM NADH. NR= $(I_0 - I_d)/I_0$, where I_0 is I_d before exposure to NADH.
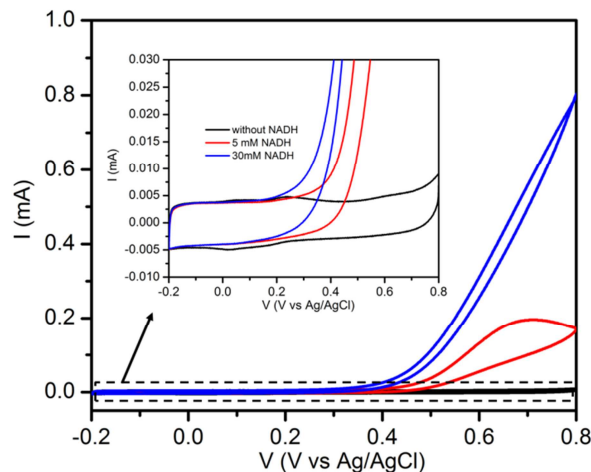

Figure 7.4 **NADH oxidation at PEDOT:PSS electrode cycled at 10 mV/s.** Oxidation starts for V=0.3 V

Since the concentration of NADH is directly related to the concentration of ethanol in the breath, [15-17] this mechanism leads to quantitative ethanol detection. This was confirmed by

exposing the OECT-breathalyzer to a series of phosphate-buffered saline (PBS) solutions containing ADH, NAD$^+$, and different amounts of ethanol. The results, shown in Figure 7.2.B, demonstrate that ethanol detection is achieved for concentrations as low as 0.0004%, and that higher ethanol concentration causes a bigger drop in I_d. The I_d drop occurs in seconds with an immediate enzyme response and steady state is reached in seconds. As a control, in absence of ADH, there is no response from the device upon addition of different ethanol concentrations (Figure 7.5).
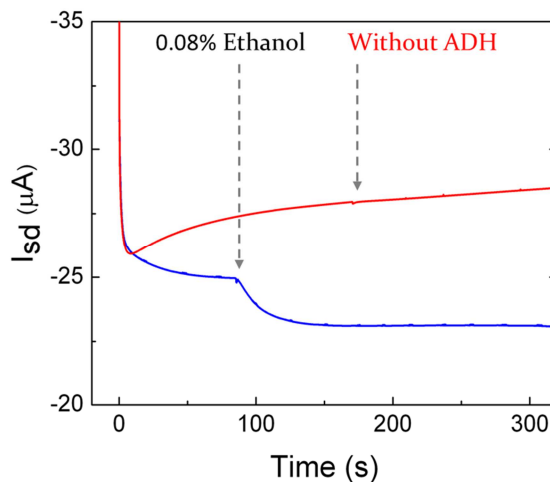

Figure 7.5 **Response of OECT to ethanol.** When ethanol is added to an OECT without the enzyme ADH no change in I_d is detected, while when ADH is present I_d drops as expected.The initial drop around 0 s corresponds to equilibration of the sensor.

We calibrate the sensor to different concentrations (Figure 7.2.C). Higher ethanol concentration corresponds to higher ΔI_d as observed with NADH (Figure 7.3). The response of the sensor is logarithmic with ethanol concentration, as expected from Eq. (3).

Finally, we demonstrate that the OECT-breathalyzer detects ethanol content in the breath of human subjects. For this demonstration, we use bovine gelatin to integrate the ADH and NAD$^+$ onto the OECT, as breathing onto a liquid electrolyte causes excessive noise and makes packaging of the OECT-breathalyzer challenging. Ethanol in the breath is related to BAC by a factor of approximately 1/2100, which tends to vary with each individual [18]. Seven volunteers participate in the breath alcohol test for BAC detection. One volunteer serves as the control, while other volunteers consume different amounts (120 ml and 240 ml) of red

wine (Les 3 filles, 2014, Merlot, 13% alcohol content). The experiment has been reproduced for each amount of wine with 3 volunteers. Thirty minutes after wine consumption, the volunteers are subject to a breath test with a commercial breathalyzer (Breathometer[TM]) for calibration and then are subject to the same test with the OECT-breathalyzer. Subsequently, the volunteer who serves as the control rinses their mouth with mouthwash (Listerine®, 21.6% ethanol content) and immediately takes another set of breath tests. The results from the two tests are compared for accuracy. The test from the volunteer serving as control (0% BAC) results in no response from the OECT-breathalyzer. In contrast, when the volunteers who have consumed wine take the test after one glass (0.01% BAC) and two glasses (0.06% BAC), an immediate response in I_d of the OECT-breathalyzer is observed (Fig. 7.6.A)
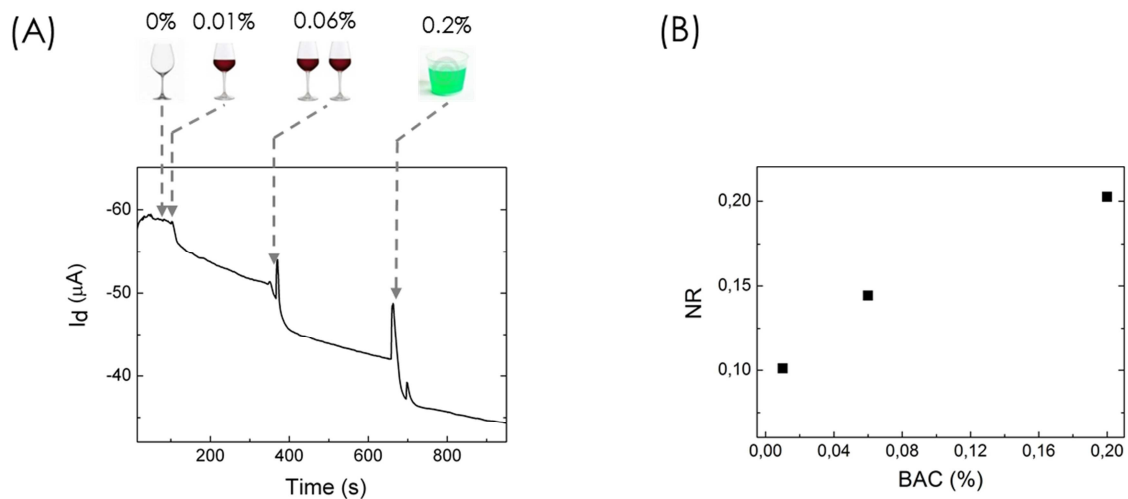

Figure 7.6 **Alcohol detection in breath.** (A) Step change in I_d when breathing 0%, 0.01%, 0.06%, 0.2% ethanol vapor on to the OECT, with $V_g = 0.5$ V, $V_d = -0.7$ V. Breath alcohol concentration is tested 30 minutes after drinking one glass of wine (0.01%) and two glasses of wine (0.06%). 0.2% breath ethanol vapor is from mouthwash, which contains 21.6% alcohol. The BAC is calibrated with a commercially available breathalyzer before testing on the device. **(B)** Normalized response (NR) of I_d is plotted at different breath alcohol concentrations (BAC). NR = $(I_0 - I_d)/I_0$.

This response scales with the amount of alcohol consumed. The test corresponding to mouthwash registers an apparent BAC of 0.2%, consistent with the high alcohol concentration in this solution. (Figure 7.6.B). Similarly to commercial breathalyzers, the OECT-breathalyzer does not seem to be affected by variation in breathing time from different volunteers as

indicated by the small spread in the data for the NR (Figure 7.6.C). We suggest that as long as a volunteer breathes on the OECT-breathalyzer long enough, the ethanol concentration on the device will equilibrate with the ethanol concentration in the breath. This proof-of-concept demonstrates that this simple OECT-breathalyzer is able to detect BAC in human subjects with performance comparable with a commercial breathalyzer.

7.3   Discussion and Conclusions

We demonstrate the first alcohol sensor made with an organic electrochemical transistor integrated with the enzyme alcohol dehydrogenase and its cofactor. This OECT-breathalyzer is easy to fabricate using printing techniques, requires no metal deposition, and is made on an inexpensive, disposable, and biodegradable paper support. The use of a gel to immobilize the enzyme and its cofactor makes the device robust and easy to use. We show that the OECT-breathalyzer detects ethanol in both solution and vapor (such as breath). We conduct preliminary tests with a limited pool of human volunteers and compare the performance of the OECT-breathalyzer with the performance of a commercial breathalyzer. The OECT-breathalyzer is able to detect the consumption of just one glass of red wine. For further optimization, studies with a larger pool of human volunteers are required. This work may help develop alcohol sensors that are easy to integrate with portable/wearable electronics such as smartphones and smart watches. These devices could, in turn, prevent a vehicle to start if they detect the driver to be under the influence and therefore reduce alcohol-associated traffic accidents.

7.4   Materials and Methods

PEDOT:PSS ink: The PEDOT:PSS ink consists of the commercially available PEDOT:PSS (Heraeus, Clevios PH1000) dispersion with 20 wt% ethylene glycol (Sigma Aldrich) and a combination of organic solvents. We add 0.8 wt%

glycidoxypropyltrimethoxysilane (GOPS, Sigma Aldrich) to the ink to prevent delamination, and 0.3% surfactants to match the surface tension of the ink with the substrate.

Ink-jet printing: We use a Dimatix DMP-2800 inkjet printer to print the OECT onto a coated paper (Arjo Wiggins, Inc.). In this study, two layers of PEDOT:PSS are deposited for a total thickness of 190 nm. The printed device is cured in a conventional oven at 160 °C for 30 min. The dimensions of the channel are 1 x 5 mm^2 and 2 x 5 mm^2 for the gate (Fig. 1). For the alcohol solution measurements, 9 mM NAD$^+$ (Sigma Aldrich) are mixed in 0.1 M standard phosphate buffer solution (PBS, Sigma Aldrich). For each measurement, 1.5 mg/mL ADH (Sigma Aldrich) in PBS is added to the in NAD$^+$ and PBS mix at a 1:10 ratio of the total volume. The pH of the electrolyte is adjusted to 8.2 and measured with a pH meter to meet the requirements of the enzyme. A PDMS well is attached to the OECT to confine the electrolyte, defining an active device area of 4 x 4 mm^2. The well is filled with 20 μL electrolyte. For the alcohol vapor measurements, we formulate a 2 wt% bovine gelatin (Sigma Aldrich) in PBS, containing the same proportion of ADH and NAD$^+$ as in the liquid electrolyte above. 15 μL gel solution is drop-casted onto the device and cured at 4 °C for 30 min to form gel.

OECT Electrical Characterization: Electrical characterization is conducted with an Agilent 4155C semiconductor parameter analyzer. During the experiment, V$_g$ varies from 0 to 0.7 V and the V$_d$ from -0.8 to 0 V. For the measurements, we apply constant V$_g$ = 0.5 V and V$_d$ = -0.7 V respectively. Soft carbon electrodes connect the OECT contacts and the Agilent. We prepare different concentrations of ethanol solution in DI water: 0.0004 wt%, 0.004 wt%, 0.008 wt%, 0.01 wt%, 0.03 wt%, 0.04 wt%, 0.08 wt%, 0.1 wt%, 0.12 wt%, 0.15 wt% and measure the response of the device for each concentration three times. During the alcohol solution tests (Fig. 2), we first wait for 120 s until the source drain current (I$_d$) stabilizes after the application of bias on the OECT, and then add 2 μL of ethanol solution to the electrolyte at a 1:10 ratio. For the BAC tests (Fig. 3), we replace the electrolyte solution with gel on top of the OECT. Volunteers consuming different quantities of alcoholic beverages first have their BAC tested with a commercial breathalyzer: The Original Breathometer (Breathometer, Inc.), and then breathe onto the OECT-breathalyzer for a certain duration. The experiment has been tested three times for each concentration with volunteers. The methods were carried out in accordance with the approved guidelines, and all experimental protocols were approved by

the direction of research of the Ecole des Mines de St. Etienne. All volunteers provided informed signed consent to participate in the study.

7.5   References

1   Park, K. K. *et al.* Capacitive micromachined ultrasonic transducers for chemical detection in nitrogen. *Appl. Phys. Lett.* **91,** 094102, (2007).

2   Steven B. Karch, M. D. F. *Drug Abuse Handbook, Second Edition.* 1129 (CRC Press, 2006).

3   U.S. Environmental Protection Agency, Potassium Dichromate Listing Background Document
For The Inorganic Chemical Listing Determin Ation. Date of access: 07/09/2015.
Link:
http://www3.epa.gov/epawaste/hazard/wastetypes/wasteid/inorchem/docs/pot-dich.pdf

4   Breathometer Inc., *Calibration Service*, Date of access: 07/09/2015. Link: https://www.breathometer.com/calibration

5   Cui, G. *et al.* Disposable amperometric glucose sensor electrode with enzyme-immobilized nitrocellulose strip. *Talanta* **54**, 1105-1111, (2001).

6   Strakosas, X., Bongo, M. & Owens, R. M. The organic electrochemical transistor for biological applications. *J. Appl. Polym. Sci.* **132**, 41735, (2015).

7   Lin, P., Yan, F., Yu, J., Chan, H. L. & Yang, M. The Application of Organic Electrochemical Transistors in Cell-Based Biosensors. *Adv. Mater.* **22**, 3655-3660 (2010).

8   Rivnay, J., Owens, R. M. & Malliaras, G. G. The rise of organic bioelectronics. *Chem. Mater.* **26**, 679-685 (2013).

9   Berggren, M. & Richter-Dahlfors, A. Organic bioelectronics. *Adv. Mater.* **19**, 3201-3213, (2007).

10   Scheiblin, G. *et al.* Screen-printed organic electrochemical transistors for metabolite sensing. *MRS Communications*, 5, 507-511 (2015),

11   Andersson Ersman, P., Nilsson, D., Kawahara, J., Gustafsson, G. & Berggren, M. Fast-switching all-printed organic electrochemical transistors. *Org. Electron.* **14**, 1276-1280, (2013).

12   Mannerbro, R., Ranlöf, M., Robinson, N. & Forchheimer, R. Inkjet printed electrochemical organic electronics. *Synth. Met.* **158**, 556-560, (2008).

13   Kitagawa, Y., Kitabatake, K., Kubo, I., Tamiya, E. & Karube, I. Alcohol Sensor Based on Membrane-Bound Alcohol-Dehydrogenase. *Anal Chim Acta* **218**, 61-68, (1989).

14   Bernards, D. A. *et al.* Enzymatic sensing with organic electrochemical transistors. *J. Mater. Chem.* **18**, 116-120, (2008).

15   Shan, C. *et al.* Electrochemical determination of NADH and ethanol based on ionic liquid-functionalized graphene. *Biosens. Bioelectron.* **25**, 1504-1508, (2010).

16   Raj, C. R. & Behera, S. Mediatorless voltammetric oxidation of NADH and sensing of ethanol. *Biosens. Bioelectron.* **21**, 949-956, (2005).

17   Ramesh, P., Sivakumar, P. & Sampath, S. Renewable surface electrodes based on dopamine functionalized exfoliated graphite: NADH oxidation and ethanol biosensing. *J.Electroanal. Chem.* **528**, 82-92, (2002).

18   Alobaidi, T. A. A., Hill, D. W. & Payne, J. P. Significance of Variations in Blood - Breath Partition-Coefficient of Alcohol. *Brit Med J.* **2**, 1479-1481 (1976).

Conclusion

In this thesis, I present the work conducted on optimizing an inkjet printing-based fabrication approach for low cost, disposable and wearable organic electronic devices for medical diagnostics and biosensors platform.

Driven by the ever growing demands in healthcare industry for cheaper faster and more accurate diagnostic devices that can provide critical information about the health status of a patient, significant effort has been dedicated the last decades in finding alternative diagnostic tools that can fulfil the aforementioned requirements.

Electrophysiological monitoring can undoubtedly provide a wide range of information regarding the health condition of a patient even at very early stages of certain pathologies. For instance, the early detection of cardiovascular related disease. Current limitations to the commercial electrophysiological monitoring devices include chronic inflammatory reactions after repetitive use and contact with the human skin. It is thus of critical importance to develop such devices that are patient compliant for daily and prolonged use,

With the emergence of conducting polymers, such stringent requirements could be fulfilled due to a unique set of advantages such as the mixed ionic and electronic conduction, the good mechanical properties as well as the soft nature and biocompatibility of this new class of materials. Besides, their ease of processability allows for their integration with low cost fabrication approaches rendering them ideal candidates for biomedical diagnostic applications.

An easily customizable and versatile technique such as the inkjet process combined with the use of conducting polymer- based inks, PEDOT:PSS in this case, is the main focus of the present work aiming in the development of the next generation of cutaneous biomedical devices.

In this thesis I initially introduce the biopotential electrodes and specifically their use in electrophysiological applications. I also study a wide range of different types of low cost and disposable substrates for the printed electrodes and compare the performance of the resulting devices with respect to the commercial electrodes. Specifically, the substrates I focus on include: paper, textile and tattoo. Short and long term measurements of the printed electrodes

on paper were conducted for ECG recordings, and their performance was found to outperform the commercially available ones.

Next, I demonstrated the feasibility to develop printed electrodes on wearable devices and used it for both EMG and ECG recordings. Especially in the case of ECG recordings using the wearable electrodes, an ionic gel was used at the skin/electrode interface in order to improve the contact with the skin and thus the quality of the recordings.

Going one step further from wearable to fully conformable devices toward the ultimate goal of e-skin, I developed a printed electrode on commercially available temporary tattoos and demonstrated its feasibility in EMG recordings. In this approach, I tried to establish a smart interface connection between the data acquisition system and the tattoo electrode, a major challenge in e-skin related applications. Particularly, I used a dry PEDOT:PSS printed textile to replace the traditional wiring and thus provide the required connection to the data acquisition setup without damaging the tattoo electrode.

Last but not least, more complex electronic components like the Organic Electrochemical Transistor (OECT) were realized using the inkjet printing method on paper-based substrates. Initially, the resulting devices were tested and compared with spin-coated state-of-the-art OECTs of similar geometry. The performance was found to be comparable, thus encouraging their implementation as transducing elements in point-of-care testing applications. In particular, I developed a disposable Breathalyzer to detect alcohol levels in breath. To do so, the gate electrode of the OECT (printed, PEDOT:PSS as well) was functionalized with the enzyme, alcohol dehydrogenase along with its co-factor, to confer the required specificity for alcohol. The resulting disposable biosensors were tested on human volunteers with varying alcohol concentration on their breath, and the data acquired were compared with commercially available breathalyzer further confirming their accuracy.

Overall, based on the encouraging results I obtained with the organic printed electronic devices that I developed and tested for different healthcare applications, I anticipate that this work will pave the way to next generation low cost, disposable multi-parameter monitoring devices. In particular, the ultimate goal would be to combine, in one platform, different types of devices for electrophysiological monitoring and/or biosensing toward personalized and connected healthcare diagnostics intelligent system.

Appendix A

Electrical characterization of the PEDOT:PSS printed on glass slide
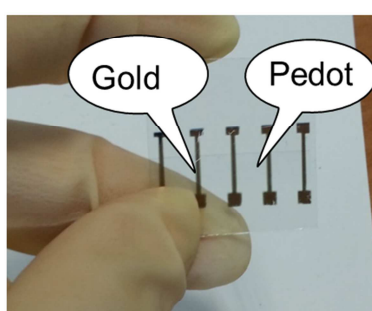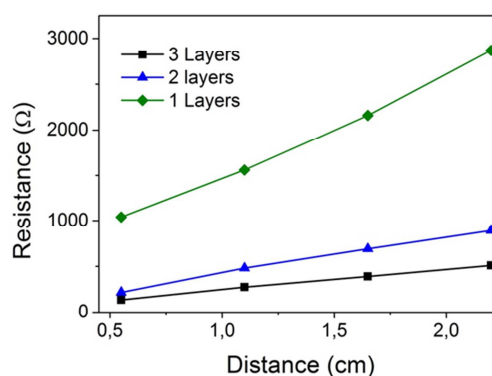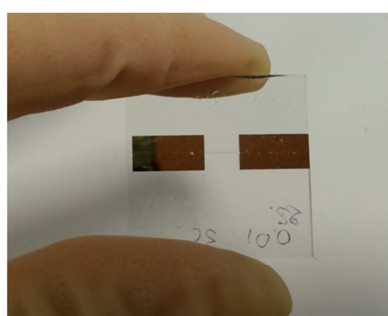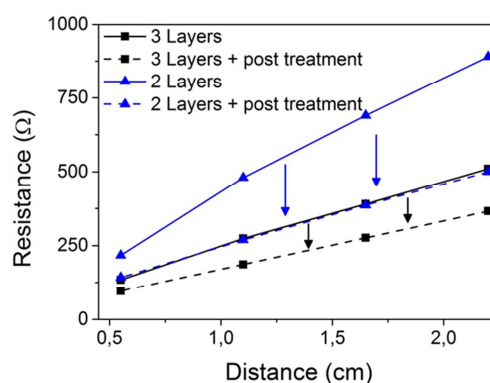

(a)   (b)

Figure A.1 (a) Photograph of the printed PEDOT:PSS rectangle (35mm x 5mm) on a classic glass slide, 100 nm of gold is deposited on top of the conducting polymer by evaporation , (b) Resistance measured vs. the distance for 1, 2, 3 layers respectively.

(a)   (b)

Figure A.2 (a) Photograph of the inkjet-printed PEDOT:PSS rectangle (35mm x 2mm) on a classic glass slide, 100 nm of gold is deposited on top of the conducting polymer by

evaporation , (b) Resistance measured vs. the distance for 2, 3 layers respectively before and after post treatment Post treatment was consisting of immersion in sulfuric acid (1M) following the protocol proposed by Xia et al [1] .
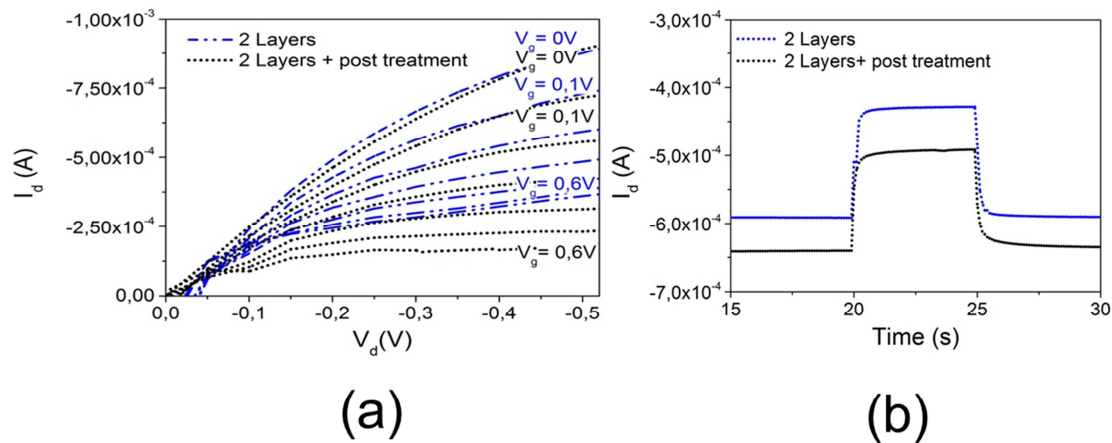

(a)

(b)

Figure A.3 (a) Id versus Vd for OECTs printed on glass slide before and after sulfuric treatment, (b) Drain current transient of the printed transistor after applying 0V-> 0,1V to the gate for 5s before and after treatment

References

1.   Xia, Y., Sun, K. & Ouyang, J. Solution-Processed Metallic Conducting Polymer Films as Transparent Electrode of Optoelectronic Devices. *Adv. Mater.* **24,** 2436–2440 (2012).

Appendix B

This work is based on the following publication:

"Fully Printed Organic Electrochemical Transistor on Paper for Glucose Sensing"

C. Davidson, **E. Bihar**, A-M Pappa, V. Curto, G. Malliaras**,** NNIN Research Accomplishments (2011)

Abstract

Inkjet printing is a versatile, low-cost, and non-contact fabrication method for electronic devices. In this study, an all-plastic organic electrochemical transistor (OECT) using an aqueous ink consisting of poly(3,4-ethylenedioxythiophene)-poly(styrene sulfonic acid) (PEDOT:PSS) was printed on a paper substrate and was employed as the transducing element of a glucose biosensor We functionalized the gate, printing on top of it an ink comprising chitosan/ferrocene, a common electron mediator. For the enzymatic-based sensing of glucose, glucose oxidase (GOx) was added in the electrolyte solution of phosphate buffered saline. Initial results exhibit a detection range between 2.70 and 10.00 mM after successive additions of different concentrations of glucose which is consistent with that concentration in blood. Those results pave the way to establishing a paper-based, simple and low cost biosensing platform suitable for point of care diagnostics.

Introduction

OECTs have recently gained great attention, due to their advantages such as biocompatibility, ease of fabrication and operation in low voltages making them ideal candidates for bioelectronic applications. PEDOT:PSS is a conductive polymer ideal for fabricating OECTs due to its high conductivity, commercial availability, and its exceptional films forming properties [1] . In our study, we focus on inkjet printing the biomedical device. Indeed inkjet presents advantages as speed, flexibility, and low cost [2] and it offers the possibility to print on a multitude of substrates, including paper which is an eco-friendly, disposable and inexpensive alternative to plastics.

In our work, we detect the presence of glucose inducing the enzyme specific reaction of glucose coupled with ferrocene an electron mediator as shown in Figure 1.
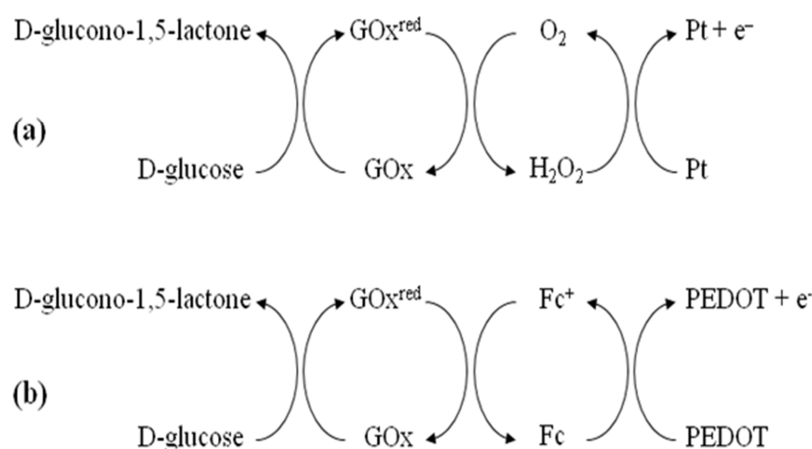

Figure 1. Reaction Cycle for glucose detection using a ferrocene mediator

Ferrocene acts as an electron shuttle from the GOx to the PEDOT:PSS gate, causing de-doping of the channel and thus decreasing the drain current. This decrease is proportional to the concentration of glucose in the working solution [3].

Experimental Procedure

We used a Dimatix Materials Printer (DMP) to print the device and its dimensions are shown in Figure 2. The channel and gate dimensions (length and width) were respectively 5mmx1mm and 5mmx2mm. We printed 2 layers of pre-developed recipe of PEDOT:PSS ink to fabricate the channel, drain source and gate of the transistor.

For the electron mediator solution preparation, a chitosan/ferrocene solution in acetic acid (0.3%wt) was first made by dissolving 15 mg of chitosan/ferrocene copolymer in 5 mL of 0.2 M acetic acid. To match this solution with the requirements of inkjet (rheological properties of the ink), we added a surfactant (Dynol 810) and a flush solution (water and ethylene glycol).

We run cyclic voltammetry using a Platinum wire as counter electrode, an Ag/AgCl reference electrode, and our ink's preparations as the working electrode, and can be seen in Figure 3, to assess the electrochemical performance of the ink.

Electrical characterization of the printed devices was carried out at a constant gate voltage of 0.5 V and a drain voltage of -0.7 V. In order to confine the electrolyte, a polydimethylsiloxane (PDMS) well was placed on top of the gate and channel and the electrolyte (16 μL) and the enzyme (2 μL) were added. After stabilization of the drain current, we added different concentrations of glucose solutions . Figure 4 shows the device response to incremental steps in glucose concentration.

Results and Discussion

Figure 2 shows the cyclic voltammograms of the chitosan/ferrocene ink after addition of surfactant, after further addition of flush solution, and a control of PEDOT:PSS. The peaks that can be observed at around 0.4 V and 0.1 V for both inks containing chitosan/ferrocene solution, confirm the electrochemical activity of ferrocene. Following that, the devices were fully   printed.
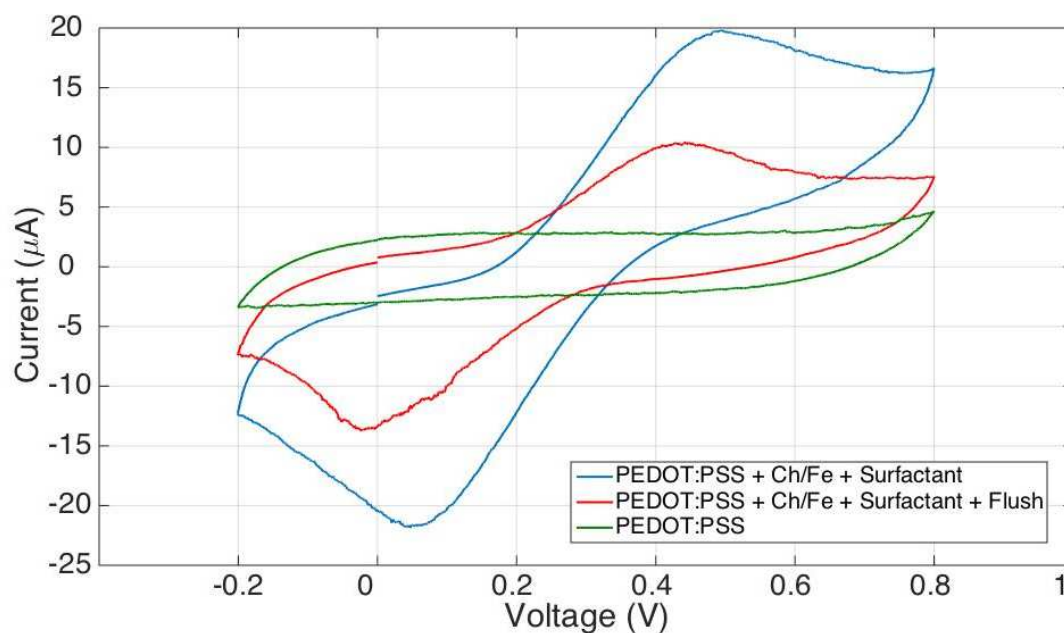
Figure 2. Cyclic voltammograms for different chitosan/ferrocene inks compared to PEDOT:PSS

There is a clear color change between the gate (brown) and the rest of the device (blue) (Fig. 3) indicating that the chitosan/ferrocene ink was successfully printed selectively onto the gate of the device.
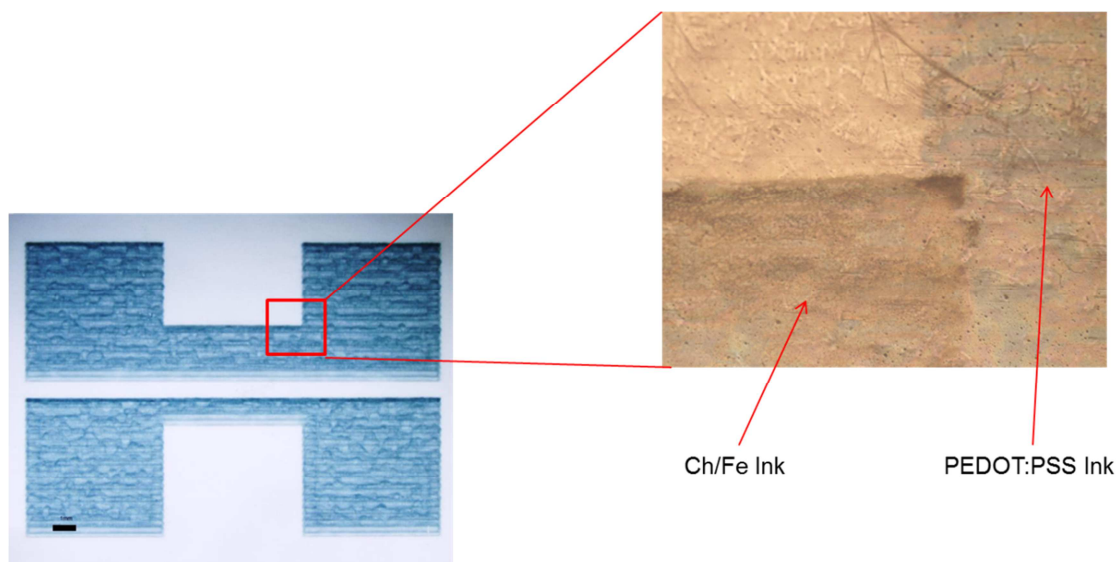

Figure 3. Fully printed OECT with zoom on gate border

Figure 4 shows the device response upon successive additions of different glucose
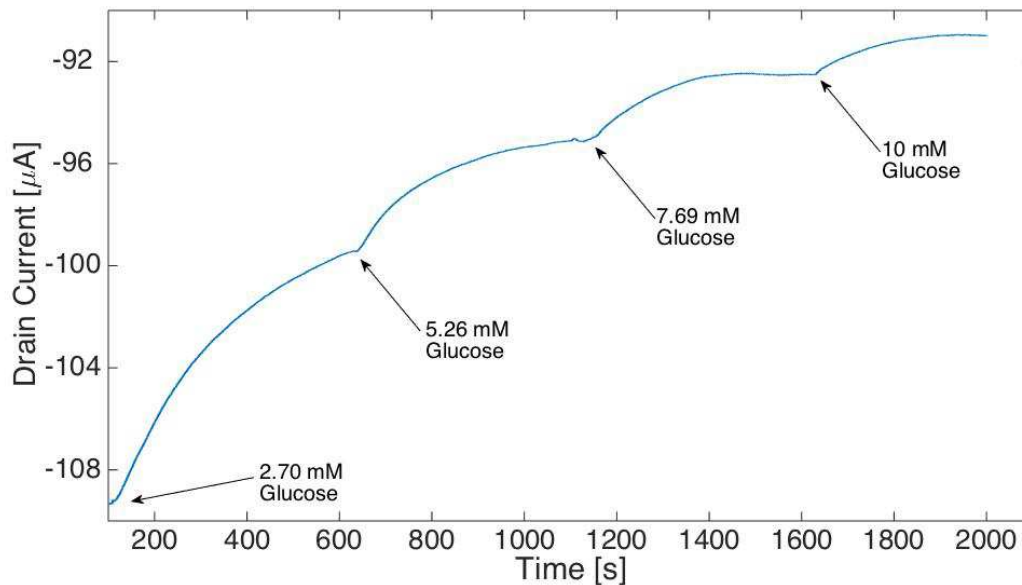
concentration onto the device.

Figure 4. Device response

There are clear changes in the current values for a range of concentrations 2.70 mM and 10 mM which are consistent with those in human blood [4].

Conclusion and Future Work

In this study, PEDOT:PSS and chitosan/ferrocene –based inks were successfully printed on paper towards the development of an all printed paper OECT based glucose sensor. The detection of glucose was successful in a range of concentrations between 2.70 and 10.00 mM, similar to that in human blood. There is room for optimization, e.g. immobilizing the enzyme in the printed layer and improving the sensor's sensitivity to the µM range for the detection of glucose in saliva. This work shows great potential as a disposable noninvasive sensing platform for point of care diagnostics.

References:

[1] Shim N. et al. *Sensors.* **2009**, *9*, 9896-9902

[2] Yun Y.H. et al. *Anal. Sci.* **2011**, *27*, 375-379

[3] Strakosas X., Bongo M., Owens R.M. *J. Appl. Polym. Sci.* **2015**, *132*, 41735.

[4] Panchbhai A.S. et al. *J. Oral. Maxillofac. Res.* **2012**, *3(3):e*

École Nationale Supérieure des Mines

de Saint-Étienne

Eloïse Bihar

Inkjet printed organic electronic devices for biomedical diagnosis

Speciality : Microelectronics

Abstract : Currently, there is a tremendous effort on the development of biomedical devices in healthcare industry for the early diagnosis, prevention or treatment of chronic disease. With the evolution of microelectronics industry and their direct implementation in the biomedical arena, innovative tools and technologies have come to the fore enabling more reliable and cost-effective treatment. The last decade, conducting polymers have attracted special attention due to their unique set of features such as combined ionic and electronic conduction, rendering them an ideal alternative to the inorganic materials used for electrophysiological applications. In this thesis I focus on the integration of the conducting polymer namely PEDOT:PSS with printing technologies towards the realization of high performant biomedical devices.

In the first part of this study, I focus on the optimization of the conducting ink formulation. Following, I emphasize on the fabrication of inkjet printed PEDOT:PSS based biopotential electrodes on a wide variety of substrates (i.e., paper, textiles, tattoo paper) for use in electrophysiological applications such as electrocardiography (ECG) and electromyography (EMG). In an initial approach, electrodes on paper and printed wearable electrodes were fabricated and investigated for long-term ECG recordings. Last but not least, conformable printed tattoo electrodes were fabricated to detect the biceps activity during muscle contraction for a period of seven hours. In order to enable a reliable connection of the tattoo with the electronic acquisition system, the conventional wiring was replaced by a simple contact between the tattoo and a similarly ink-jet printed textile electrode.

In the last part, I present the potentiality of inkjet printing method for the realization of organic electrochemical transistor (OECTs) as high performing biomedical devices. As proof of concept, a paper disposable breathalyzer comprised of a printed OECT and modified with alcohol dehydrogenase was used for the direct alcohol detection in breath, enabling future integration with wearable devices for real-time health monitoring. Their compatibility with printing technologies allows the realization of low-cost and large area electronic devices, toward next-generation fully integrated smart biomedical devices.

École Nationale Supérieure des Mines

de Saint-Étienne

NNT : *2016LYSEM036*

Eloïse Bihar

Réalisation de dispositifs biomédicaux par impression jet d'encre

Spécialité: Microélectronique

Mots clefs : Jet d'encre, bioélectronique, électrodes, biodétection, OECT,PEDOT :PSS,

Résumé :

De nos jours, le domaine biomédical est en pleine croissance avec le développement de dispositifs thérapeutiques innovants, bas coût, pour le diagnostic, le traitement ou la prévention de maladies chroniques ou cardiovasculaires. Ces dernières années ont connu l'émergence des polymères semi-conducteurs, alternative intéressante aux matériaux inorganiques, présentant des propriétés uniques de conduction ionique et électronique.

Tout d'abord, j'ai axé mes travaux de recherche sur le développement et l'optimisation d'une encre conductrice à base de PEDOT:PSS, parfait candidat comme matériau, pour la transduction des signaux biologiques en signaux électriques, compatible avec le process jet d'encre, pour la réalisation de dispositifs imprimés. Puis mes travaux se sont orientés vers la conception et l'étude d'électrodes imprimées sur supports papiers, tatous et textiles permettant des enregistrements long termes d'électrocardiogrammes (ECG) ou électromyogrammes (EMG), présentant des performances similaires aux électrodes commerciales, utilisant un système d'acquisition spécifique pour la mesure d'activités électriques de tissus musculaires. Puis dans un second temps, je me suis penchée sur l'impression sur support papier, de transistors organiques électrochimiques (OECTs) fonctionnalisés, afin de permettre la détection d'éléments biologiques ou chimiques comme l'alcool.

Ces travaux proposent une nouvelle voie pour la conception de dispositifs innovants biomédicaux à bas couts, imprimés, permettant la personnalisation des produits pouvant être intégrés dans des dispositifs biomédicaux portables ou dans des vêtements « intelligents ».